ADVANCED MASTERS IN STRUCTURAL ANALYSIS
OF MONUMENTS AND HISTORICAL CONSTRUCTIONS

Master's Thesis

Juan Mora Gómez

Innovative retrofitting materials
for brick masonry infill walls.

University of Minho

Czech Technical
University in Prague

Education and Culture

Erasmus Mundus

DECLARATION

Name:	Juan Mora Gómez
Email:	jmoragz@gmail.com

Title of the MSc Dissertation:	Innovative retrofitting materials for brick masonry infill walls.
Supervisor(s):	Graça Vasconcelos / Raul Fangueiro
Year:	July 2012

I hereby declare that all information in this document has been obtained and presented in accordance with academic rules and ethical conduct. I also declare that, as required by these rules and conduct, I have fully cited and referenced all material and results that are not original to this work.

I hereby declare that the MSc Consortium responsible for the Advanced Masters in Structural Analysis of Monuments and Historical Constructions is allowed to store and make available electronically the present MSc Dissertation.

University:	University of Minho
Date:	17 July 2012
Signature:	

Master's Thesis

Juan Mora Gómez

Innovative retrofitting materials for brick masonry infill walls.

A la curiosidad y paciencia del lector.

ACKNOWLEDGEMENTS.

ABSTRACT.

Last seismic events in Southern Europe have highlighted the vulnerability in the most usual constructive typology in contemporary architecture: framed structures with masonry infills. Contemporary structures have a good capacity to withstand these actions, given that they were considered for their design according to modern codes. Nonetheless, nonstructural elements as masonry infills show a high degree of damage even for medium magnitude earthquakes, causing casualties and high economic losses. For decades, these elements have been considered as nonstructural and therefore they were not requested to have resisting conditions.

Given this, there is a large segment within the building stock in seismic prone areas that needs to undergo preventive action, specially for out-of-plane loads. This can range from a mere union of the infills to the frame structures to a reinforce of the elements, which can also be applied to the case of already damaged elements. The potential benefits go beyond the mere stability of nonstructural elements, as this would improve the behaviour of the whole structure to face seismic events.

Some new fibre-based materials for structural reinforcement based in braiding techniques have been developed in the last years in the Universidade do Minho, as an alternative to conventional FRP rods. These materials have several advantages, out of which it can be remarked the possibility of designing the composition according to mechanical requirements and the implication of low-tech and low-cost procedures for its production.

The main purpose on this thesis will be the assessment of the application of this material as reinforcement for clay brick masonry, using the technique of Textile Reinforced Mortars, considering out-of-plane actions. This has been done through a basic experimental campaign in which it has been evaluated the improvement in the behaviour of masonry samples subjected to flexural loads. The material was applied with variations in reinforcement ratio in order to have some parametrical confrontation. Other samples included commercial solutions, so as to have a reference on already existing materials, and the control samples were unreinforced.

The obtained results for the innovative materials were highly satisfying in terms of ductility enhancement, obtaining big deformations with a considerable flexural capacity, and a considerable increase in strength. Furthermore, the use of different materials within a composite results in the combination of its properties.

The future development and enhancement of this material presents a high potential as an economic and easy to apply method for brick masonry reinforcement, with the possibility of tailor-made properties..

RESUMO.

Os recentes eventos sísmicos ocorridos no sul da Europa destacaram as vulnerabilidades de um dos sistemas construtivos mais utilizados na arquitectura contemporânea: estruturas em pórtico preenchidas com paineis de alvenaria. Enquanto as estruturas modernas, dimensionadas de acordo com os códigos em vigor, resistem bem a esse tipo de acções, o mesmo já não se passa com os elementos não-estruturais. De facto, é comum os paineis de alvenaria sofrerem elevados danos, mesmo para sismos de intensidade media, causando vitimas fatais e elevadas perdas económicas. Durante décadas estes elementos foram considerados como sendo não-estruturais e consequentemente nunca lhes foi exigido quaisquer propriedades the resistência.

Sendo assim, é natural que nas zonas sismicas exista uma larga porção de patrimonio edificado com necessidade de sofrer medidas preventivas, especialmente para acções fora do plano.Estas medidas podem significar desde a simples união dos paneis à estrutura até um reforço dos elementos individuais da alvenaria, o qual pode ser aplicado mesmo que já existam danos. Os potenciais benefícios destas técnicas vão para além da mera estabilidade destes elementos uma vez que o seu reforço poderá implicar uma mehoria das caracteristicas sismicas da estrutura como um todo.

Durante os últimos anos a Universidade do Minho tem vindo a desenvolver novos materiais à base de fibras como alternativa aos sistemas convencionais de polimetros reforçados com fibras (FRP).. Estes materiais possuem várias vantagens entre as quais se destaca a possibilidade de poderem ser dimensionados com base em requisitos mecânicos de uma forma barata e tecnologicamente acessível.

O principal objectivo desta tese é a avaliação da aplicação deste material como reforço de alvenaria de tijolo cerâmico, utilizando a técnica de argamassas reforçadas com texteis e considerando acções fora do plano. Este estudo foi realizado através de uma série de ensaios experimentais simples, na qual foi avaliada a melhoria do comportamento de várias amostras sujeitas a cargas de flexão. Vários espécimens foram preparados com diferentes densidades de reforço, de modo a possibilitar a comparação de vários parâmetros. Outras amostras incluíram soluções comerciais, de forma a ter uma referência de materiais já existentes, e amostras de controlo não-reforçadas.

Os resultados obtidos para os materiais inovadores foram altamente satisfatórios em termos de aumento de ductilidade, tendo-se verificado deformações elevadas enquanto mantendo uma capacidade de suporte de carga considerável, e um aumento da capacidade de carga no estado fendilhado.

O continuado desenvolvimento e aperfeiçoamento destes materiais apresenta um elevado potencial, sendo um método economico e de fácil aplicação em alvenaria de tijolo cerâmico.

RESUMEN.

Los últimos eventos sísmicos en el Sur de Europa han puesto de relieve la vulnerabilidad de una de las tipologías constructivas más usuales de la arquitectura contemporánea: las estructuras porticadas –metálicas o de hormigón- con cerramientos de ladrillo. Si bien las estructuras soportan bien las acciones, los elementos no estructurales como fachadas o petos sufren graves daños, provocando altas pérdidas económicas y víctimas mortales incluso para acciones sísmicas de mediana magnitud. Durante décadas, estos elementos constructivos se han considerado no estructurales, y por tanto no se les han exigido condiciones de resistencia.

Nos encontramos por tanto con un amplio sector del parque inmobiliario en zonas de riesgo sísmico necesitado de acciones de prevención. Dichas acciones incluyen una mejor unión de los cerramientos a la estructura general, así como posibles refuerzos de los elementos en sí. El beneficio, más allá de la estabilidad de los elementos en sí, incluye un mejor comportamiento de la estructura general ante acciones sísmicas

En la Universidade do Minho se han venido desarrollando nuevos materiales de refuerzo estructural, basados en la técnica del entrenzado de fibras, como alternativas a las barras de FRP convencionales. Estos materiales están compuestos por un núcleo de material resistente rodeado de una funda entrenzada de material económico, que mejora la adherencia del material al mortero a la vez que protege al núcleo del ataque alcalino. Entre sus ventajas, la posibilidad de diseñar composiciones del material dependiendo de los requerimientos mecánicos y el uso de una tecnología sencilla y de bajo coste. La producción y caracterización de estos materiales será tratada a fondo en este trabajo.

La validación de estos nuevos materiales en su aplicación al refuerzo de muros de fábrica de ladrillo se ha hecho mediante una campaña experimental básica, comprobando la mejora que supone su uso en la resistencia a flexión unidireccional de unas muestras de obra de fábrica, realizados con los materiales más usuales para esta solución constructiva. Se ha intentado confrontar el resultado de estos materiales, con parámetros variables, con el de materiales disponibles comercialmente, así como con muestras de control sin refuerzo.

Los resultados obtenidos para los materiales desarrollados son muy satisfactorios en cuanto a la mejora de la ductilidad, obteniendo grandes deformaciones manteniendo la capacidad de carga, incluso para ratios de refuerzo relativamente bajos. Para los ejemplares con más refuerzo, se observa además una redistribución de tensiones dentro de la fábrica, dando lugar a un fallo a flexión muy dúctil y a un comportamiento con incremento de resistencia en el estado fisurado.

El desarrollo de este material presenta una gran potencialidad como método económico y de fácil aplicación para el refuerzo de muros de fábrica

CONTENTS.

LIST OF FIGURES.

LIST OF TABLES.

LIST OF ABREVIATIONS.

RC – reinforced concrete

URM – unreinforced masonry

CM – confined masonry

RM – reinforced masonry

FRP – fiber reinforced polymers

GFRP – glass fiber reinforced polymers

CFRP – carbon fiber reinforced polymers

TRM – textile reinforced mortar

LVDT – Lineal variable differential transducer

CHAPTER 1. INTRODUCTION.

The development of reinforced concrete along last century was supported by exhaustive research, mathematical and physical theorization and modelling, and consequent progressive improvements that made it the most affordable and reliable material for structural design. This way, now days this is the prevalent typology within the contemporary built stock in Europe. Experience and research helped to develop standards and building codes increasingly strict and safe, with a better understanding of actions such as earthquake, and solutions to face them.

Nonetheless, this increasing structural requirements were mainly applied only to the purely concrete or metallic structural skeleton, neglecting the non-structural elements such as the brick masonry infills that for decades have constituted the most common solution for enclosing and façading. These elements have undergone development, but regarding mainly their enclosing and isolating functions, and forgetting their resisting role, since this requirement is only evidenced in limited, and normally accidental occasions.

Last seismic events in Southern Europe have shown that the contemporary building stock can withstand earthquakes reasonably well under the point of view of collapse, when compared to the ancient and traditional masonry structures, which show a higher vulnerability. Nonetheless, the damages in non-structural elements have been a major cause of both casualties and economic loss [1] [2]. Failure and overturning of façades and parapets induced by out-of-plane load, and major damage of the infills for in-plane loads are common in reinforced concrete buildings even if the main structure remains undamaged. This shows that a big part of the building stock is highly exposed to high cost damages and to life security even for medium-size seismic events.

Preventive actions should consider the enhancement of the behaviour of this non-structural elements, both by considering an adequate connection between the supporting structure and the infills (a solution more frequent now days, but quite rare in buildings from past decades), and by retrofitting them by means of affordable and feasible techniques.

Given this, the objectives of any constructive solution that might be developed to enhance the behaviour of these non-structural elements to earthquakes and other accidental loads such as blast- should be in principle three:

- Enhancement of the ultimate strength of the element, both for safety reasons and for contributing to the seismic response of the whole structure.
- Enhancement of the deformation capacity, in order to obtain a ductile failure from a potentially brittle material such as masonry, also with the scope of safety.

- Raising the cracking load for the element, reducing the damage and thus the economical losses.

Several materials and techniques have been developed and tested as retrofitting possibilities for these elements, from the early application of ferrocement to the more recent retrofitting technique based on Fibre Reinforced Polymers (FRP). Their application can range from the preventive aspect for hazardous elements previous to their damage, to the strengthening in lightly damaged elements, preventing further damage in future seismic events.

In a first approach, FRPs seem to have the best mechanical performance for this kind of application. They provide both high strength and a fairly ductile behaviour. On the other hand, their application has many disadvantages due to the use of resins for the matrix. One of the developed alternatives has been textile reinforced mortars (TRMs), that use the same reinforcing fibres, mainly glass and carbon, but within a textile structure and embedded in a mortar matrix. This solution is more recent and few studies are available on its performance when applied in the retrofitting of masonry infill walls. With this respect, among the problems to be solved is the possibility for the composite material to debond, which implies an ineffective use of the material, and the potential reactivity of the mortar to some of its components that can lower its durability.

1.1. Objectives of the thesis

Following the need of studying retrofitting strategies to improve the seismic behaviour of masonry infill walls, textile reinforced mortar technique was adopted to be analysed in the scope of this thesis. The textile materials used here continue a research line of development of braided materials carried out in University do Minho [3]. The textile materials are proposed as an alternative to conventional FRP rods, produced using simpler and lower cost technology (braiding). In short, these materials consist of a core of high resistance material such as carbon or glass fibres, coated on a braided tubular structure of cheaper material, namely polyester. This external braid should carry out two important functions: improving the bonding to the mortar in which the rods will be embedded, through the creation of a ribbed structure in the braided shell, and the protection of the inner core to the potential reactivity of the alkali components of mortar. Previous research studied the application of these materials as an alternative to steel reinforcement of concrete [4] [5] [6].

Thus, the main objective of this thesis is to assess the behaviour of these innovative materials in the retrofitting of typical brick masonry infill panels. Though the experimental campaign only focuses on contemporary materials, the applications are wider, and could be extrapolated easily to historical masonry.

In detail, the objectives are: (1) study of innovative materials for retrofitting masonry infill walls based on textile reinforced mortar (textile braided materials embedded in mortar); (2) characterize the

performance of the innovative retrofitting techniques in the improvement of the out-of-plane behaviour of masonry brick walls; (3) comparison of the innovative solution with other existing techniques.

In relation to the previous work [3], which compared distinct internal core material for the braided bars (carbon fibre core, glass fibre core and polyester), some improvements and modifications have been made, such as the development of the ribbed structure to improve the bonding, and the application of a resin in the braided bars to make it more effective in the resistance of the composite material. Besides, in this thesis only one type of reinforcing material (glass fibre) was considered in all the samples, to have the possibility of assessing the effect of varying parameters affecting the density of reinforcing material, such as the amount of reinforcement and the spacing of the rods. There will be also a comparison with two commercial solutions of meshes to be embedded in mortar.

Both the production of the strengthening materials and the obtaining of data for analysis imply large amount of laboratory work due to (1) the semi-manual process of production of the braided materials and to the need of a thorough characterization of all the implied components and (2) the experimental campaign for the evaluation of the performance of the developed materials as a retrofitting technique for the enhancement of the out-of-plane behaviour of masonry infill walls and their comparison. Here, there will be a special care on the analysis of improvement on strength and deformation capacity of the retrofitting materials, as well as possible comparison with the commercial solutions, both quantitatively and qualitatively, as well as with other research on TRM available in literature.

The designed experimental campaign is quite basic, studying only the improvement of behaviour to simple flexure as comparable parameter, given that this is only a first approach to the use of the material in masonry reinforcement. Further empirical studies, with improvements drawn from this thesis, should go further for a more realistic behaviour of reinforced masonry under seismic loads.

1.2. Organization of the thesis

The thesis is divided into five chapters besides the introduction (Chapter 1).

In the second Chapter, it is provided a wide review on general topics related to both masonry and seismic actions. This is mainly centred on the current building codes and standards, and their consequences on building techniques.

In Chapter three, a literature review on the specific topic of masonry infills, their behaviour under seismic actions and the most usual retrofitting techniques used nowadays, leading to the starting point of the innovative materials.

Chapter four is fully dedicated to the innovative reinforcing materials. It is explained their development through a literature review, their production in the textile laboratory of University of Minho, and a thorough description of its material and mechanical characterization.

Chapter five explains the application of this reinforcing materials to masonry samples, and goes through the whole experimental campaign. This includes the design of the samples and the experimental setup, the mechanical characterization of the masonry components, an analytical estimation of the expected behaviour based on material models, and the analysis of the results obtained from the experimental campaign. This analysis will be done both for each typology of reinforcement considered and comparing the different solutions among them.

In Chapter six the conclusions and recommendations for future development are provided.

There is also an appendix of annexes, including all sort of data that can be helpful for further understanding of the reader of certain points of the work done.

CHAPTER 2. MASONRY INFILLS UNDER SEISMIC ACTIONS: GENERAL OVERVIEW.

Through this section, the main background of the particular research done in this thesis will be reviewed in order to give an initial thread to the further development of specific parts of the whole frame here described. This first part will consist in an introduction to the two main topics to be treated in the research project: masonry infills and seismic behaviour.

First, there will be a description of the typology of masonry infills in reinforced concrete structures, and their importance within the contemporary building industry. The overview includes aspects about their possible classification with structural implications and some problematics, according to the European reference codes.

Then, a short introduction into a complex topic, the seismic behaviour of reinforced concrete structures and the influence of masonry infills in it, with a review on the most important research carried out about the topic.

Finally, some qualitative parameters of the infill that will affect its behaviour, as well as an initial approximation to the estimation of the seismic requirements for this type of element.

2.1. Characterization of masonry infills.

2.1.1. Historical introduction.

The first hint when trying to define masonry solutions refers to the period in which it was built. Even if it's a rough generalization, in Europe, and even more in earthquake-prone zones of Europe (approximately the South and Mediterranean Basin) the development and application of constructive solutions for masonry infills of reinforced concrete structures was very similar.

Starting at the beginning of the XX century, a new type of structural typology replaced the traditional building technique based in structural masonry walls. Skeleton structures have a precedent in timber structures, that were normally infilled with masonry or adobe. Nonetheless, the real development of this type came with the development of reinforced concrete and steel in industrial production. This materials became the cheapest and quickest solutions for building. From then on, this structural type was further developed and improved and gained popularity, specially after Second World War and the reconstruction of European cities, and was applied to all typologies of buildings in industrially developed countries and specially all over Europe. This implied a revolution not only for the construction processes but also for the architectonical possibilities. The structural function was separated from the protection and isolation of internal spaces, which traditionally had been all carried out by structural masonry walls.

At the beginning, mixed structures with perimetral structural masonry walls and internal columns and floor slabs made in reinforced concrete were more common [7], but the later development, together with the bad structural behaviour of this typology (specially to seismic loads) led to what nowadays is the most common structural typology of reinforced concrete skeleton with non-structural masonry infills.

The composition of this infills was developed and improved according to the increasing requirements of thermal and acoustical isolation and humidity problems, as well as the technical development of new solutions and materials: perforated clay bricks, isolating layers, air gaps, porotherm style blocks, etc. This evolution is depicted in Figure 1.

In a similar way, the connection of the infill with the main structure and the internal connection among masonry layers was progressively improved. Being non-structural elements, their behaviour and their influence in the behaviour on the main structures was at first considered irrelevant, and therefore they were only designed for their self-support. This is a conservative position when considering only vertical forces. But later experience with seismic events led to a better understanding of the structure as a whole, and, as will be discussed later, their effect started to be studied carefully, both for the importance of their failure (heavy elements causing casualties) and for their contribution to the resistance of the main structure.

As a result of this studies, new building codes have been developed, being the last one in Europe Eurocode 6, and Eurocode 8 for prescriptions in earthquake-prone areas, and their national versions. In the codes, better detailing and connection are prescribed on the scope of a better performance.
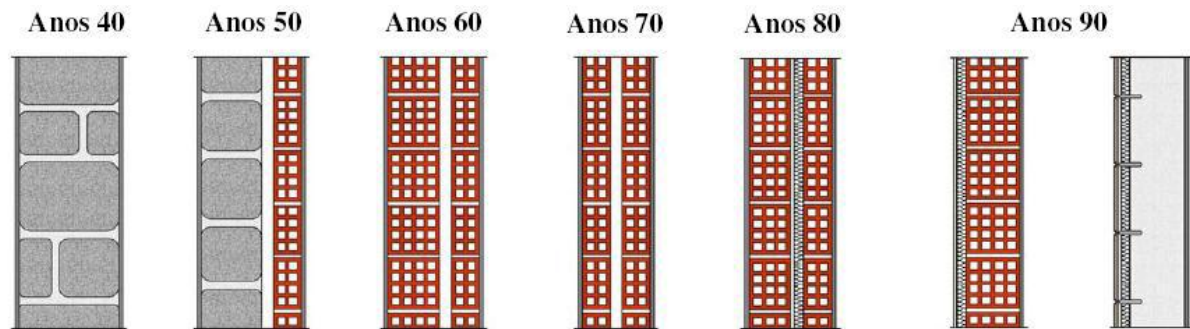
Figure 1. Evolution of masonry infill walls in Southern Europe. [8]

As seen in Figure 1, the development of new building codes has lead to the increased general use of multilayer walls, lighter and thinner. As it will be seen afterwards, this parameters have an implication on the behaviour of the infill to seismic actions, and therefore for the consideration of different retrofitting solutions.

In spite of the development and improvement of the codes and requirements for new buildings, there has been a long period in which there were nor regulation neither experience with this type of walls, specially for their performance under earthquakes. This leads to a considerable percentage of the building stock to be considered as risky, given the possibility of failure of their infill walls and partitions. In risky areas, there might be a need of retrofitting the most dangerous elements or of strengthening elements damaged in previous seismic events.

2.1.2. Classification: material, typology.

Masonry infills can be designed according to many types of constructive solutions. On the purpose of assessing the performance of a given wall to seismic actions, the first step will be to give a classification according to the details and requirements. Though Eurocode 6 is specifically for masonry with structural purposes, the materials and classification can be applied for infills, given the similar typologies. For each type of solution considered within this classification, the modelling and further estimation of strengths and failure modes will be different. The parameters that rule the classification will define very important features of the masonry elements, such as its weight and slenderness (which will define its own behaviour), the flexural strength, the consideration of some kind of bonding among the main structure and the infills, or as indicated by Tomazevic, the robustness of the brick itself [9].

First classification can be done according to the use of reinforcing elements within the masonry element. Reinforcement has a very important effect on improving the resistance to shear, and, mostly,

to flexural requirements. Therefore, reinforced masonry will have a completely different behaviour from unreinforced masonry.

- Unreinforced masonry. It's the simplest typology, with no reinforcing elements. The whole structural resistance to shear and flexural requirements relies on the masonry elements and the bonding among them. As a result, this is the weakest type. Given its lower costs and the lack of structural requirements in infills, it is the most extended type.
- Reinforced masonry. The masonry has steel reinforcing elements that improve its tensile behaviour enhancing the response to flexural actions. This reinforcement can be set in several ways: reinforced grouted masonry (specific masonry systems such as mono-layer enclosures), bed joint reinforcements, etc.
- Other metallic elements that could be inserted are connection among infills and RC structures to ensure its stability. This are highly recommendable in seismic-prone areas.

Other classification is according to the constructive detail, mainly referring to the number of layers composing the infill.

- Simple leaf masonry. It's the simplest unit. Within the leaves composing a wall, a very important parameter will be how the blocks or bricks are arranged so that a proper interlocking is guaranteed.
- Double leaf masonry. Leaves are joined by a mortar layer and some ties, which could be masonry blocks in a perpendicular direction, or some metallic elements.
- Cavity wall. a wall consisting of two parallel single-leaf walls, effectively tied together with wall ties or bed joint reinforcement. The space between the leaves is left as a continuous cavity or filled or partially filled with non-loadbearing thermal insulating material. EC 6 establish a minimum of 2 ties each squared metre to consider that there's a connection among leaves.

Another important aspect is the classification and characterization of the materials used to make the masonry. Their properties will influence on the mechanical properties of the whole element.

- Blocks: clay (usually burned), calcium silicate, aggregate concrete, and autoclaved aerated concrete. Stone is also considered, even if its use is anecdotic for the type of walls considered in this thesis. The influence of the block typology is further detailed in FEMA 306-8.2. Their properties and its determination are regulated by UNE-EN-752.
- Mortar: It is necessary to define the binding material (cement, lime..), the proportions of water:sand:binder, and finally its class, according to the compressive strength (M2, M5...). Its properties will permit to classify it as general purpose mortar (joint thickness >3mm), thin layer mortar (joint thickness <3mm) and lightweight mortar. Determination of properties according to UNE-EN-1015.

Last mention is to the geometry of the blocks. It is important to define not only its dimensions (which can vary from small bricks to relatively big blocks of thermal clay), but another very important parameter as the percentage of perforation, its direction, and the thickness of the material webs and shells among them. This, according to EC6, allows to make a classification that is then used to determine the equations and correction factors used for each type:

- Group 1: Massive blocks or very little perforated, though this typology is more used in structural masonry. Figure 2, first row.
- Groups 2 and 3: Vertical perforations, in increasing percentage. Figure 2, second row.
- Group 4: Horizontal perforations. Being the cheapest and lightest and the ones with highest isolation properties, these are the most commonly used for masonry infills. Figure 2, third row.
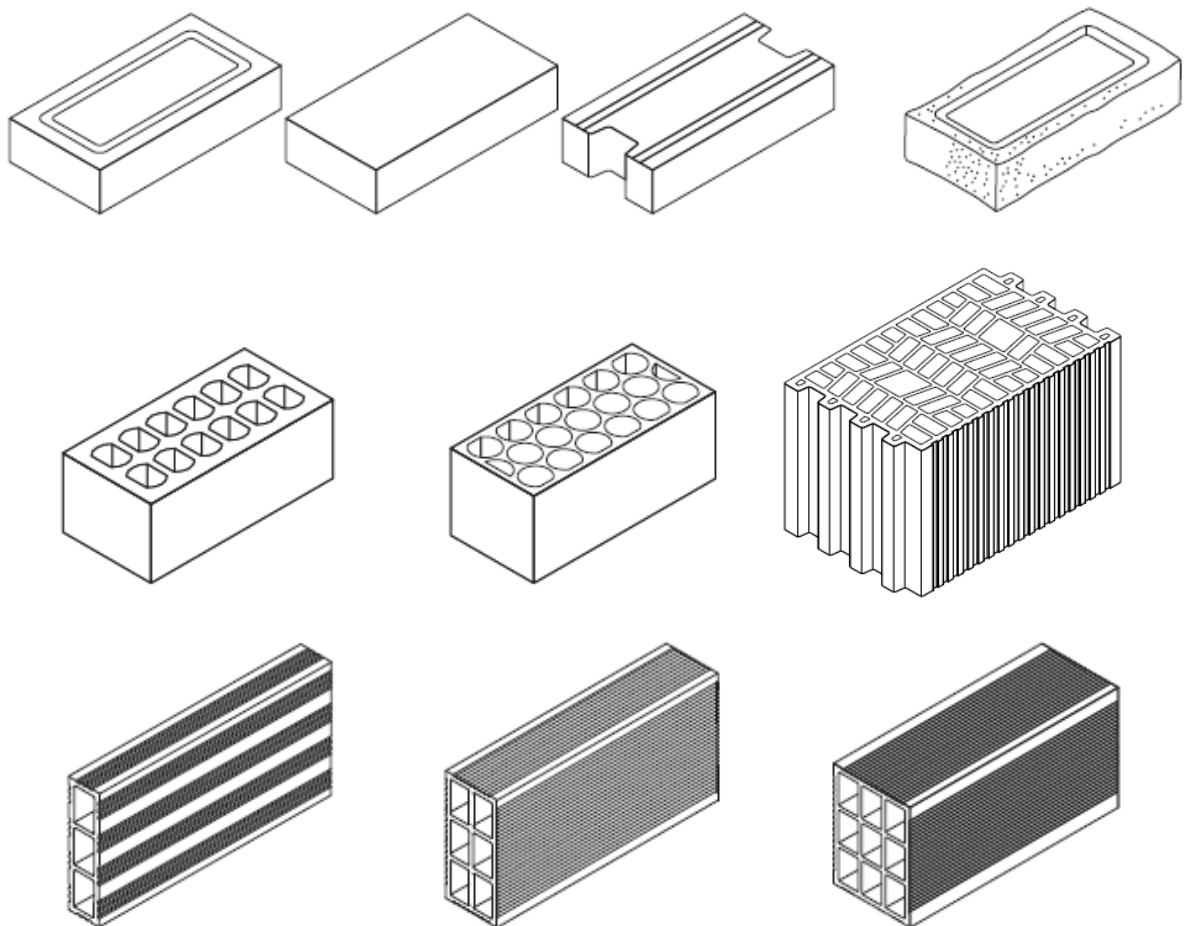
Figure 2. Most usual block typologies, according to the percentage of voids and the necessity of rendering. [10]

2.1.3. Mechanical characterization of existing masonry.

Besides characterizing the masonry by its material quality and composition, there must be an assessment on its quantitative properties, so that this values can be compared with the requirements according to the expected seismic action and thus stating whether reinforcement is necessary.

For existing masonry, this implies testing an statistically relevant number of samples in order to get significant values. The number of samples or tests depends on the size of the building, the area covered by the masonry infills, etc. A more exhaustive description of the minimum number of tests can be found in FEMA 273. The tests can be carried out in different ways.

- Destructive tests: extraction of samples. The experimental determination of mechanical properties of masonry samples should be done according to UNE-EN-1052. The samples can be tested as extracted, or if the conditions are not good, they can be rebuilt from the materials extracted.
- Minor-destructive in situ tests such as double Flat-jacks (for compressive strength and elastic modulus), bond-wrench method (flexural tensile strength), shear tests (Shear strength) or equivalents.

American codes and guidelines such as FEMA 273 introduce the concept of knowledge factor, κ, in which the properties of the elements are reduced if there is uncertainty about its values.

The full characterization of existing infill masonries, as for any other masonry, implies the determination of the following parameters:

- The compressive strength, f_k
- The shear strength, f_v
- The flexural strength, f_x
- The stress-strain relationship, σ-ε.

In addition to mechanical characteristics specified by EC 6, the following mechanical properties of masonry and masonry elements are also needed for numerical verification:

- The tensile strength, f_t, as an equivalent to shear strength, f_v.
- The modulus of elasticity, E.
- The shear modulus, G
- The ductility factor (indicator), μ, which is a typical mechanical property of a masonry wall and cannot be attributed to the masonry alone.

Otherwise, in case that this data is not available, the values can be estimated according to the nominal properties of blocks and mortar, and according to the group classification of masonry blocks. From this properties, EC6 proposes an estimation of the normalised compressive strength, and from there, estimations of the other characteristic values. Nonetheless, this estimations are very approximated

and according to Tomazevic [7], they can be either very conservative or even non conservative depending on the type of brick.

This testing is valid for non-damaged masonry, as the parameters define the linear behaviour of masonry. Once the masonry is cracked, damages have surpassed this elastic behaviour and thus mechanical characterization becomes more complex and depending on many more parametres.

In FEMA 306 [11] the effect of damage is considered for the calculation through a series of reducing factors applied to the characteristics of the walls: stiffness reduction factors (λ_K), strength reduction factor (λ_Q) and a displacement reduction factor (λ_D). This factors are deduced according both to tests and to a somehow subjective classification of the damage.

2.2. Behaviour of masonry infills under seismic action.

2.2.1. Influence of infill walls in the general structural behaviour under seismic actions.

Systematic calculation of structures by mathematical methods and models were developed parallel to the success of reinforced concrete skeleton structures. Previously, the dimension and design of masonry wall structures was more a matter of constructive practice and tradition, including the seismic-positive detailing and position of the walls. Since the development of skeleton structures released the walls of a structural performance, they were no more considered as a resistant part of it, but just as a load. This is often seen as an inaccurate but safe consideration.

For the behaviour under vertical loads, this is partly true, and not considering their effect in the transmission of actions to the soil can be just a conservative approach, as any increase in stiffness results in a better behaviour facing deflections.

For horizontal actions such as earthquake or even wind, nonetheless, this is only partly true. Two main factors are ignored if the infills and partitions are not taken into account for the modeling of the structure under this actions:

- The very high in-plane stiffness of walls, that can help to reduce the large deformations of the structure and therefore the efforts on the nodes.

- The capacity of energy dissipation due to the cracking of walls, that releases the main RC structure of a part of the effects of the earthquake.

Kappos [12] found that taking into account the infill in the analysis resulted in an increase in stiffness as much as 440%, and at the serviceability level over 95% of the energy dissipation is taking place in the infill walls after their cracking. Therefore, a properly designed and executed constructive solution of masonry infills can be considered the first line of defence of the structure against earthquake actions.

Some investigations and experimental work comparing the resistance of frames with and without infill show the positive effect of the infill for in-plane loads [13].

This way, normally the masonry infills have a positive effect on skeleton structures, as they provide them of resisting parametres that in bare structures should be carried by the joints. This way, enhancing the behaviour of the infill can have a effect of retrofitting the whole structure, given the positive effect of the masonry. The enhancement should be designed carefully, attending to the state of the walls to be reinforced and their distribution. Some studies have carried out this strengthening and analyzed its effects using FRP materials [14].

Nonetheless, the main risk of the infill walls within RC structures are local failures due to discontinuities on the stiffness of the main structure, that lead to concentrations of stress in certain points that are likely to fail. The experience on previous seismic events point to three main types of problems:

- ROTATION OF STRUCTURE. Irregular distribution of the walls in plan. This creates an eccentricity of the stiffness of the structure that leads to a rotational effect. The rotation of the whole structure creates very large deformations in the columns situated farthest from the rotation centre.
- SHORT COLUMNS. Infill walls that are not continuous through all the height of the frame. This is very typical for some types of windows, This can lead to an effect called "short column". The parts of the column that are not within the infill, being more flexible, have to deform jointly with the larger columns that are not into infill. Being very short and stiff, this columns are very likely to fail, as they will be subjected to a high level of shear force which can lead to shear failure of the column.
- SOFT STOREY. Irregular distribution of stiffness along the height of the structure. A very common case is that of buildings in which the lower story has no partitions and the façade is not infilled due to commercial, parking or pedestrian use. This way, the story has the least stiff structure, and furthermore the accumulation of the forces from all the upper stores.

Many times, this local failure effects are caused because of the opening in the infills, as they represent unpredictable discontinuities. That's why the behaviour of infills with openings should be better analyzed not as an infill but just as a part of it, divided into sub-components as strong columns or piers of masonry attached to the RC elements. Among the possible interactions, important examples are the strong columns and piers inducing shear failure in the beams, or strong spandrel components reducing the ductility by causing short-column effects. This effect of openings was studied, among others, by Syrmakezis and Asteris [15].

Another important factor for considering the modeling is the nature of seismic loading. Vintzeleou and Tassios [16] found through experimental finding that the contribution of the infill wall to the frame

lateral stiffness is greatly reduced when the structure is subjected under reversed cyclic loading, as in real structures under earthquake conditions.

This problems can be solved through a proper architectural design of the distribution of the infills, that should avoid irregularities if the infills are supposed to work jointly with the structure under seismic actions. Those infills that are required architectonically but not structurally (or that induce to irregularities in plan or in height) should be structurally disconnected from the framed structure through joints, so that they offer no unexpected resistance (given that this resistance would lead to irregularities) when the structure is deforming under seismic actions.

Besides of the local effects and the general improvement of the resistance to lateral loads, some researches study the influence of masonry infills on the whole structure in terms of modification of the dynamic properties.

Kose [17], after modeling structures both with and without infills, concluded that the presence of infills lowers the fundamental period of a structure between 5 and 10%, and between 6 and 10% if they were acting as shear walls. This implies an underprediction of the fundamental period of this building type if the current codes are applied. The percentage of shear walls was the second most important parameter after the height of the building when calculating the fundamental period. The percentage of infill walls and the number of bays had almost the same effect on the fundamental period of the building models.

Madan and Shentivel [18] verified experimentally the effect of improvement of seismic behaviour of RC structures when infilled, as well as the weakening effect of the soft story created by discontinuity of the distribution of infills in the elevation.

2.2.2. Importance of the constructive detail and execution of the infills.

The main parametres that will define the seismic behaviour of infills will be the presence or absence of reinforcement (as bed-joint reinforcement, or in grouted cores), the specific connections with the frame and a correct tying of different wall leaves among them.

From the starting design phase, some factors such as the selection of a given type of brick or the slenderness of the element have to be carefully considered, since generally speaking, hollow bricks with a very high percentage of voids or with too thin shells, as well as very slender walls, are parametres that will lead to a very poor performance of the infill and probably to a brittle failure [1].

A poor control of the execution of the constructive element normally leads as well to a poorer performance of the walls, that could be due to a bad quality mortar or an inhomogeneous resistance of the infill, bad implementation of connection to the main structure, bad connection among wall leafs, or use of materials with imperfections.

But another very important factor is neglected many times. This is the selection of constructive details and the execution of the infills, that in many cases can increase the effect of seismic actions, specially for out of plane failure. This is specially important for the detailing of ties and the evaluation of brick resistance [1].

With the development of improvements regarding condensation and isolation of buildings, a very common practice was that of the thermal bridge correction using perforated bricks coating the structural elements. To get a uniform external surface, the façade infills are then displaced out from the border of the slabs or beams supporting them, as seen in Figure 3. This has been widely used, following the rule of supporting only 1/3 of the section of the wall in the structural element. Nonetheless, this solution was quite frequently bad executed, so it's not unusual to find infills with even less support. This leads to a big eccentricity of the infills, making overturn of the whole infill much more likely.

Other very important constructive element for the infills are the metallic connections to guarantee the union among frames and infills. Its influence was studied by Liauw [19], concluding that they have a very positive effect not only making that frame and infill work together and with higher stiffness, but also raising the strength of the ensemble and preventing the failure of the infill.
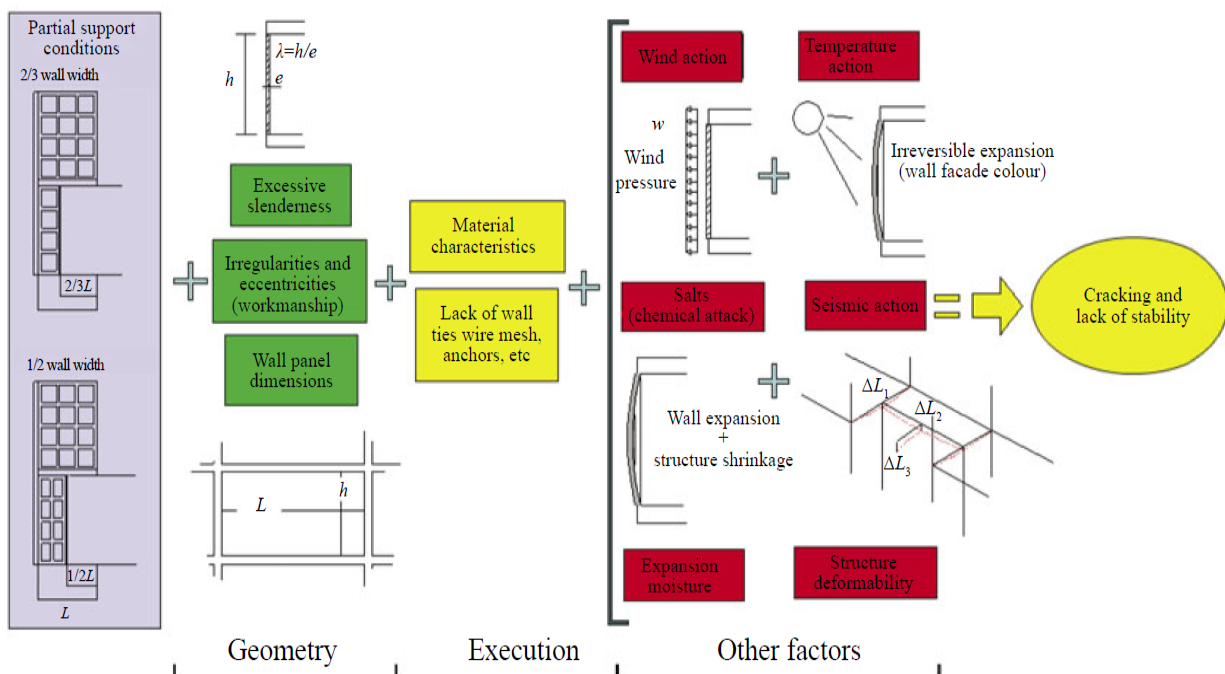
Figure 3. Design and construction parametres affecting the infill performance . [1]

2.4.   Estimation of the requirements according to EC8.

Last words in this chapter will be to review the code requirements for masonry infills. The estimation of the seismic action on the masonry infills depends mainly on three factors: the seismic risk, measured as the strongest earthquake expected for the region, as can be seen in Figure 4, the height of the infill, and the fundamental period of the main structure.

The most used method, due to its simplicity, is done as static-equivalent force. As it will be seen later, there are numerical and physical models that imply a more precise description of the elements. Nonetheless, this models are developed only for the wall infill locally. Thus, the effect of an earthquake in an infill wall, within a given structure, shall be calculated specifically through numerical and non-linear methods, and so far there is no systematic method as for RC structures.
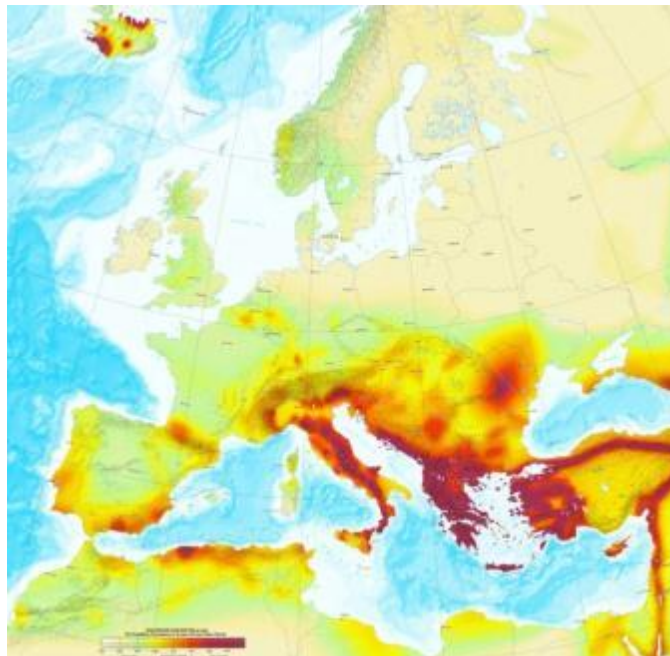
Figure 4. Seismic hazard in Europe, measured as expected peak ground acceleration with 10% of probability of excedence in 50 years (source: European Seismological Commission, 2003) Many of the seismic regions, such as the Mediterranean area, share common constructive practice.

The estimation of in-plane requirements for infill walls in a given structure is complicated to calculate under simplified rules, given that it is highly dependant on the deformation of the main structure, and the calculus of this will normally imply a numeric calculation of the RC structure with an estimation of the displacements in order to a further analysis of the effect on the infills.

The estimation of the out-of-plane requirements for infills can be determined as for nonstructural elements. Masonry infills are considered nonstructural elements if they are constructed after the hardening of the main structure, they are not connected to the main structure, and they are in contact with the main structure. The calculus is done considering the building as a single-degree-of-freedom

structure, and therefore does not consider effects of reduction or amplification of the ground vibration that can occur as a result of the filtering of the signal through the primary structure (i.e., the RC structure)

The effects of the seismic action may be determined by applying to the nonstructural element a horizontal force F. This methodology is used in many of the papers later analyzed.

$$F = \frac{S\ W\ \gamma}{q}$$

(Eq. 1)

where

F_a is the horizontal seismic force, acting at the centre of mass of the non-structural element in the most unfavourable direction;
W_a is the weight of the element;
S_a is the seismic coefficient applicable to non-structural elements, calculated according to the expression defined later;
γ_a is the importance factor of the element;
q_a is the behaviour factor of the element;
The seismic coefficient S_a may be calculated using the following expression:

$$Sa = \alpha S \frac{3(1 + z/H)}{(1 + (1 - Ta/T1)2) - 0,5}$$

(Eq. 2)

where

α is the ratio of the design ground acceleration on type A ground, ag, to the acceleration of gravity g (See map);
S is the soil factor;
T_a is the fundamental vibration period of the non-structural element;
T_1 is the fundamental vibration period of the building in the relevant direction;
z is the height of the non-structural element above the level of application of the seismic action (foundation or top of a rigid basement); and
H is the building height measured from the foundation or from the top of a rigid basement.
The value of the seismic coefficient Sa may not be taken less than αS.

Further specifications for the verification of the safety of this elements and general warnings about the negative effect of infills is provided in a specific section.

In American codes FEMA, some models are proposed that allow a better estimation of the effect for the in-plane action, both as a stiffener of the whole structure and as an action to be withstood by the infill.

Some modifications of the fundamental periods are proposed by Tomazevic [7], so that the influence of the infill in the whole system is taken into account.

Other approach is done by Menon and Magenes [20] [21], who develop a semi-analytical expression specifically for the out-of-plane demands to be applied to URM buildings, to take into account the filtering effect . Nonetheless, there could also be a further application to RC structures.

CHAPTER 3. EFFECT OF SEISMIC ACTIONS ON INFILL WALLS AND RETROFITTING TECHNIQUES: STATE OF THE ART

After exposing the general technical criteria for assessing the classification, state and requirements related to masonry infills, it will be exposed a short overview of the particular problematics, more closely related with the study object of this thesis. Many concepts are still unclear are until now days under research development.

First, it will be discussed how the seismic forces affect masonry infills in a qualitative way: damage patterns and degrees, individualization of different modes of damage and failure, and their particular relations with the properties of the masonry and its constitutive materials. This will be illustrated with examples from the last seismic events in Europe and how they affected this building typology.

For the quantification of this effects, there will be a short overview of the models developed for the calculation and prediction of the mechanical properties and the nonlinear behaviour of the composite frame-infill. Nonetheless, given the complexity of this topic, only general ideas will be discussed.

Then, a listing of the most frequent reinforcement techniques applied to this particular problematics, specially the ones that are going under research. There will be particular emphasis on the research about their advantages and disadvantages and, if available, comparison among different techniques.

Finally the topic of Textile Reinforced Mortars and their use for seismic retrofitting will be presented, with an outlining of the latest advances in the field.

3.1.   Effect of seismic actions on masonry walls: In plane action.

In-plane actions are quite well studied, given that this behaviour is related with the contribution of the infills to the seismic resistance and the composite frame-infill behaviour.

The behaviour of infills under this action is strongly connected with shear strength of the wall, along with the deformability of the frame supporting it. Since frame and infill are supposed to work as a composite element, the failure mechanism will depend mainly on the ratio or strength and stiffness of the wall and those of the frame. The most desirable situation is a relatively weak infill, given that the order of failure for the elements should be infill – beam – column. The relation of strength among mortar and brick will be the main parametre to define the expected mechanisms of failure within the infill.

The interaction infill-frame is another determinant parameter. At a low lateral load level, an infilled frame acts as a monolithic load resisting system. As the load increases and the first cracking appears, the infill tends to partially separate from the bounding frame and form a compression strut mechanism which may or may not evolve into a primary load-resistance mechanism of the structure, depending on the strength and stiffness properties of the infill with respect to those of the frame. [22] This model of behaviour is shown in Figure 5 and Figure 6.

A failure in which the infill can be a risk for human life is unlikely, as it is necessary a big deformation or buckling of the infill to provide a complete expulsion or overturning of the material out of the structure.
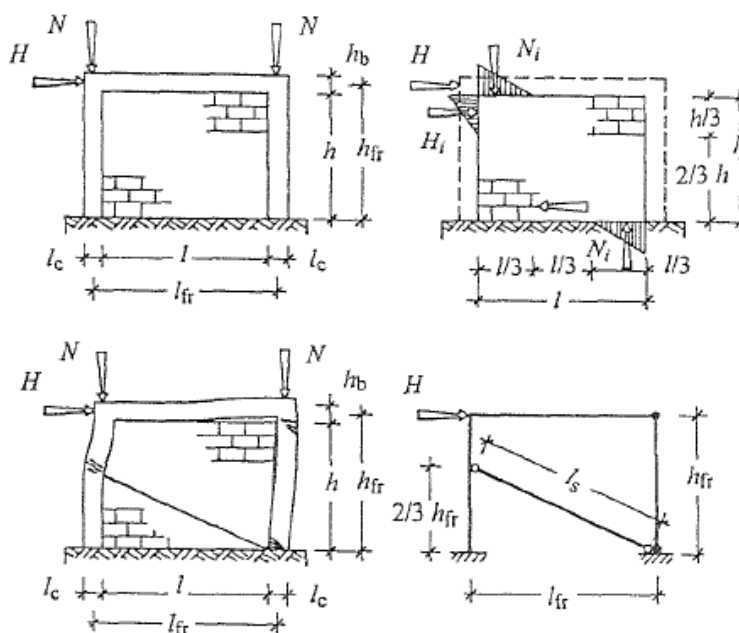
Figure 5. Modeling of seismic behaviour before and after detachment of masonry infill [7]

Under small deformations, the stiffness and behaviour are dominated by the panel stiffness characteristics such as the slenderness. As the deformation increases the panel characteristics will be a function of its element properties such as the mortar strength. Normally, the failure of the infill will occur as a combination (e.g. corner crushing and diagonal tension) of the individualized modes (will be discussed further in next pages) that can be seen in Figure 6:

- Corner crushing mode.
- Diagonal compression.
- Sliding shear.
- Diagonal cracking mode.
- Frame failure.

Other important aspect to consider is the presence of openings in the infill, as the failure will be strongly connected to their shape, size and position within the "diagonal strut". For this cases, the failure modes are much more complex, depending on multiple factors and with not-evident relation among them [22]. Some proposed models imply the calculation of multiple struts [23]. An experimental campaign to relate the crack pattern and the reduction of strength of the infill with the size and the position of the openings was carried out by Asteris [24], observing a very complex behaviour, different from the strut model (that will be explained in next subsections), and individualizing some patterns and failure modes related with very specific models of openings.
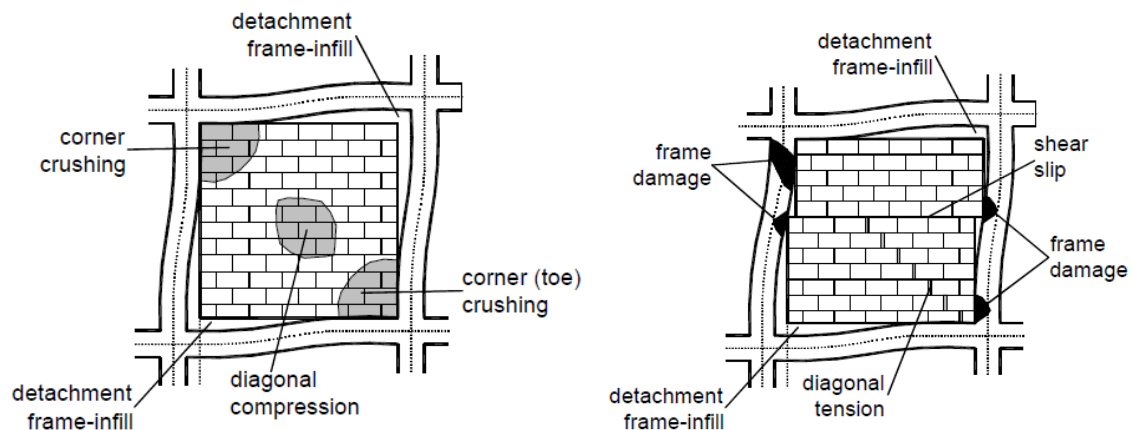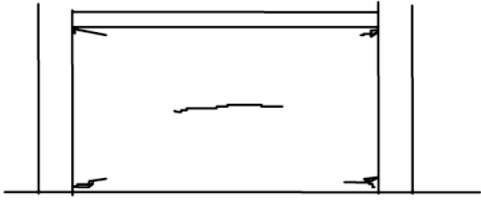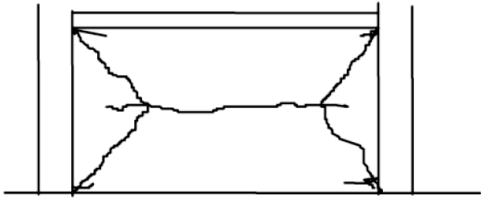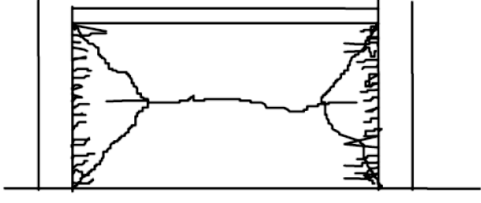
Figure 6. Modes of failure of infilled frames [24].
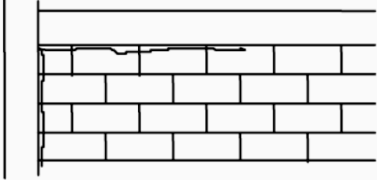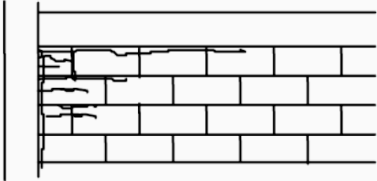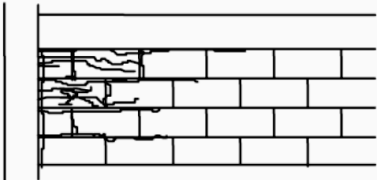
*Table **1**. Typical degree of damage for bed joint sliding [11]*

Severity	Description of Damage	Performance Restoration Measures
Insignificant $\lambda_K = 0.8$ $\lambda_Q = 0.9$ $\lambda_D = 0.9$	*Criteria:* Crushing of mortar around perimeter of frame. This is particularly noticeable adjacent to the columns near the corners of the infill panels. *Typical appearance:*	Repoint spalled mortar. Inject cracks.
Moderate $\lambda_K = 0.5$ $\lambda_Q = 0.8$ $\lambda_D = 0.8$	*Criteria:* Crushing of mortar and cracking of bricks extend over larger zones adjacent to beam and column *Typical appearance:*.	Remove damaged bricks and replace.
Heavy $\lambda_K = 0.4$ $\lambda_Q = 0.7$ $\lambda_D = 0.7$	*Criteria:* Significant crushing of mortar and bricks extends around most of the perimeter frame, particularly along the height of the column. *Typical appearance:*	Remove and replace infill, or patch spalls. Apply shotcrete, ferrocement or composite overlay on infill.

Sliding shear.- This mode is associated with infill of weak mortar joints and a strong frame. In this case, infill panels crack along the bed joints instead of along the diagonal, creating, horizontal cracks that might occur across several bed joints as an assembly of units slides to accommodate the deflected shape of the frame. Might imply damage in the frame due to short column effect and is therefore highly undesirable. In this situation, plastic hinges can form at the mid-height of the frame. For reinforced concrete frames, the columns will have a high tendency to develop shear failure.
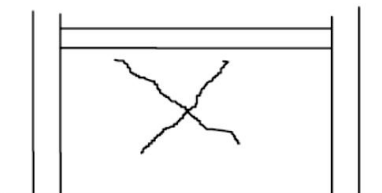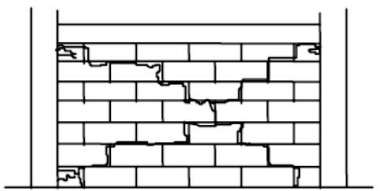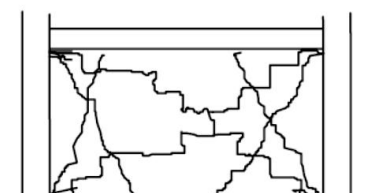
Another mode of failure related to this mode is characterized by the sliding of multiple bed-joints in the masonry infill. Very often, this occurs in infills with weak mortar joints, and can result in a fairly ductile behaviour, provided that the brittle shear failure of the columns can be avoided. [22]

*Table **2**. Typical degree of damage for corner crushing [11]*

Severity	Description of Damage	Performance Restoration Measures
Insignificant $\lambda_K = 0.9$ $\lambda_Q = 0.9$ $\lambda_D = 1.0$	*Criteria:* Separation of mortar around perimeter of panel and some crushing or mortar near corners of infill panel *Typical Appearance:.*	• Repoint spalled mortar. • Inject cracks.
Moderate $\lambda_K = 0.6$ $\lambda_Q = 0.8$ $\lambda_D = 0.8$	*Criteria:* Crushing of mortar, cracking of blocks including lateral movement of face shells. *Typical Appearance:*	• Remove and replace damaged units. • Inject cracks around perimeter of infill. • Apply composite overlay at damaged corners.
Heavy $\lambda_K = 0.5$ $\lambda_Q = 0.7$ $\lambda_D = 0.7$	*Criteria:* Loss of corner blocks through complete spalling of face shells. Diagonal (stairstep) cracking and/or bed joint sliding may also be evident. *Typical Appearance:*	• Remove and replace infill or apply composite overlay on infill.
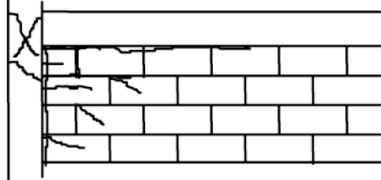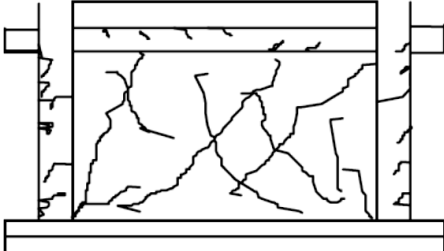
Corner crushing.- This mode is usually associated with in-filled frames consisting of a weak masonry infill panel surrounded by a frame with weak joints and strong members. [24]

Table 3. Typical degree of damage for diagonal tension cracking [11]

Severity	Description of Damage	Performance Restoration Measures
Insignificant $\lambda_K = 0.7$ $\lambda_Q = 0.9$ $\lambda_D = 1.0$	*Criteria:* Initial hairline cracking occur on diagonals in masonry. This is mostly associated with breaking of the bond between mortar and bricks. Cracking mostly concentrated within center region of panel *Typical appearance:*.	Measures not necessary for structural performance restoration. (Certain measures may be necessary for the restoration of nonstructural characteristics).
Moderate $\lambda_K = 0.4$ $\lambda_Q = 0.8$ $\lambda_D = 0.9$	*Criteria:* Hairline cracks fully extend along diagonals following the mortar courses in a stairstep fashion, but sometimes propagate through bricks. Some crushing and/or "walking-out" of the mortar may be observed. Cracks mostly closed due to confinement provided by frames. *Typical appearance*	Repoint spalled mortar. Remove and replace damaged masonry units.
Heavy $\lambda_K = 0.2$ $\lambda_Q = 0.5$ $\lambda_D = 0.8$	*Criteria:* Cracks widen to about 1/8", and are usually associated with corner crushing. Much loss of mortar is evident. More than one diagonal crack is generally evident. Crushing/cracking of the bricks is also evident. Portions of the entire infill may "walk" out-of-plane under cyclic loading. *Typical appearance:*	Remove and replace damaged infill, or patch spalls. Apply shotcrete, ferrocement or composite overlay.

Diagonal tension cracking.- This mode is associated with a weak frame or a frame with weak joints and strong members in-filled with a rather strong infill. When the masonry units are strong relative to the mortar, diagonal tension will result in a stair-stepped pattern of cracks through head and bed joints. When the mortar is stronger than the units (which is rare), cracks will develop through the units as well as the mortar and follow a line normal to the direction of the principal stress. With the stair-stepped cracks, shear can continue to be resisted after cracking by the development of a compressive stress normal to the bed joints, characterized as a compression strut.

Table 4. Typical degree of damage for corner crushing and diagonal cracking [11]

Severity	Description of Damage	Performance Restoration Measures
Insignificant $\lambda_K = 0.9$ $\lambda_Q = 1.0$ $\lambda_D = 1.0$	*Criteria:* Separation of mortar around frame occurs first in beam-to-infill interface. Some hairline cracks may be evident along mortar courses.	Repoint spalled mortar. Inject cracks.
Moderate $\lambda_K = 0.6$ $\lambda_Q = 0.8$ $\lambda_D = 0.8$	*Criteria:* For a ductile (strong column-weak beam) frame design, yielding of longitudinal reinforcement occurs first in beam, with minor cracking in columns. Compression splitting occurs in corner blocks. Some hairline X cracks may be expected in beam-column joint *Typical appearance:.* 	Remove and replace damaged masonry units. Inject cracks.
Heavy $\lambda_K = 0.5$ $\lambda_Q = 0.6$ $\lambda_D = 0.6$	*Criteria:* Extensive cracking in beam and column hinge zones, leading to spalling of cover concrete in frame. Diagonal cracking passes through blocks. Faceshells spall off in corners, and also across a critical shear plane at mid-height of infill *Typical appearance:.* 	Remove and replace infill. Remove and patch spalled and loose concrete in frame. Inject cracks.

Diagonal compression.- This mode is associated with a relatively slender infill, where failure results from out-of-plane buckling of the infill. The cracks propagate from one loaded corner to the other; and these can sometimes be jointed by a horizontal crack at mid-height. In this case, the infill can develop a diagonal strut mechanism that can eventually lead to corner crushing and plastic hinges or shear failure in the frame members.

3.3.   Effect of seismic actions on masonry walls: Out of plane action.

While in-plane actions account for a high percentage of the damage, out of plane actions are the major cause for casualties related with failing of infill walls, given that it is related to overturning and failing of heavy constructive elements.

The two main factors to define the infill behaviour will be its flexural strength (and also connected to its slenderness) and the connection to the main structure. In this case, the structure and the infill will not work that much as a composite structure, and the failing of the wall is regarded more as a local failure, mostly related to overturning and loss of equilibrium, or in case of damage, to big displacements. [7]

A masonry panel restrained by a bounding frame can develop a significant out-of-plane resistance due to the formation of an arching mechanism, as seen in Figure 7. The resistance provided by the arching mechanism depends on the height-to-thickness (slenderness) ratio of the infill and the compressive strength of masonry, and of course on the restraining effect of the frame. Previous earthquake damage, causing diagonal tensile cracking or slight detachment from the frame, weakens the strength of the infill to out-of plane actions [22]. [25].

In out-of-plane tests, the development of cracks is normally characterized by a precocious cracking of mortar joints and development of membrane stresses, showed by cracks dividing the panels in separate segments. As the forces are increased, this segments move out of the wall plane, sliding from the columns faces, and developing the characteristic arcs, until the final failure of the wall panel [26].

Latest research is oriented on investigation on the parametres of the main structure affecting the out of plane action affecting the infill, such as amplification of the vibrations caused by the natural frequencies of the structure [20].
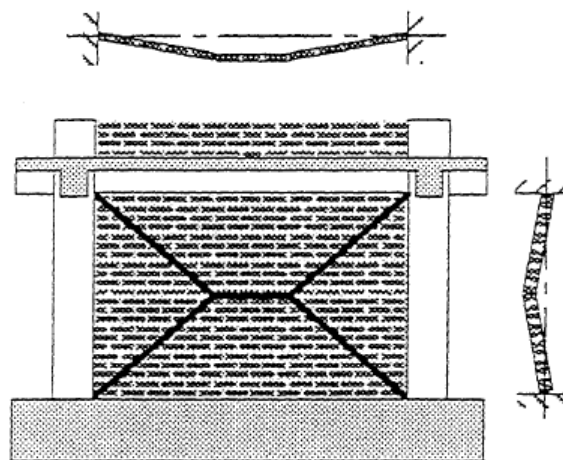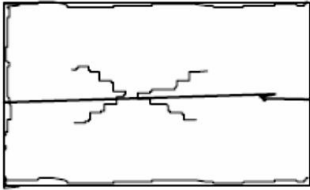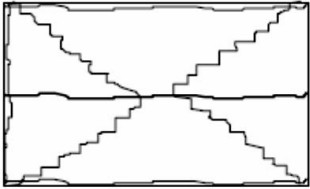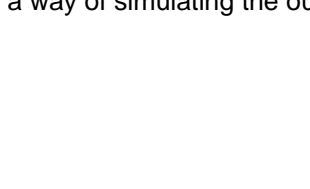
Figure 7. Typical crack pattern and dislocation for out of plane actions [25]

Table 5. Typical degree of damage caused by out-of-plane actions [11]

Severity	Description of Damage	Performance Restoration Measures
Insignificant $\lambda_K = 0.9$ $\lambda_Q = 1.0$ $\lambda_D = 1.0$	*Criteria:* Flexural cracking in the mortar beds around the perimeter, with hairline cracking in mortar bed at mid-height of panel.	Repoint spalled mortar.
Moderate $\lambda_K = 0.9$ $\lambda_Q = 0.8$ $\lambda_D = 1.0$	*Criteria:* Crushing and loss of mortar along top, mid-height, bottom and side mortar beds. Possibly some in-plane damage, as evidenced by hair-line X-cracks in the central panel area. *Typical appearance:* 	Apply shotcrete, ferrocement, or composite overlay to the infill.
Heavy $\lambda_K = 0.5$ $\lambda_Q = 0.6$ $\lambda_D = 0.9$	*Criteria:* Severe corner-to-corner cracking with some out-of-plane dislodgment of masonry. Top, bottom and mid-height mortar bed is completely crushed and/or missing. There is some out-of-plane dislodgment of masonry. Concurrent in-plane damage should also be expected, as evidenced by extensive X-cracking. *Typical appearance:* 	Remove and replace infill.

In Table **5** it is visible how the damage of the infill overcomes as bidirectional flexural damage. Due to the anisometric properties of masonry, the damage occurs first on the direction in which it has less flexural strength, this is, with bending perpendicular to the bed joints.

The damage pattern can also be associated with that of punching, and some experimental campaigns have taken this testing as a way of simulating the out of plane performance of masonry [27].

3.4. Examples in last European earthquakes. Lorca, L'Aquila.

Following the theoretical examples, describing and showing pure failure mechanisms, degrees of damage, etc., some real examples will be shown. The images of damaged buildings have been selected from the typology studied in this project.

Figure 8. Typical diagonal in-plane cracking of infills [28] L'Aquila.

Figure 9. Out-of plane failure, overturning of the external leave or the whole infill [28]. L'Aquila.

Figure 10. Failing of the exterior leaf due to improper connection [1] L'Aquila.

Figure 11. Out of plane damage in several degrees: from diagonal-central cracking to complete overturning and expulsion of infills [28] L'Aquila.

Figure 12. mix of in-plane and out-of-plane actions in a free corner [29] Lorca.
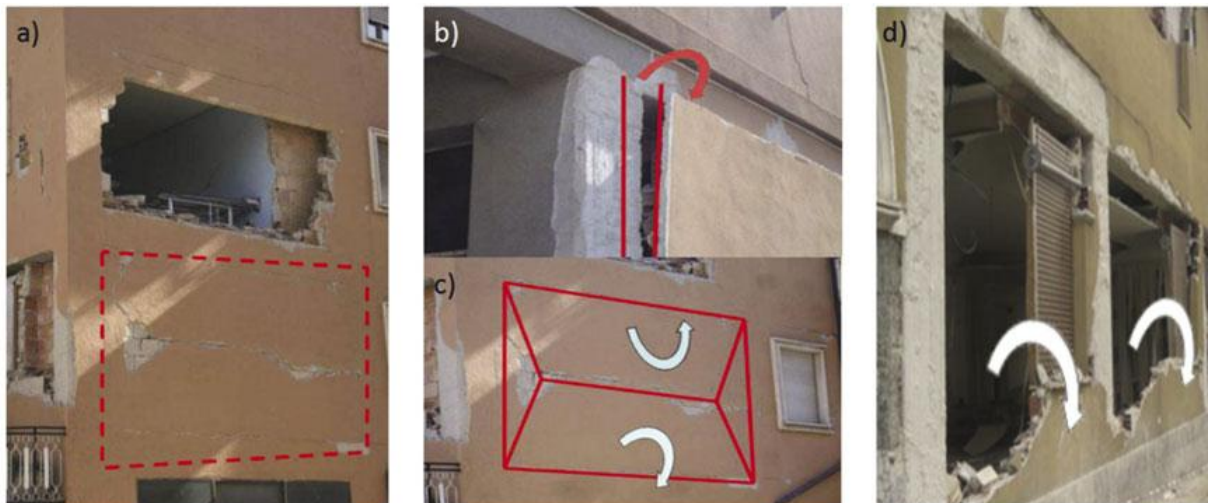
Figure 13. (a) Out of plane collapse of infill walls;(b) Wall panel rotation; (c) Horizontal hinge formation; (d) Total collapse of the single leaf wall [1] L' Aquila.
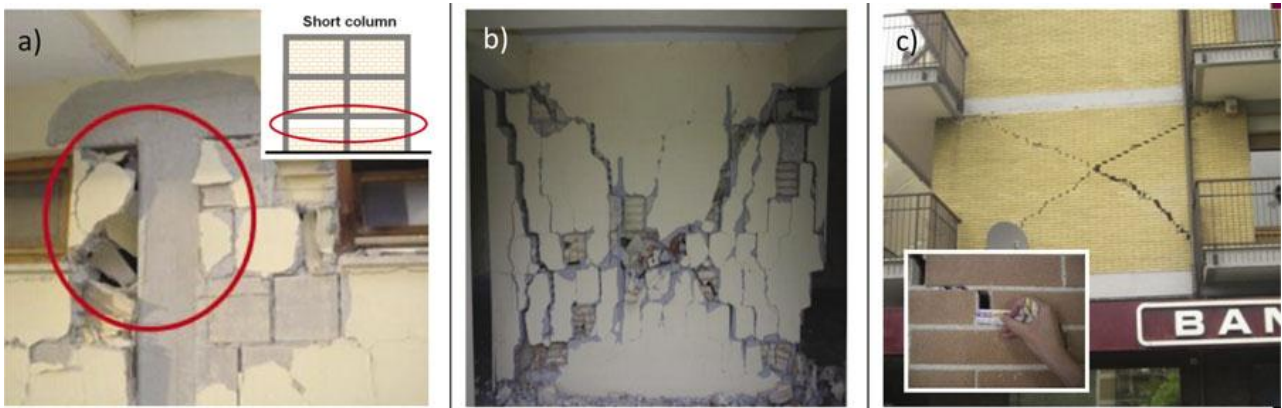
Figure 14. (a) Short column and corner crushing of the infill; (b) In–plane cracking and crushing of masonry wall (c) Horizontal bed joint sliding [1] L'Aquila.

Figure 15. L'Aquila. [30]

Figure 16. L'Aquila. [30]

3.5. Modeling of infill walls.

The physical and mathematical modeling of infill walls has proved to be a very complex issue. This is due mainly to the complexity of both the element (composed material subjected to shear and bonding) and the difficulty to determine the nature of the connection among the infill and the principal structure.

Several approaches have been tried in order to describe and predict their behaviour. Among them, limit analysis methods that account for a variety of possible failure modes seem to be the most promising approach. Nonetheless, they need to be further refined and extensively validated in a systematic manner before they could be used in a building-code approach. Sophisticated finite element models have also been developed to analyse infilled structures. While these models are general and widely applicable to different infilled frames, they should be used with caution because they could be easily misused due to the high degree of idealization, and lead to unconservative results. [23]

3.5.1. Numerical approaches.

3.5.1.1. In-plane behaviour.

This models have been developing since the early 60's (Stafford Smith), and the most developed model has been the strut analogy, that idealizes the infill as a compression element reinforcing the frame for its shear deformations. In the equivalent strut idealization, the infilled frame is viewed as a frame braced by a compression diagonal as seen in Figure 17. The equivalent strut idealization of the infilled frame can be justified as follows: After the first deformation of the infilled frame, infill and frame are separated due to the developing of tensile stresses in the interface mortar. Therefore, contact is maintained only at opposite corners, at the ends of a compression diagonal that forms through the infill panel, as explained in Figure 6.

Most remarkable models were the one developed by Wood, in 1978 and Liauw in the late 80s. Although these methods of analysis have shown to be reasonably successful in predicting the strength capacity of infilled-frame systems, its roots are in elasticity or rigid plasticity, making it either difficult or impossible to extend the findings to inelastic (elasto-plastic) behaviour, especially if cyclic loading is to be considered [31] [32].

The equivalent-strut method of analysis has become the most popular approach for analyzing infilled frame systems. Some codes such as FEMA 273 [23] includes formulation in this model to estimate the stiffness and shear strength of the elements, as well as the deformation acceptance criteria.

The formulation given to state the width of the masonry strut to be considered as resisting element depends on the state of the infill, and as well on the author. [7] [25] [24] [12] [19]

Another interesting study was done by Shing and Mehrabi [22], who studied the different possible failure mechanisms for masonry infills within equilibrium kinematics.

In spite of the general success of modeling infilled frames with solid panels, major difficulties still remain unresolved regarding the modeling approach for infilled frames with openings. Such frames, in practice, are commonplace and are perhaps the norm rather than the exception. [24]
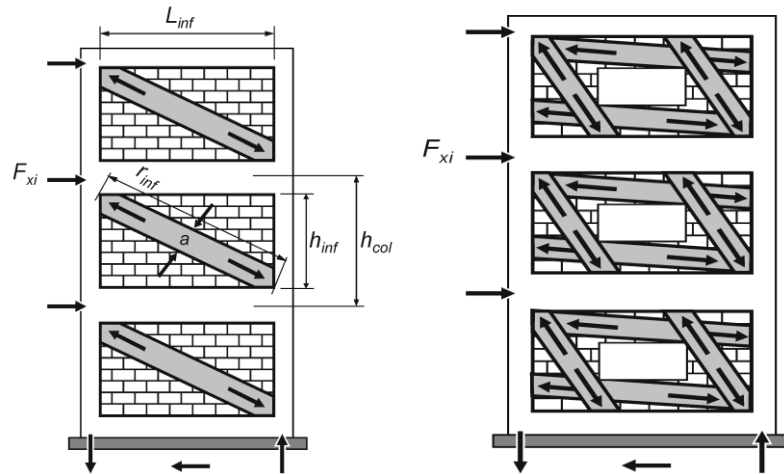
Figure 17. Strut analogy [33]

3.5.1.2. Out-of-plane behaviour.

The local failure of the infills is caused mainly by out-of-plane actions. The most usual models rely on the arching action of the masonry. Masonry infills have been observed to withstand much larger lateral loads than would be predicted on the basis of conventional bending analysis. Experimental work has shown that fixed-end brick beams have 3 to 6 times the load-carrying capacity of simply supported beams, due to arching action [32] [25]. Nonetheless, for the consideration of this arching effect, it is needed a thorough characterization of the stress-strain properties of the masonry in compression. Specific formulation and examples of calculation of the maximum estimated load can be found in publications by Angel [25].

The recent Italian building standards [NTC, 2008 and Circolare Applicativa, 2008] recommend verification of local collapse mechanisms in existing URM buildings through limit equilibrium analysis based on rigid body kinematics, as depicted in Figure 18. This implies stating that the failure is more likely to happen due to loss of equilibrium than due to extended failure of the material. Safety check for the ultimate limit state is fulfilled if the ultimate displacement capacity of the local mechanism of a masonry portion is greater than the demand.
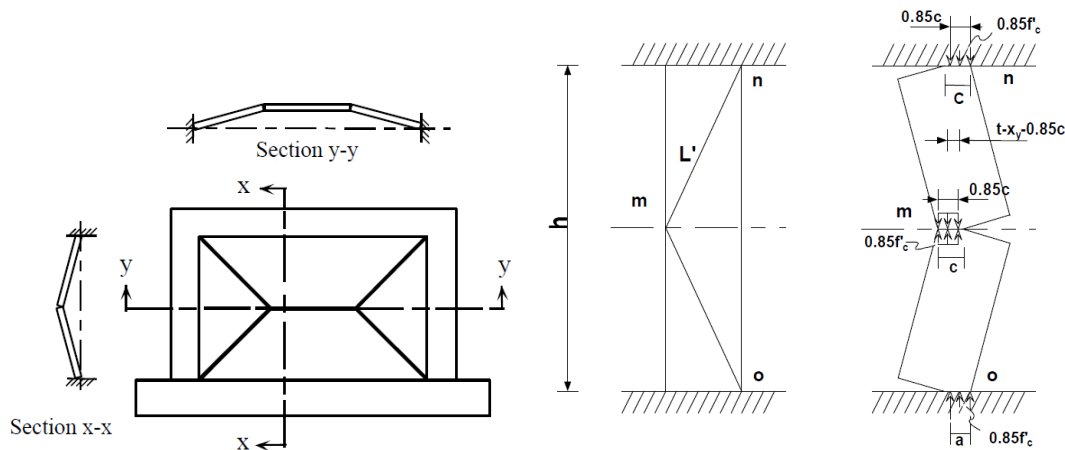
Figure 18. Limit equilibrium analysis in out-of plane failure of masonry infills [32]

3.5.2. FEM.

Computer-modeling of masonry infilled steel or concrete frames is complicated due to a series of parametres defining both material and interfaces which idealization is not clear. This increases the already complicated models currently under research for masonry. Examples of this are: the nonlinearity of the masonry material, the existence of the mortar joint planes of weakness, the masonry block geometry, cracking and crushing of the infill wall, nonlinear frame behaviour and relative movement along the frame-wall interface. This latter effect is a highly nonlinear contact problem existing because of the typical construction practice of not creating any positive connection between the infill wall and the surrounding frame. Factors affecting the contact behaviour include: coefficient of friction, cohesion, maximum shear stress developed at the interface and normal and shear contact stiffness. [34]

In literature, it's found that two approaches have been employed to model the masonry, depending on how the composition of the masonry is treated:

- Homogeneous models or macro-element models developed either directly from masonry models or via homogenization techniques. The infill is substituted by an element that has the same ideal properties than the whole panel. They are useful mostly to assess the effect of panels in the whole structures. The use of strut analogy in RC structures is within this case.

- Heterogeneous models or micro-elements models, where the individual units and mortar joints are modeled separately. They are based on the finite element method which generally utilize 3 types of elements for providing the masonry infill wall, frame and the interaction between them. In most cases, special attention has been focused on the contacting elements between frame and masonry infill walls. This models are more appropriate to study local effects of the actions within the masonry.

Interesting examples of modeling and the obtained results can be found in:

El-Dakhakhni [34] used the numeric modeling for a parametrical study on the effect of openings in infill walls, using parametres as Drucker-Prager failure criterion, with a yield surface that does not change with progressive yielding.

Some studies [35] have been also done trying to match the experimental and the FEM results for cyclic loading on infilled frames of two bays, with good accuracy of the obtained results by both methods.

Chidiac and others [36] used FEM to simulate the out-of-plane actions on masonry walls, stating the importance of a correct geometrical definition of the blocks, including the hollows.

3.6. Analysis of the retrofitting schemes used for masonry infill walls.

Seismic retrofit is the range of actions and interventions carried out on structures or nonstructural elements before damage, or in cases of slight damage, in order to improve their behaviour to face a potential earthquake event. For an important part of the contemporary housing stock, and specially for the one built before the development of specific seismic building codes, this is an important action to be fulfilled, since the infills were not designed to withstand any horizontal action.

Retrofitting of the infills normally aims three purposes: increasing the strength, specially to shear (in-plane actions) and bending (out-of plane actions), increasing the stiffness (in order to avoid damage that result on economical losses), and increasing the deformation capacity (mostly in order to avoid full failure and falling of heavy pieces). The choose on a specific technique shall depend on a careful balance of its benefits (increase in stiffness or strength or deformability or a combination of them) and its disadvantages (cost, modification of structural behaviour, architectonical concerns...) [37].

Besides, proper connections among structure and infills can modify decisively their behaviour, in an even more evident way for out-of-plane behaviour.

The result of retrofitting, along with an improvement of the behaviour of the infill itself, can be also an improvement of the behaviour of the whole structure, given the contribution of the infills to stiffen the structure and to dissipate energy once cracked.

Given the characteristics of masonry infills, the techniques conventionally used for unreinforced masonry are not completely applicable. The most usual typology of construction of infills is walls built into the structure, forming discontinuous panels. Furthermore, they are very usually composed by two layers separated by an air gap and isolation materials. This implies that affordable and feasible reinforcement techniques are limited to the ones that can be applied externally, and moreover, only on the external side since the internal is not always accessible without major destruction of the façades.

This way, some techniques such as coring, bed-joint reinforcement or grouting, very used and providing satisfactory results for structural masonry walls [37], are not to be considered as possible solutions for infills.

In the next pages, some of the most used retrofitting techniques used will be discussed and, when possible, compared, according to previous research.

3.6.1. Steel fiber composite concrete shot.

This technique, compared to other methods, can result more economical, due to the simplicity of the materials, and quicker in its application, specially for large surfaces. Some research was done comparing this solution to other cementitious composite overlays and with ferrocement [27]. Among the conclusions, it is remarkable:

- Most frequent failure mode is pullout of the fibres, due to lower bonding relatively to other techniques.
- Good behaviour under distributed load conditions.
- Significant enhancement of both maximum load and deflection when compared to unreinforced walls. Nonetheless, the results are much lower than the ones with steel mesh.

3.6.2. Steel meshes.

This is the oldest type of reinforcement, consisting on quite widespread and economic materials. Among its disadvantages, the problems on durability if applied in normal thickness render layers.

Manuel Pereira [38] compared samples of masonry infill walls non-reinforced, with steel bed-joint reinforcement and with steel mesh reinforcement. His conclusions is that, among this three, the ones with steel meshes show the highest values of strength and highest deformation capacity.

Research by Rupika compared steel, polypropylene and glass fibre meshes [39]. Steel meshes raise highly the strength, but not so much the deformability. ferrocement overlays were further able to provide the same stiffness to the wall until it reaches the ultimate load without any intermediate drops in load and with controlled crack width opening. On the other hand, when compared to other solutions, the increase of deforming capacity is low, and the failure tends to be brittle.

In the same research it is stated that the same values of strengthening and of energy dissipation are achievable with glass fibre meshes, but only when including very large amounts of reinforcing material.

3.6.3. Polymeric grids.

Based on very economical materials, this kind of reinforcement was studied for widespread retrofitting in developing countries. Its disadvantages are linked to the material, such as low resistance and not very well studied durability.

Research by Sofronie [40] focuses on the high deformability capability, and therefore its good performance for increasing ductility and even safety. On the other hand, damage of the constructive element is not avoided. It is recommended for retrofitting schemes comprising whole buildings, as means of tying.

In the previously mentioned research by Rupika [39] comparing to fibreglass or steel meshes, it is evident its very low strengthening capacity. Even very large reinforcement ratios did not contribute to increase the wall strength prior to compressive failure of the walls due to the very low stiffness of the material. However, the observed results showed that although specimens failed in flexural compression, polypropylene mesh was able to safely contain failed wall specimens without dropping dangerously.

3.6.4. Bed joint reinforcement.

This technique is only applicable for new masonry, given that the inclusion of proper bed-joint reinforcement in already existing panels would imply a large amount of work that makes it difficultly feasible. Nonetheless, lightly reinforced masonry is an economic and promising technique for new masonry.

Research by Penna, Calvi and Bolognini [41] show the increment of lateral strength and displacement capacity, as well as energy dissipation, of horizontally reinforced in-fill panels. The comparison with other reinforcement techniques shows relevant advantages:

- Truss reinforcement improve the structural effectiveness of bed joint reinforcement both reducing anchoring lengths and allowing the transversal connection of double veneer walls.
- The presence of even slight horizontal reinforcement is very effective in cracking control.
- Masonry spandrel beams and lintels can be easily built using bed joint reinforcements which provide flexural strength;
- Beneficial effects on the frame structural response.

In research by Pereira [38], it is stated that this type of reinforcement don't add any flexural strength in the direction perpendicular to them, as was expected. Nonetheless, the increasing in flexural strength in the direction perpendicular to bed joints that is lower than the one corresponding to the walls reinforced with steel mesh overlay, but all the same increases the flexural strength in 250%, and provides a very high deformation capacity.

3.6.5. Near surface mounted reinforcing bars.

This technique is widely used in masonry, and it can be interesting for masonry infills with exposed brickwork. In this technique, the reinforcement is inserted in slots within the bed joints, in case of unidirectional reinforcement, and also in slots implying both head joints and brickwork in the case of bidirectional reinforcement. Among its advantages, low technology and little workmanship required, no visual impact, and good protection of the reinforcement material due to its position within a mortar element. This technique is particularly interesting, given that a further application of the materials developed for this thesis (in their version of single rods instead of woven meshes) could be using this technique.

Turco and others studied the use of NSM circular and rectangular FRP bars for flexural and shear reinforcement, embedding them both in latex-modified cementitious matrix and in an epoxy-based matrix [42]. Among their main conclusions:

- Big increase in flexural strength and pseudo ductility, with an increased capacity of up to 2.5 times for shear and from 4.5 to 26 times in the case of flexural strength.
- Good performance of glass FRP in spite of its low elastic modulus.

- Low bond in sand-coated FRP bars + cementitious matrix or in smooth FRP bars + epoxy matrix. Higher bond with rectangular bars.
- Better performance of low bond systems for shear strengthening, as sliding provides a better redistribution of stresses.
- Similarity of results for epoxy and cementitious matrixes.

Galati, Tumialan and Nanni made a parametrical study [43], in which it was analyzed the influence of the bar shape (i.e., circular vs. rectangular), FRP material, dimension of the groove and type of embedding material (i.e., epoxy or cementitious-based paste).

- Flexural capacity increased from 2 to 14 times, as well as strength and pseudo-ductility.
- Three modes of failure: Shear, debonding of reinforcement, and flexural failure by failure of reinforcement or crushing of masonry. For large amounts of reinforcement, shear was the controlling mode. For the rest, debonding was more frequent than pure flexural failure.
- Sliding of FRP bars imply higher ductility.

Ismail and Ingham used twisted metal bars in this technique for in-plane shear actions [44] studying the effectiveness of the reinforcing schemes to restrain the diagonal cracking failure, in vertical, horizontal and grid pattern. The analysis focused on earthquake-related parametres, including shear strength, drift capacity, pseudo-ductility, shear modulus and elastic modulus.

- The improvement in shear strength ranged from 114% to 189% except for specimens strengthened using a horizontal pattern.
- The horizontal reinforcement scheme was effective in bridging diagonal cracks which formed close to peak load, and allowed the wallets to deform further until ultimate failure occurred.
- The vertical and grid reinforcement schemes performed the best in terms of increases in strength and displacement capacity.
- All strengthened wallets (except those that were strengthened using horizontal schemes) displayed ductile failure modes and continued to resist load at the completion of testing.

3.7. Use of textile reinforced mortar (TRM) as a retrofitting technique for masonry infill walls.

3.7.1. Textile reinforced mortar in structural reinforcements.

The development of textile materials starts with the development of high-performance fibres such as fiberglass (in the 30s) and carbon fibres (early 60s), developed for high tech industry such as the aeronautics.

Its application in the building industry as part of reinforcement of cement-based materials starts in the beginning of the 80s, and they were through a slow process of investigation until the late 90s [45].

The concept, as for steel-reinforced concrete, consists in the application of a material highly resistant to tensile stresses, embedded in a mortar matrix that acts as the bonding agent with the main structure to be reinforced. The advantages of fibres is their smaller diametre, and their higher strength, that makes this solution specially suitable for reinforcements of already existent elements. This materials consist on of long woven, knitted or even unwoven fiber yarns in at least two directions.

The most basic application is the fibre reinforced mortar, which consists in a mixture of mortar with a percentage of fibres randomly distributed within its composition. It is generally used as shotcrete, and it's becoming widespread for tunnel reinforcements. Some factors affecting the effectiveness of this solution are the slenderness and length of fibres, and the size of aggregates in the mortar matrix, since they define the bonding properties and thus the capacity to behave as a composite.

More complex solutions using the same kind of material imply defining a direction for the reinforcement, according to the material requirements due to the design of the structure. This way, the fibres can develop their maximum capacity. The constructive solutions are unidirectional and bidirectional meshes of reinforcement. The first investigated solutions were related to its tensile properties and its application to reinforcement of reinforced concrete structures, that made it suitable for the reinforcement of beams (both for bending and shear) or the jacketing and confinement of columns. The application as a method of jacketing for retrofitting or reinforcement of masonry walls is a relatively new concept still under investigation, with many parametres still to be defined. Nonetheless, it is already one of the recommended reparation techniques in some guidelines. [46]

Among the parametres that affect the performance of the reinforcement, there are some remarkable ones:

- Density of the mesh, depending on quantity of fibres in each thread (defined by mass) and the separation among them.
- Properties of the mortar, affecting the bond between the element and the reinforcement.
- Properties of both mortar and textile surfaces, affecting the bond among them to make the composite work as such.

In this investigation, the resisting thread (namely carbon fibre and glass fibre) is covered with other materials such as polyester forming a braid, in varied dispositions and geometries, with the main purpose of improving this bond matrix-textile and besides providing protection to the resisting material.

3.7.2. TRM vs. FRP – Researches by Papanicolau and Triantafillou

TRM is being developed mainly as an alternative to fiber reinforced polymers, that have seen a great development and widespread use in the field of structural reinforcement. Nonetheless, some disadvantages, mainly linked to the use of resins as bonding agents, are leading to the investigation of other materials of similar behaviour. Some of the most remarkable are:

- High costs, due to both the materials and the requirement of highly skilled workmanship.
- Necessity of good protection against fire action, given its very low performance in this situations.
- Impermeability both to water and to vapour, that can lead to internal structural problems.
- Hazards of using resins: dissolvents, toxic vapours, etc.
- Difficult reversibility of the strengthening, which is specially problematic for historical structures or in cases where problems such as cracking must be checked afterwards.

The use of an inorganic matrix would solve most of these problems, given that the properties of cementitious binders are more alike to the properties of concrete, and also masonry. Nonetheless, its behaviour is not still fully investigated and there are many parametres that must be studied to get to a better understanding of the behaviour of this material, as well as its advantages when compared to other reinforcement techniques.

Studies by Papanicolau and Triantafillou have compared the performance of FRP and TRM for many applications, in some studies directly related with the subject of investigation of this thesis: reinforcement of masonry for both in-plane and out-of-plane actions. [47] [48]. In this research, several samples were studied with variation on parametres such as the quantity of reinforcement.

They found that, compared with FRP overlays reinforcement of the same fibre density, TRM had an effectiveness of 60-70%. Nevertheless, the deformability was increased in 15-30%.

The conclusions are that, in general, but specially for out-of plane actions (which are usually the ones to cause major damage during earthquakes), TRM is a very promising technique, thanks to its capacity of rising highly the deformability of the infill walls before the collapse, as well as its strength.

Papanicolau et al made an intensive experimental campaign comparing many types of TRM, from high-tech (basalt fibres) to low-tech (polypropylene) and FRP. They obtained good results for TRM, specially for ductility and out-of-plane resistance, for which the TRM, even in its lower-tech solutions, outperformed FRP. For in-plane testing, the results of TRM were slightly lower than FRP, about 30%. [49]

3.7.3. Expected modes of failure in walls reinforced with TRM.

From the theoretical definition, some singular failure modes can be distinguished. In practice, final failure in tests show a mix of several factors. The preponderance of a particular one will depend highly on factors such as the relation between tensile capacity of the reinforcement and compressive capacity of the masonry, and the bonding strength of the reinforcement to the wall and inside the proper reinforcement. The individual modes for flexural (or out of plane) tests can be stated as follows [49] [50]:

- Failure of the wall implies crushing of the bricks, Figure 19. This is a brittle failure, and implies that the tensile capacity of the reinforcement is too high for very low resistance bricks. Its occurrence, under flexural requirements, normally happens after cracking of the reinforcement and the masonry, raising the neutral axis and making the compressive zone very small.

- Debonding of the matrix from the wall, Figure 20. This can be due to low resistance of the mortar of to a inaccurate preparation of the wall surface. It implies a non-efficient behaviour of the reinforcement, given that it cannot develop its full capacity.

- Debonding of the composite, Figure 20. Slipping of the fibres within the matrix is a very common failure for TRM solutions. It an undesirable failure for the same reasons than exposed previously. The research on improving bonding capacity of fibres is one of the major topics within TRM development.

- Tensile failure of the fibres, Figure 22. This is the most desirable failure mode, since the capacity of the fibres is effectively added to the wall strength, and the properties of strengthening and improving of the deformation capacity are taken to the maximum. This also implies a better distribution of the stresses. [50]

Figure 19. Failure by deep cracking and crushing of brick. [50]
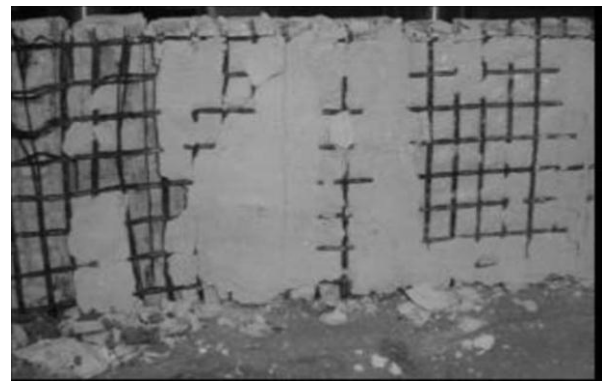
Figure 20. Debonding and disintegration of the mortar matrix. [50]

Figure 21. Slipping of the fibres within the mortar matrix [49].

Figure 22. Tensile failure of fibres [50].

3.7.4. Commercial solutions: overview.

When compared to the wide development of FRP solutions by many chemical – textile companies, the range of commercial solutions for TRM are quite reduced. Meshes are still highly intended for nonstructural reinforcement, such as anti-retraction meshes, and as such, the products don't give a thorough definition of its mechanical properties in their brochures.

They consist mainly in unidirectional and bidirectional woven meshes. Their stability is provided by the woven union of the braids. The reinforcing material is always exposed, even if in many cases it's conveniently treated (for example, bitumen-covered glass fibre) to improve their durability within a mortar matrix.

Unidirectional meshes are composed of threads of a higher density and quality on the main direction, and threads of inferior quality in the transverse direction which function is just conforming the mesh. This meshes are theoretically indicated for reinforcement of elements with well-defined principal stresses, such as the tensile face in a bending element.

In bidirectional elements, the thread in both directions have the same properties.

In the next section, two particular solutions will be analyzed, since they will be used in the experimental campaign.

CHAPTER 4. DEVELOPMENT OF TEXTILE BRAIDED MATERIALS.

This Chapter is focused on the material used for the retrofitting of masonry infill walls, both from the manufacture and mechanical characterization point of view. Inclusively, its production has been one of the challenges in this thesis, given its innovative nature.

The reinforcement typology of textile braided composite rods has been applied in previous studies in University of Minho, and its application to masonry strengthening is on its first steps. This implies that these materials should be carefully studied in order to have a better insight on the mechanical behaviour and to better understand its performance as a retrofitting technique for out-of-plane loading acting in the walls.

The process of manufacture of the composite strengthening materials will be studied and described. The manual component is important, compared to industrially produced meshes, and the control and methodologies to obtain a homogeneous material in the required quantity are important to obtain final coherent results.

The resulting rods will be analysed in all its features, from the material components to the geometrical and mechanical properties, obtained according to standardized tests for similar materials such as plastic composites.

Finally, there will be a brief comparison among the proposed material and commercial solutions, considering both material features and mechanical properties, which will allow a better understanding of the final results of the testing campaign of the materials once applied on the masonry samples.

4.1. Innovative materials: braided fibre-reinforced rods.

The application of textile materials, as reviewed in the state of the art, is a technique with some years of research and development, with some commercial implementations already available. The most common used fibres are glass and carbon due to the junction of good mechanical properties with durability and chemical resistance. Other developments are carried out with polymeric grids [40], or natural fibres like sisal or jute [51], having as main inconvenience the quick degradation.

A second generation of this kind of materials is currently being developed with the aim of improving the behaviour and effectiveness of the resisting fibres, by means of their use within composite materials, and especially within braided composite textile materials under the form of rods [5]. These were developed as an alternative for steel reinforcements, given its higher strength, its resistance to corrosion, the lower diameter and the possibilities offered by the insertion of a rib structure to improve the bonding to the matrix. The further application of this technology is the retrofitting of masonry, still in early steps of assessment and main topic for this thesis.

The resulting material is very similar to FRP rods, in the sense that they are a composite material with fibres within a resin matrix [48]. They are called in bibliography BRC, or braided composed rods. When compared to FRP rods, their production implies a series of advantages:

- Lower cost and higher availability, since the production is carried out in simple and low-tech machinery, compared to the high tech required for production of pultruded FRP, and out the same materials (fibres, resin).
- Wide range of possibilities in mixing different fibres, according to the required results.
- Simpler production, done in only one step and by non-qualified workmanship.
- Current research in self-monitoring materials.

Its innovation is linked to the use of different materials within a composite trying to gather the better of each one's properties. The resisting fibre, stronger and more expensive, is inserted within an external textile braided tubular structure with low mechanical properties and cheap. This shell, not being necessarily resistant, should carry out two functions: improving the bond among the mortar matrix and the fibres and protecting the fibres from the potential chemical reactivity of the matrix.

Bonding is a major problem in the application of very strong materials for reinforcement. Failures by slipping of the fibres within the mortar or concrete matrix are very common, and it can imply an ineffective use of the material, given that it is not allowed to develop its maximum stress. Given the economical and environmental costs of these materials, especially carbon and glass fibres, it is desirable to obtain a bonding strength such that the tensile failure of the fibre occurs before the slipping. In the experimental campaign, this implies the evaluation of the failure mode of the walls regarding the tensile failure of the fibreglass.

4.2. Material composition.

The composite material developed for this work can be briefly described as a braided external tubular structure made of cheap polymeric fibres (namely polyester) around a core of fiberglass, with the addition of polyester resin to the braided material to guarantee the bonding among them (Figure 23). The choice on fibreglass instead carbon is due to its lower cost, higher availability and its better behaviour in terms of ductility, given that carbon, even having a higher tensile strength, shows also a lower elongation in rupture and higher stiffness. The commercial reference is EC13 408 Z28, with the following technic characteristics and further information provided in annex 1

- EC: Classification as E-Glass, a low alkali glass. This type of fibreglass is relatively low-cost and very available when compared to other types of fibreglass or carbon fibre.
- 13: Diametre of the fibres, in microns.
- 408: Linear mass, 408 tex (or grams / kilometer) per yarn.
- The mechanical characterization can be estimated as an ultimate strength of 270 N per yarn, with a final strain of 2.4%, taken from previous researches [52].

Two different types of reinforcement are produced according to the number of yarns of fibreglass composing the core. The reinforced core is composed by 2 or 4 yarns of fiberglass, being designated by 2G or 4G fiberglass respectively.

The braided tubular structure is composed by 15 simple yarns of high resilience polyester. Additionally, more 8 yarns added as a simple braid were used to provide the braided rod with a ribbed structure intended to improve the bonding between the rod and the rendering mortar. The polyester yarn is mainly defined by its linear mass, of 110 tex, giving a total of 2530 tex in the external tubular structure. The polyester was chosen for the braid due to its abrasion resistance and very low cost.

After the braided rod was produced, a polyester resin was applied along the surface of the braid aiming at improving the bond between the braid rod and the reinforcing fibres. The polyester resin was selected due to its lower cost and toxicity compared to epoxy resins. It is activated through addition of 2% of Methyl Ethyl Ketone Peroxide.

15 Polyester yarns for the braided shell

1 Basic braid composed of 8 polyester yarns for rib structure

2/4 Fiberglass yarns for the main reinforcing function

Final braided product (with rib structure)

Figure 23. Materials used in the manufacture of the braided retrofitting materials:

4.3. Manufacture of the retrofitting materials. Methodology.

The composite braided rods consist of a new material and have to be manufactured in a self–manufacture process with the use of technology and machinery limited to the laboratory disposition of the textile department of University of Minho. After manufacturing of the braided rods, it is intended to weave them into a mesh with a certain spacing in order to apply the textile bi-directional mesh in the masonry infill panels and evaluate its resisting contribution to out-of-plane resistance and deformation of the walls. A big part of the manufacturing the retrofitting materials is a manual process, namely the resining of the rods or weaving of the rods into meshes .

The braiding technique consists on two sets of bobbins, spinning one clockwise and the other anticlockwise, as the yarns in them are intermingled. As a result of the braiding of the yarns in longitudinal and transversal directions, a tubular structure is produced around the core, as can be observed in Figure 25. The required machinery is relatively simple and well known in textile engineering, generally known as standard braiding machine as seen in Figure 24.

A special disposition has been developed regarding the composition of the shell. The braided tubular structure for the shell can be produced with thicker yarns included in it, creating a helicoidal rib to improve adhesion between them and the mortar matrix [4]. In this case, these thicker yarns, which are used in the braiding machine in a rate of 15 normal to 1 thicker, is composed by a simple braid of 8 yarns. The procedure can be described by the following steps:

1.- The first element to be manufactured is the basic external helicoidal braid, composed by 8 yarns of polyester. This is done in the same braiding machine, and with the same braiding velocity than the final braided material.

2.- Afterwards, it is necessary to prepare the specific bobbins of the machine by winding the materials in them at constant velocity of 40 m/min, with an appropriate winding machine.

3.- Then, the production of the reinforcement rods can start, as seen in Figure 25. An important parameter to be controlled in this process is the braiding velocity imposed to the machine, since it is related with the braiding angle. For this process, the velocity was kept constant at 54 cm/min.

4.- The final step of the preparation of the rods implies tensioning them with 100N force, and then to stabilize them, as seen in Figure 26. The tensioning was done by attaching the braided rods to a stable structure on one end, and hanging weight on the other end. Once tensioned, it can be resined, a process that is done manually as seen in Figure 27. This is done by external impregnation in polyester resins. Along with the stabilization of the rods and keeping the tension, it is intended to ensure the bonding and the unitary behaviour of both external tubular structure and core. For other research applications, the technique of resining was different [6]. The resin was applied to the core, before its insertion in the braided tubular structure. Nonetheless, this technique was not recommended for this project, due to two main disadvantages: (1) the difficulty to apply this technique for the much

larger required amount of material, and (2) the rigidity of the obtained rods, which would be a problem for the weaving.

Finally, the resin cured for 24 hours previously to the cut of the rods according to the required measures for the assemblage of the meshes.

Figure 24. Braiding machine.

Figure 25. Detail of the braiding process.

Figure 26. Tensioning of the produced material.

Figure 27. Manual application of polyester resin.

4.4. Geometrical characterization of the braided materials.

Braided materials can be characterized mainly by two features: braiding angle and diameter. In this case, it will be analysed as well the angle formed by the rib structure.

Figure 28. Equipment for the determination of geometrical properties.

Figure 29. Measurement of the diametre with Vernier caliper..

The diametre of the rods has been determined by its measure with a Vernier caliper (Figure 29) with 0.05 mm accuracy for the measurement. The difficulty comes from the helicoidal rib of the external braid, which makes the diametre irregular. For each 2G and 4G composite rods 20 measures were taken in order to have a good average as characteristic feature. The characteristic data obtained is:

- 2G rods: Average of 2.05 mm, with minimum of 1.95 mm and maximum of 2.6 mm. The resulting area is 3.301mm^2.
- 4G rods: Average of 2.16 mm, with minimum of 2.1 mm and maximum of 2.7 mm. The resulting area is 3.664 mm^2.

Other possible definition of the diameter is through the formula of the theoretical diameters, in which the porosity of fibres is taken into account, and only depends on the materials. Nonetheless, this formula is for rounded fibres and would give just an approximate value.
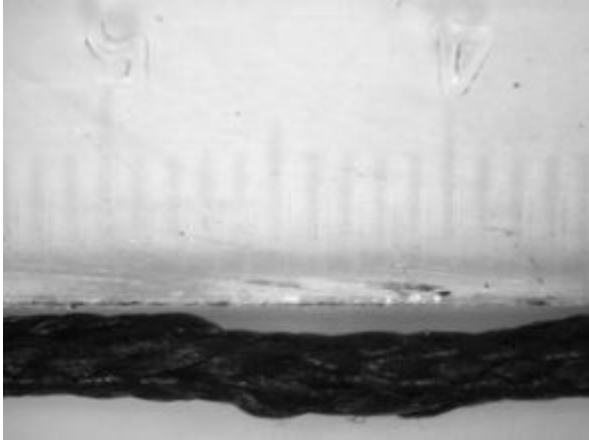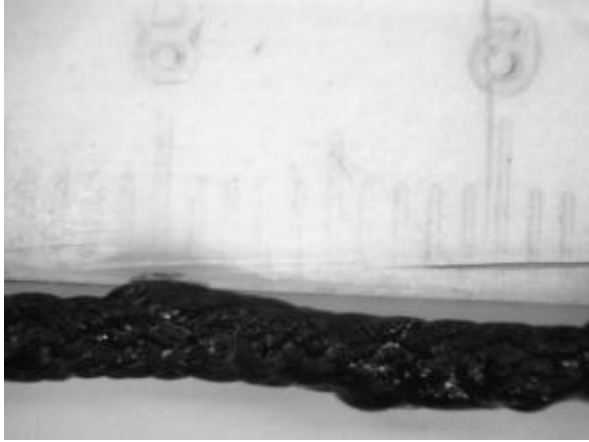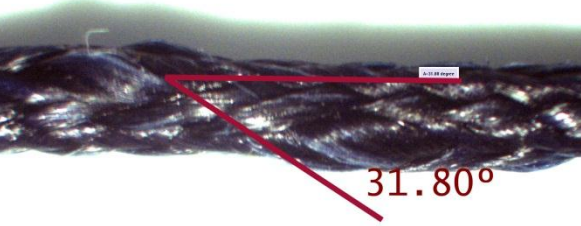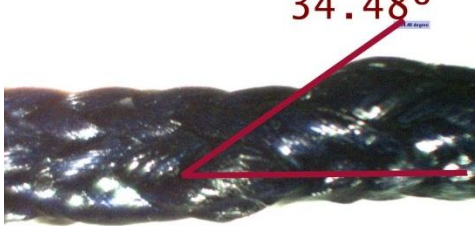
$$D = 4.44 \sqrt{\frac{Tex}{\rho} \cdot 10^{-2}}$$ **(Eq. 3)**

For the external shell, composed of 15+8=23 yarns, 110 tex each, which makes a total of 2350 tex, with a density of 1.4 g/cm^3. This gives a diameter of 1.81 mm, and an area of 2.54 mm^2.

For 2G fibreglass, we have 816 tex and a density of 2.55 g/cm^3. The theoretical diameter is 0.79 mm. The total theoretical area of fibreglass is 0.501 mm^2, and a total area of 3.041 mm^2.

For 4G fiberglass, with 1632 tex and a density of 2.55 g/cm^3. The theoretical diameter is 1.12 mm. The total theoretical area of fibreglass is 0.985 mm^2, and a total area of 3.52 mm^2.

Table 6. Geometrical characterization of produced materials.

Figure 30. 2G rods. Magnification.	*Figure 31. 4G rods. Magnification.*
Figure 32. 2G rods. Braiding angle: 24.1º	*Figure 33. 4G rods. Braiding angle: 25.7º*
Figure 34. 2G rods. Rib angle.	*Figure 35. 4G rods. Rib angle.*

The braiding angle is defined as the angle formed by the yarns braided around the core and the axis of the rod. This feature is important as bonding properties are highly affected by the characteristics of the braid and its rib structure. In previous studies by Gonilho and Fangueiro, it was observed that for each core-reinforced fabric, there is a braiding angle that ensures an optimum mechanical performance. For a braided fabric produced with six bobbins of polyester yarns and two simple braids, and a core reinforcement of 1800 tex fibreglass, this angle was stated in 23º-24º [5].

This characterization was made with optical amplifier (Figure 28) and corresponding image-treatment software. The obtained data is the average of three measures, and the measured entity is as defined graphically in Table 6.

4.5.   Manufacture of textile braided meshes.

In the next step of the production of the reinforcements, the produced rods were assembled into a bidirectional mesh. A woven structure for the mesh was preferred to the simple superposition of the rods in perpendicular directions, due to a better self-stability of the mesh before its implementation and a better guaranteed bidirectional behaviour.

The meshes were assembled according to the defined measures (Figure 36), with spacing of 60 or 30 millimeters. The manual character of this procedure implied difficulties such as ensuring accurate constant spacing among the rods.

The joining of the two perpendicular directions of yarns in the mesh was done by application of polystyrene resin on them. To guarantee a correct application, the curing period was of 24 hours. The aim is to improve the natural stability of the mesh to make sure its application to the wall in correct conditions.
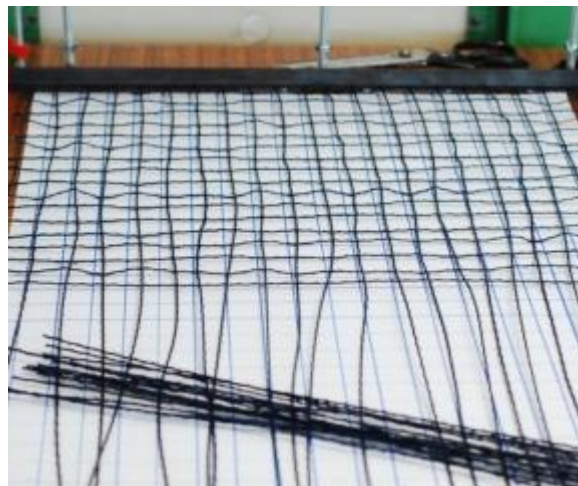
Figure 36. Manual assembly of the mesh.

4.6. Mechanical characterization of braided bars. Uniaxial tensile tests.

4.6.1. Test set-up and procedures.

The produced materials were tested according to standards in order to obtain their mechanical properties, namely breaking strength (equivalent to tensile strength), elongation and modulus of elasticity. This was done in a dynamometer, following the routine procedures in textile tests. [3] [6].

The dynamometer (Figure 37) consists in a device of two clamps used for measuring the force needed to keep a constant velocity in their opening. The material is grabbed by the clamps and tensioned until breaking, obtaining data of elongation related to the applied force.

Samples of each 2G and 4G rods, as well as external braid without any reinforcement, were prepared according to the standards and requirements of the testing machine. From previous experience it can be said that it is not convenient to grab the rods directly with the clamps. An alternative procedure is based on the use of holding plates on each end, made of a composite of fibreglass and epoxy resins, in order to obtain the breaking of the bars in the middle of the sample and not at the fixed ends of the specimen. The length of the samples was 100 mm, and the holding surfaces were 70x50mm^2.

Given that there is no specific standard for this material, the ASTM – 5034: textile break strength and elongation through grab test was used. The measurement equipment was a dynamometer Hounsfeld H100KS, and the test was setup with the following parametres:

- Extension: 100 mm (which means the maximum possible elongation is 100%)
- Gauge length: 100 mm (length of the sample, distance between claws).
- Speed 5 mm/min
- Preload 10 N

Figure 37. Equipment used for the tensile tests.

The first test campaign led to inconclusive results (Figure 38), as the breaking of the material was delayed for an unexpectedly high elongation. By observing in detail the behaviour of broken samples, see Figure 39 and Figure 40, it was concluded that the breakage of the specimens was due to slipping of the fibreglass core within the braided shell. Given the short length of the samples, this behaviour cannot be taken as representative, since it happens due to the close distance to the free end of the braid. Other cause of failed tests was due to inaccurate curing of the resin, that lead to slipping of the rods within the resined plates without failing, as seen in Figure 41.
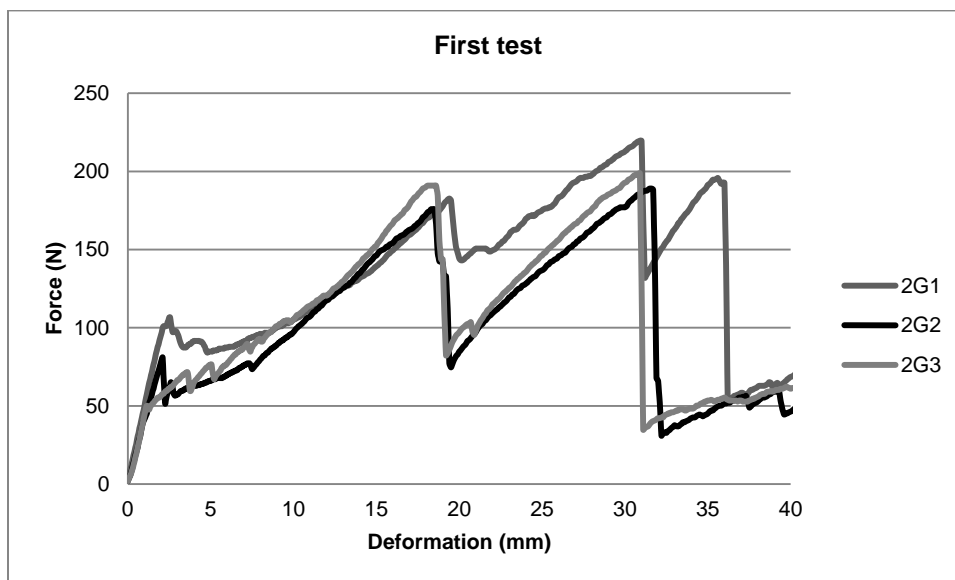
Figure 38. Force – elongation graph for 2G rods in the first tests.

It is observed that after a first expected linear stretch of the force-deformation diagrams, there was a first yield, subsequent hardening and other yield points. This is interpreted as the tensile behaviour of the fibre within the external braid. First, both materials deform together, and the commanding elasticity is the one of the fibreglass, much stiffer. Then, the fibreglass slides into the shell, twice, but due to friction it gives some hardening (Figure 39). The final breaking point is related with the elongation capacity of the polyester fibres.

After this experience, the samples were redesigned to guarantee that the behaviour of the material would be as expected. The core was taken out of the braid, embedded in resin and thus firmly bonded to the support plates, as seen in Figure 42. In this way, the length of both materials during the test is maintained and the breaking points of each component will be attained according to their tensile strength and elongation.
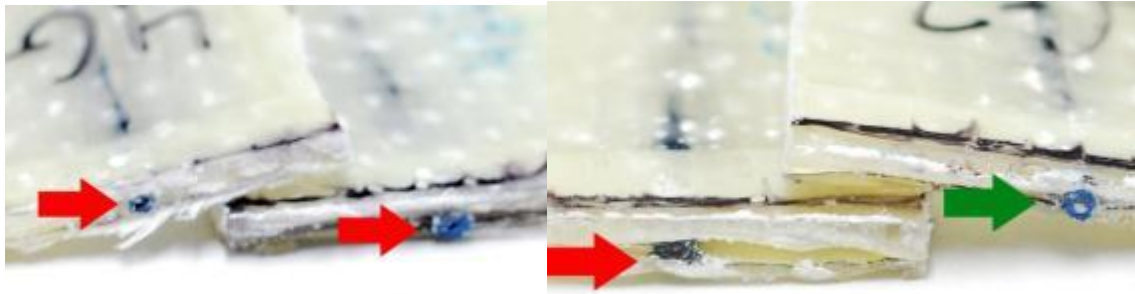
Figure 39. Red: points where sliding is noticed. Green: sample where the core did not slide.

Figure 40. Example of broken sample. The sliding of the fibres is not noticeable at first glance.

Figure 41. Other type of failing: the whole rod slides into the composite plates.
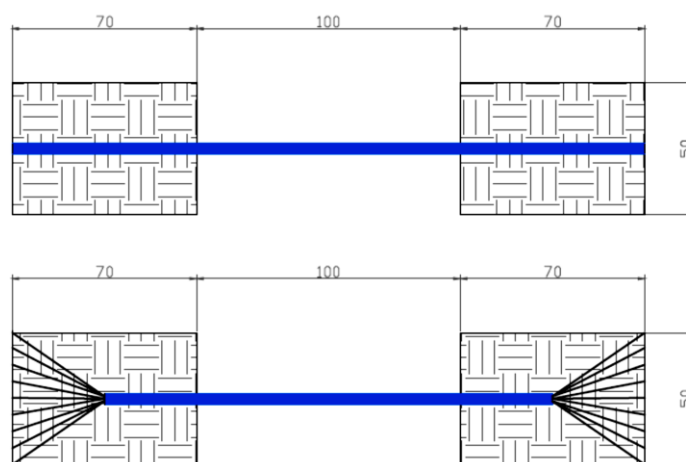
Figure 42. Up: first test samples. Down: second test samples, exposing glass fibres.

4.6.2. Results of the tests.

From the results of the tests, it can be obtained the three parametres defining a tensile reinforcement material, as it's seen in FiguresFigure 43,Figure 44Figure 45:

- Ultimate load, and derived from its area, ultimate strength,
- Ultimate elongation, and derived from the sample length, ultimate strain,
- Stress-strain diagram, and from the slope of the calculated regression line, the estimated elasticity modulus.

The force-elongation diagrams obtained in the tensile tests of the external braid without reinforcement prepared according to the procedure previously described are shown is Figure 43. It is seen that its behaviour is quite uniform. The elasticity modulus shows a very low value when compared to materials normally used for reinforcement as steel or strong fibres.

The initial extension of the braid presents a nonlinear behaviour, which is due to the repositioning of the fibres within the tubular structure: as the tensile stress increases and the braid stretches, the braid angle is decreasing, which corresponds to the improvement of the tensioning of the polyester fibres. After this, the external braid present a linear behaviour corresponding to a considerable higher modulus of elasticity. An important feature that should be focused is the great elongation of the braided materials and the fact that only for great elongations, the maximum tensile strength is attained. This peculiar behaviour should be attributed to the modulus of elasticity, very low when compared to materials normally used in structural reinforcement, as the deformations are expected to be small.
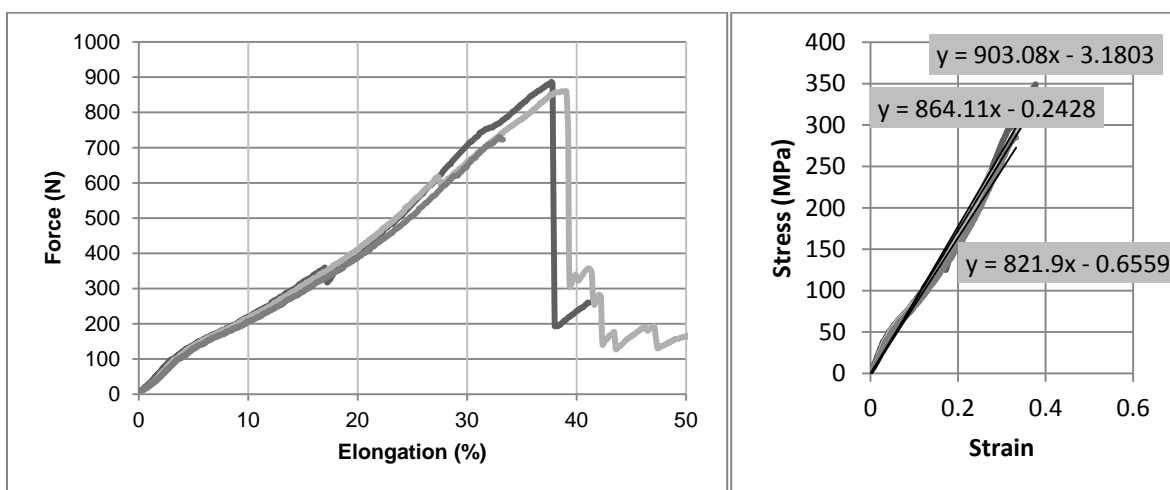
Figure 43. Tensile behaviour of external braids without reinforcement (2350 tex of polyester).
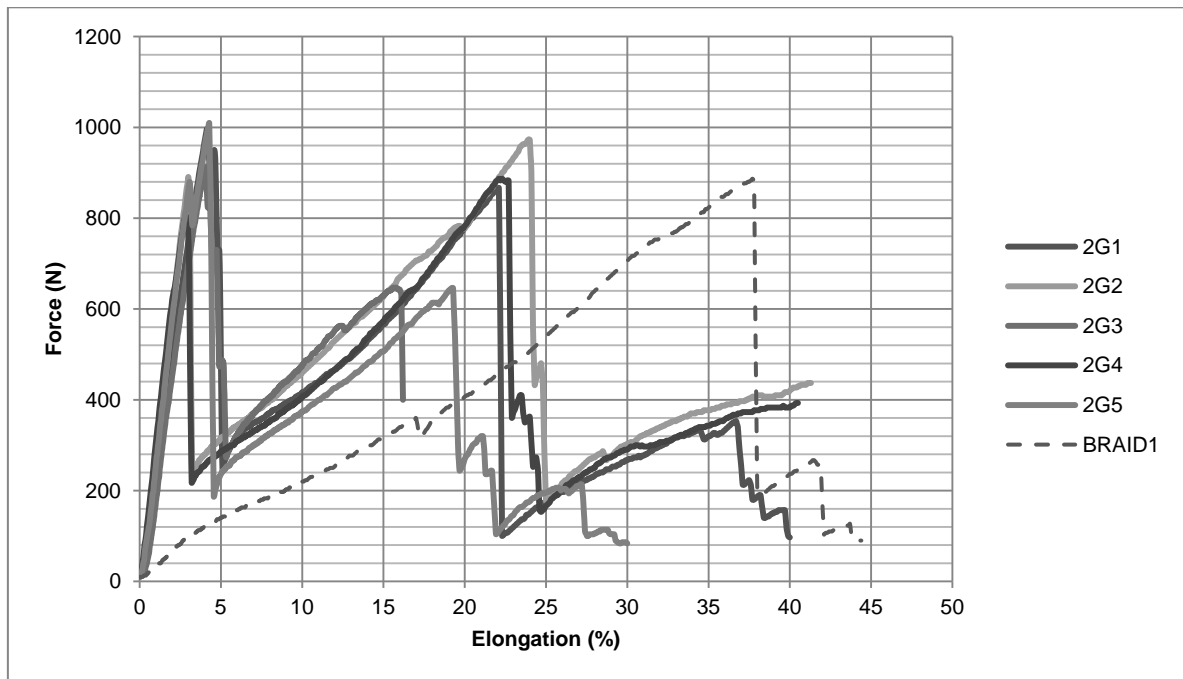
Figure 44. Force – elongation diagrams obtained for 2G rods (816 tex of glass fibre), and comparison with behaviour of external braid.
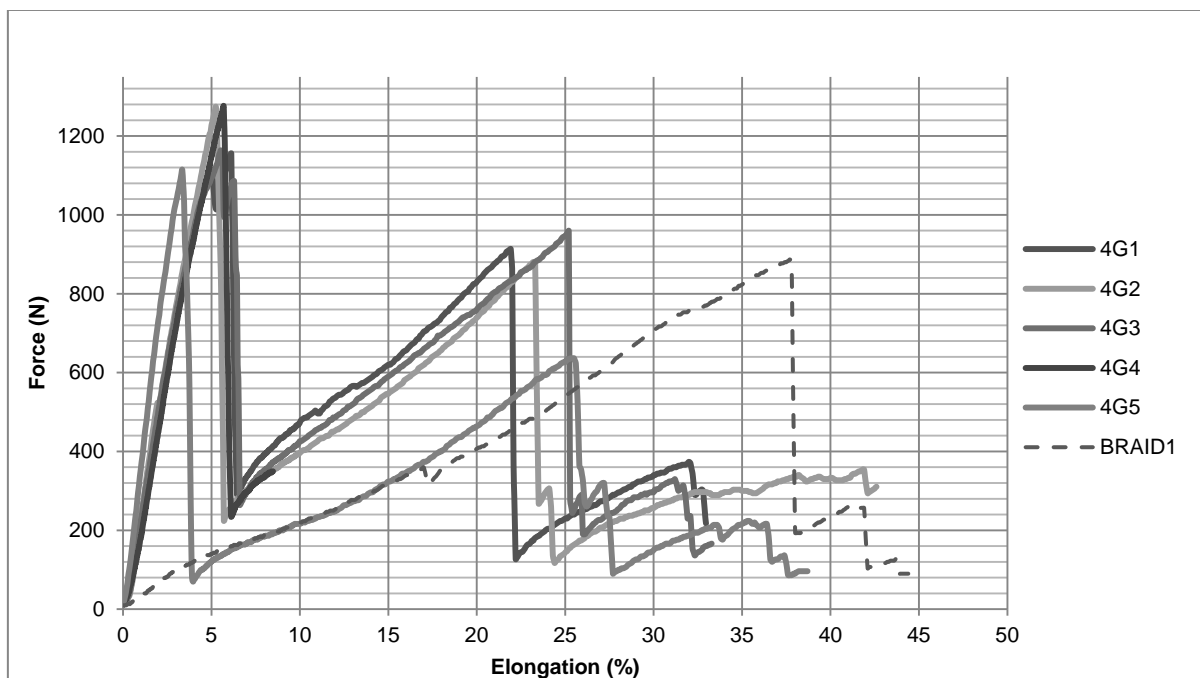
Figure 45. Force – elongation diagrams obtained for 4G rods (1632 tex of glass fibre), and comparison with behaviour of external braid.

The tensile behaviour the two different types of braided rods (2G and 4G) rods is displayed in Figure 45 and Figure 46, respectively. The obtained results are especially uniform in the first part of the deformation, even if some variation in the failure resistance of the resisting core was recorded The behaviour of the rods when only the external braid remained was more disperse.
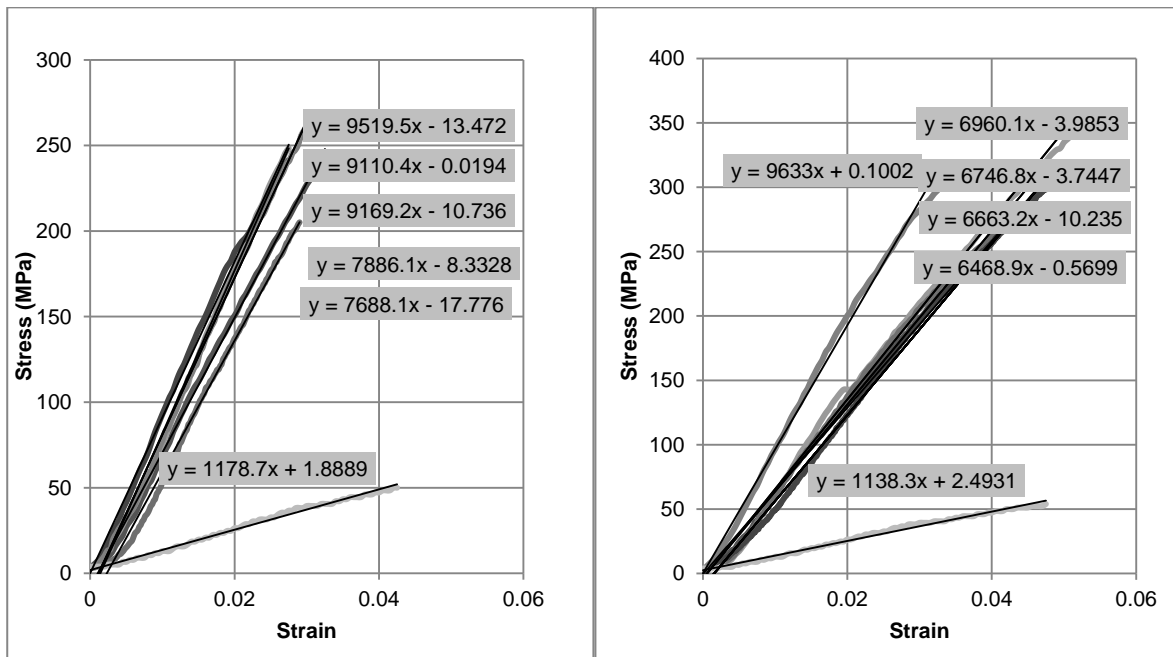
Figure 46. Calculation of elasticity of the materials. Left, 2G rods. Right, 4G rods.

4.6.3. Analysis and discussion of the results.

The behaviour of the rods must be analyzed from the point of view of a material composed by two resisting elements: an external material composed of the polyester rod and the core composed by the reinforcing materials (glass fibres). The pre-peak regime is practically linear until peak load, being the stiffness of the composite material influenced at great extent by the high elastic modulus of the core.. After the peak load is reached, an abrupt decreasing of the resistance is recorded. The stress on the composite rod decrease to the level of the force mobilized only by the external polyester braid, see Figure 47. The drop on the resistance should correspond to the failure of the core of the most part of the glass fibre behaviour. This failure cannot be seen during the tests, as the fibres break within the polyester braid, which due to its lower modulus of elasticity, is still unaffected and continues to deform. After this phase, the composite braid recover resistance up to the level of the maximum tensile force recorded in the single external polyester braid. A second yield point is reached when the braid breaks. Some residual strength remains after this, as the thicker yarn of the ribbed structure is the last one to fail.

It is interesting to compare the behaviour of the rods and the behaviour of the external braid without reinforcement, as it makes it very legible, and explains the behaviour of the material after the first

yielding point. The external braid was initially just considered as a mean of improving the bonding of the reinforcement to the mortar matrix. Nonetheless, it has been observed that its strength is considerable and comparable to the strength of the glass fibre core. , This should be attributed to the large area of material, 2.54 mm^2 compared to 0.501 and 0.985 mm^2 of glass fibres in the core. In the case of 2G rods, the strength of the braid is similar and in some samples higher than the strength of glass fibres. Nonetheless, the data considered as breaking force for these cases will be the one of the first yielding point.
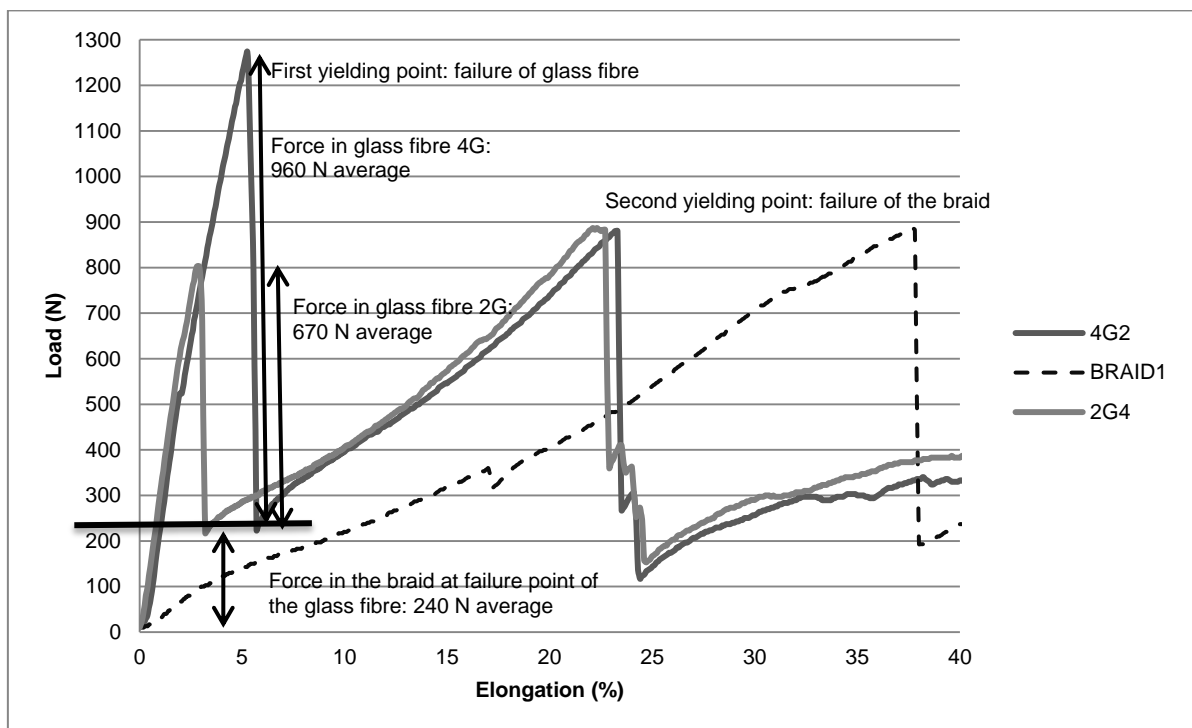
Figure 47. Analysis of results for representative examples of each element.

A summary of the results derived from tensile tests of reinforcing rods is present in Table 7. Also in the scope of direct comparison, the tensile stresses on the simple polyester braid are calculated for the elongation equivalent to the failure of fibreglass. For the effect, it was considered an average elongation corresponding to the peak stress of the composite rods of 4.6%. The simple braids are able to reach high values of stress, but only when very high deformations are reached, which is not admissible for reinforcing materials intended to improve the behaviour of stiff elements, as it would allow extensive damage before developing its strengthening capacity. On the other hand, the tensile stresses on the simple braid rods are considerably low, when the deformation corresponding to the peak stress attained in the composite rods is considered.

Table 7. Results derived from tensile tests of reinforcing rods.

	Specimen	Break Force (N)	Elongation (%)	Elasticity modulus (MPa)	Ultimate stress (MPa)
2g	2g1	997	4.15	9519	302.03
	2g2	890	3.00	9110	294.76
	2g3	913	4.04	9169	276.58
	2g4	803	2.90	7856	268.71
	2g5	1010	4.28	7668	305.97
	Average	922.6	3.67	8664.40	289.61
	Error (%)	9.473	16.49	9.86	5.65
4g	4g1	1156	6.12	9633.00	315.58
	4g2	1274	5.25	6960.00	347.57
	4g3	1164	5.52	6746.00	317.63
	4g4	1277	5.68	6663.00	348.39
	4g5	1114	3.35	6469.00	303.98
	Average	1217.75	5.64	7500.50	326.63
	Error (%)	4.866	8.46	28.43	6.66
Braid (yield point)	braid1	236	4.6	2019	92.9
	braid2	255	4.6	2182	100.4
	braid3	242	4.6	2071	95.27
	average	244.3	4.6	2090	96.19
	Error (%)	3.3	0	3.25	4.36
	braid1	887	37.7	920.43	349.21
	braid2	860.3	38.6	875.39	338.58
	braid3	730	32.9	854.85	287.40
Braid (final)	average	825.77	36.4	883.56	325.07
	Error (%)	11.60	9.6	3.25	11.59

It is also interesting to highlight the nonlinearity on the tensile resistance when analyzing the composite materials as an addition of its components. In Figure 47 it is seen how it is possible to estimate the maximum strength developed by each material in the composite: at the yielding point of the glass fibre, the remaining strength of polyester is subtracted to the total composite strength. This way, it is seen that for 4G, with double mass and therefore double resisting area than 2G, the strength is not double, but lower. This nonlinearity can be explained based on both the characteristics of the composite material and the variability induced by semi-manual production:

- Composition of the rods as a tubular structure around a fibre core, which gives two sources of nonlinearity: (1) The bonding properties among components is not very well known yet, since the addition of resin to the external surface area of the polyester braid appears to be only

superficial, and thus different to the one developed when the resin is directly applied during the manufacture of the stiff braid composite rods intended to be used in the reinforcement of concrete structural elements [6]. This can lead to a somehow independent behaviour of both materials. (2) Even if the deformation is solidary, the fibres in the core could be not perfectly aligned in the pre-tensile state, giving higher strains than expected, as the reinforcing fibres have to align in the beginning of the tensioning process, not giving any resisting force.

- Nature of the fibrous materials and the higher probabilities of having imperfect yarns, increased for materials with higher content of yarns.

- The difficulty for defining the diametre, giving that the tubular structure can allow the presence of some voids not fulfilled by the core fibres. This can lead to an estimation of a higher area, leading to lowest stress values. This can be seen in the difference among the theoretical value and the measured value of the area for the rods: in 2G, theoretical area is 3.041 mm^2 compared to measured 3.302 mm^2. For 4G, with more yarns and thus less likely of having voids, theoretical area is 3.52 mm^2 compared to 3.66 mm^2.

- The production of the materials had a highly manual component. 4G rods were produced last, having the advantage of a higher experience and thus more homogenization on processes like the resining.

- It is also interesting to notice the higher stiffness of the external braid when considered as a part of the rod than when tested as a single element. This is explainable by two factors: (1) the simple braids were not resined for the testing, though this would only affect the initial extension, and (2), the bonding between glass fibres and the external braid, that continues to act after the failure, transferring some of the stiffness of the glass fibres to the braid and thus restricting its elongation, except for the point where the glass fibre failed, as explained in Figure 48. This point matches with the point of failure of the external braid.
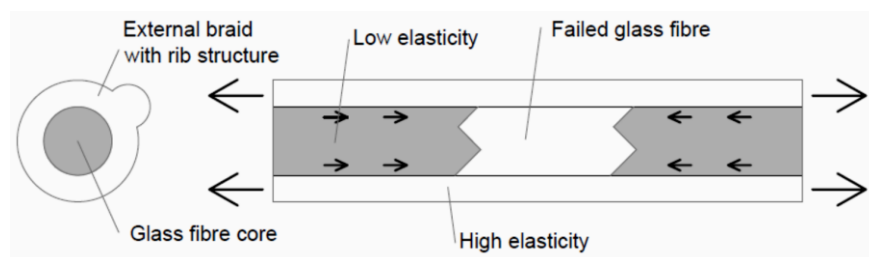
Figure 48. Internal bonding in the reinforcement rods after glass fibre failure.

- Further research including a thorough experimental characterization of the component materials is recommended in order to quantify these nonlinearities and the action of internal bonding when compared, for instance, to material models of composite sections with perfect bonding.

4.7. Commercial solutions.

One of the purposes of this research is to assess the ability of improvement of the bonding between the reinforcement fibres and the matrix mortar due to the use of braided materials. So far, commercial solutions consist just on the reinforced material, prepared to be inserted in the mortar matrix. To have a reference to compare the performance on the improving the out-of-plane behaviour of masonry infills with the material developed in the scope of the thesis, two different commercial solutions were chosen. The range of options was not very wide, but nonetheless, it was possible to choose two different solutions, being one more similar to our proposal in terms of resisting material and mass density, and the other quite different in material and disposition. This means that the comparison that will be possible to be made relates only to a qualitative overview on the performance of each material to retrofit masonry infills under out-of-plane loading.

In this section, a brief description of the commercial meshes used in the study is provided, followed by a comparison between technical properties between commercial and the novel materials developed here. comparison. The technical table can be found in Annex 1.

In relation to the commercial solutions, a mesh from the S&P Clever Reinforcement and a mesh from Mapei were used.

S&P: ARMO – mesh L 500.

This mesh is defined as unidirectional, given that the main resisting material, carbon fibres, is only disposed in one direction. In the principal direction, the elements of the mesh are composed by two yarns of carbon fibre, slightly joined by a very thin fibreglass rolled around them (Figure 49). The yarns are slightly covered with a sandy-like granular element, probably to increase the bonding properties, though there is no mention to it in the technical data. The transversal elements are composed of fibreglass, in a much lower density, probably better for stabilizing the mesh than for really give a bidirectional behaviour. The mesh is joined by weaving, and its density guarantees its self-stability. Nonetheless, the joints are easily dismantled with the hands.

Figure 49. SP ARMO L500 and its components.

MAPEI: Mapegrid G220.

This is a bidirectional mesh composed by alkali-resistant fibreglass (Figure 50). The black colour is due to the alkali-resistant treatment, based on bitumen. It is composed in both directions by two yarns of fibreglass per element, in one direction they are tightly together and in the other they are separated. The joints are somehow rigid, apparently made by pressure and heat. Its application is recommended with "high ductility mortars", such as its related product Mapei Planeitop.

Figure 50. Mapegrid G220 and its components.

4.8. Designation of the reinforcements to be tested. Comparison of mechanical properties.

For a clarification on the designation of the different solution of retrofitting materials, a systematization on the designation and comparison of the properties of the five types of reinforcements to be tested is provided.. Following the developed textile materials and the selected commercial meshes the following designations are considered:

- 2G#3 mesh: bi-directional mesh composed of 2 yarns of fibreglass, spacing 3 cm: 816 tex (grams/km) and 66 metres of reinforcement per squared metre: 53.85 grams of fibreglass/m^2.

- 2G#6 mesh: bi-directional mesh composed of 2 yarns of fibreglass, spacing 6 cm: 816 tex (grams/km) and 33 metres of reinforcement per squared metre: 27.17 grams of fibreglass/m^2.

- 4G#3 mesh: bi-directional mesh composed of 4 yarns of fibreglass, spacing 6 cm: 1632 tex (grams/km) and 33 metres of reinforcement per sq. metre: 53.85 grams of fibreglass/m^2.

- S&P ARMO L500 mesh: uni-directional mesh with 200 grams/m^2 carbon fibre, spacing 20mm.

- MAPEI Mapegrid G220 mesh: bi-directional mesh composed of 225 grams/m^2 alkali-resistant glass fibre, spacing 25 mm.

It is seen that a considerably lower mass of reinforcement material for the self-produced reinforcements was considered, when compared to commercial meshes. This should be taken in account when comparing the results on the performance of the retrofitting solutions..

For the self-produced material, one of the objectives is a parametrical comparison on how the performance is affected when doubling the mass by two different means: denser mesh and thicker rods.

Table 8. Summary of mechanical values for all used materials.

Properties	2G	4G	Mapegrid G220	S&P ARMO L500
Resisting Material	Fiberglass (composite) Bidirectional	Fiberglass (composite) Bidirectional	Alkali-resistant fibreglass Bidirectional	Carbon Monodirectional
Mass density (g/m^2)	114 / 57	114	225	200 (only main direction)
Rod spacing (mm)	30 / 60	60	25	20
Tensile strength (kN/rod or yarn)	0.922	1.217	45 kN/m	500 93.6 in flexural.
Elongation in failure (%)	3.67	5.64	<3	1.75
Elastic Modulus (MPa)	8664	7501	Not declared	160000
Ultimate stress (MPa)	289	326	2600	4300

CHAPTER 5. EXPERIMENTAL CAMPAIGN ON REINFORCED MASONRY.

The experimental campaign to be developed in this thesis is a part in a wider study of the behavior of braided textile meshes for the reinforcement of masonry infill walls. Previous studies have been done in reinforced concrete and a previous thesis in brick masonry walls.

The new materials are developed by the Textile Engineering Department of University of Minho, studying possibilities for the improvement of bonding among matrix and reinforcement, and the behavior of the reinforcement itself.

The cooperation with the Civil Engineering department implies the assessment of its implementation to real structures, so as to verify the effectiveness, to state the importance of variables such as spacing of the rods and strength, and to compare its performance with already existing commercial materials.

This verification is carried out through an experimental campaign in which wall samples are tested in simple bending in a plane perpendicular to the bed joints, as a simple but representative way to represent the behavior of infill walls under out-of-plane seismic actions.

Through this Chapter, all the experimental campaign will be described: the characterization of the masonry samples, the building process, the design of the setup of the tests, and analytical models showing expected results.

Finally, the obtained data will be exposed in a systematical system in order to have a qualitative and quantitative idea of the effect of each type of reinforcement.

5.1. Definition of the samples.

The evaluation of the effectiveness of the new materials developed in the scope of this work (Chapter 3) to act as a retrofitting technique (aiming at improving the out-of-plane behavior of brick masonry infill walls) is carried out based on an experimental campaign composed of bending tests mobilizing the flexural resistance of masonry in the perpendicular direction to the bed joints. The material was applied within a rendering mortar, using the TRM technique. Several solutions were designed using the materials developed in Chapter 3, in order to have a parametrical mean of comparison. Besides, other samples were reinforced with commercial solutions.

5.1.1. Definition of the geometry of the masonry samples.

The geometry of the samples, the setting of the flexural resistance tests and the number of tests were defined according to standards UNE-EN-1052. The bricks used in the construction of the specimens are considered to be representative of the ones commonly used in masonry infills in Portugal.

For this work, the geometry of samples was reviewed in comparison with the previous work [3], as it is considered that the span that was considered for the flexural tests should be increased. In the previous tests, the considered span was of 50 cm for samples with a wall thickness of 11 cm, which gives a relation span/thickness of about 5. This makes the samples very stiff, and even likely to develop flat arch behavior to some extent. This might not allow the reinforcement to show all their potential regarding the improvement of the capacity of ultimate deformation, which according to previous studies is one of the main factors of TRM reinforcements. On the other hand, previous studies have been carried out with larger spans [39] [48], so the results could be more directly compared. Confrontation of the samples tested in the previous thesis and the samples in this thesis can be seen in Figure 51.

Therefore, the new dimensions will be designed according to UNE-EN-1052, according to the same type of bricks as the previous works, but trying to make the span for the flexural test double of the previous one, so that the relation thickness/span of the wall is closer to 10. Papanicolau & Triantafillou used specimens with a span to thickness ratio of 1300/85 (approximately 15) and Rupika used specimens with a span to thickness ratio of 930/7 (approximately 12). This makes the results more directly comparable, even if the used materials and the test setup are very different.
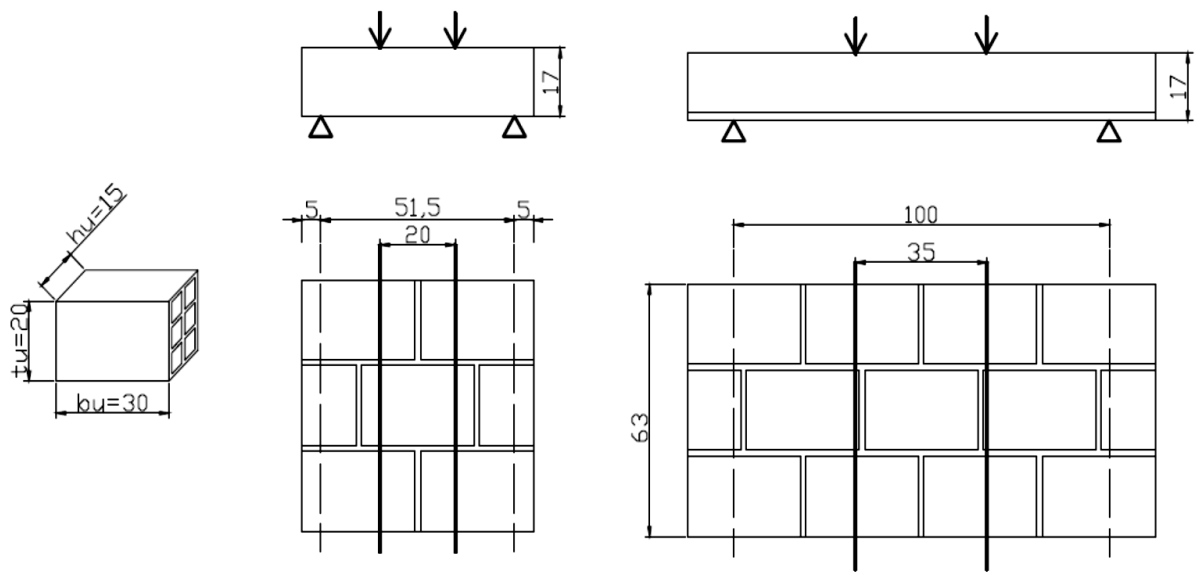
Figure 51. Left: test samples for previous experimental campaign. Right: design of samples for experimental campaign in this thesis.

The dimensions of the samples as well as the loading configuration were according to the prescriptions given in the standard. However, the loading configuration was slightly changed after two previous experimental tests due to unexpected failure mode of the samples. After this the spacing of point loads, $l_{,2}$ was reduced to 350 mm, slightly under the minimum established by the standards. A scheme of the requirements can be seen in Figure 52.
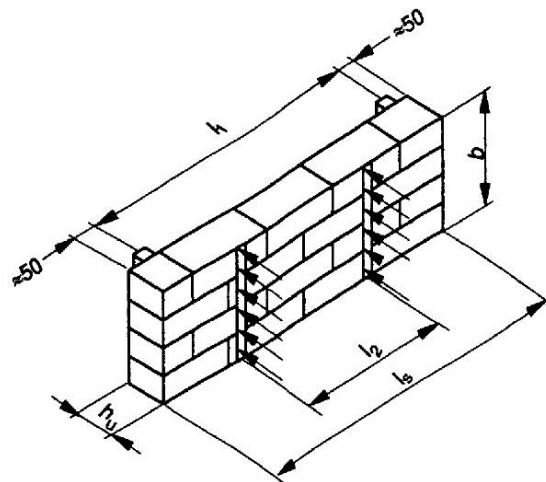
b = 630 mm ≈ $4h_u$ =680 mm (value according to three courses of bricks)

b ≥ 240 mm ; h_u ≤ 250 mm ; in every course, at least one head joint within l_2.

$0.4\, l_1 ≤ l_2 ≤ 0.6\, l_1$

Figure 52. Dimensional parameters of samples according to UNE-EN-1052.

5.1.2. Definition of the materials for the wall samples.

The brick type was selected as the most representative for simple partition walls or for simple leaves within composed enclosure walls in Portugal. The total thickness of the wall registered in codes (referring to isolation requirements) and in construction practice is of 12 cm (Spanish codes: citara de medio pie). This solution, executed with the most usual measures of bricks and with bricks with horizontal perforation, leads to a brick of nominal measures LxWxH 30x20x15, with the length in the bed joint and the height of the brick corresponding to the thickness of the wall.

The value of the characteristic strength and elasticity modulus in the normal direction to the bed joints can be taken from Pereira [38] given his studies and verifications in this type of bricks: Elasticity modulus E= 2170.8 N/mm^2 and normalized compressive strength f_b= 5.01 N/mm^2. Nonetheless, given that the flexural tests will be done in the direction of the bed joints, it will be necessary to have data for the compressive strength of the bricks in the direction of the holes. This will be obtained through uniaxial compressive tests in the direction of the perforation.

The mortar for the bed and head joints is defined as a general purpose pre-mixed mortar used for laying the mortar units corresponding to class M10. The particular properties provided by the producer are: Compressive strength f_m > 10 N/mm^2 and Bonding strength of 0.15 N/mm^2.

The mortar for the rendering and implementation of the reinforcements is defined as Argamassa de reboco, or rendering mortar, according to EN-998-1:2003 GP, CSIV: Compressive strength f_m>6N/mm^2; Adherence to concrete >0.2 N/mm^2.

Both mortars are controlled through samples taken during the construction of the specimens and then tested under flexure and uniaxial compressive strength. This procedure enables also to control the quality of workmanship and eventual irregularities presented in punctual samples.

5.1.3. Construction of masonry panels and retrofitting.

The masonry samples were built by experienced workers. Given the nature of the test campaign, it was important to guarantee the maximum homogeneity possible in the mechanical properties of the walls, and thus in their construction process. For this purpose, there was an intensive control of the mortar applied to the walls through mortar samples taken from each mix made for each specimen according to standards.

The building process of the panel walls was as follows and is shown in Figure 53:

- Soaking of the bricks previously to their application, in order to avoid quick drying of the mortar due to absorption of its water and thus to avoid a reduction of its mechanical properties and the bond adherence between the bricks and mortar.
- Initial bed joint of mortar for settlement, leveling and regularization of the bricks, allowing as well an easier handling of the samples for their removal.

- Control of the water quantity on the mortar: minimum possible to guarantee the workability, according to manufacturer's instructions, and maintaining a constant proportion mortar/water for every batch. This procedure led to approximately to the same plasticity of mortar that enabled to easily lay the bricks.
- Control of the thickness of the joints and of the dimensions of the final panels.
- Control of the planarity of the samples and of the bed joints.
- Finally, application of a rough thin layer of rendering on the bricks to improve the adhesion of the rendering.
- After execution, spilling of the walls with water to avoid a quick drying of the mortar. Then, the specimens were kept under relatively stable conditions of temperature and humidity within the laboratory.

Figure 53. Construction of the walls. Leveling and control of bed joint thickness.
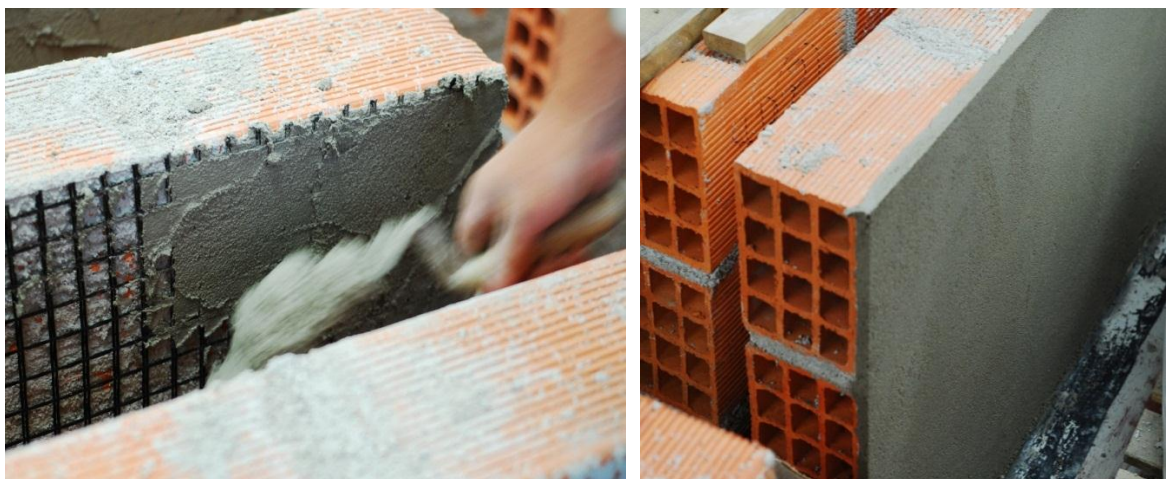
Figure 54. Application of reinforcement meshes in the render.

Two weeks later, the production of the samples was completed with the implementation of the reinforcement materials, both commercial and self-produced, within a general purpose rendering mortar, as seen in Figure 54. The process aimed, as previously explained, to obtain the highest homogeneity of conditions, taking care of following the same steps for every sample and to maintain constant conditions in the mortar.

Before the application of the retrofitting materials, the walls were swept to clean possible dust or imperfections that could affect adherence, and then spilled with water to avoid that the bricks absorbed the water of the mortar making it dry too quickly. Then, the mesh was applied within a first layer of mortar of with a thickness of approximately 6 mm. Then, a second thinner layer of mortar of about 4 mm was applied to regularize the surface, and finally a very thin layer of finishing. In average, the thickness of the render is of 12 mm.

5.1.4. Definition of the retrofitting schemes.

In total, five different retrofitting schemes will be tested. As mentioned in the previous section, the retrofitting meshes are characterized by the reinforcement density, spacing of the yarns and tensile capacity (Table 9). In Figure 55, the plans of the meshes manufactured in the laboratory of the textile Department, along with the estimation of necessary material, are provided.

A calculation of the total tensile strength for each retrofitting mesh has been done. For the commercial meshes, this value is provided as tensile strength per metre, and will be adjusted to the tensile width of the walls, corresponding to the height of the samples and equal to 610 mm. For the produced materials in the present work, it will be taken as the value resulting by multiplying the mean tensile strength of each type of rod by the number of rods according to each retrofitting scheme. This is an approximate calculation and need to be confirmed by further tensile tests on the produced meshes. As this work was out of the experimental plan, approximate values are provided.

*Table **9**. Definition of retrofitting schemes.*

Retrofitting material	Reinforcement density (g/m^2)	Spacing (mm)	Tensile Capacity (kN)
2G #6	57	60	9.22
2G#3	114	30	18.44
4G#6	114	60	11.97
Mapei	225	25	27.45
S&P	200 (unidirect.)	20	57.1
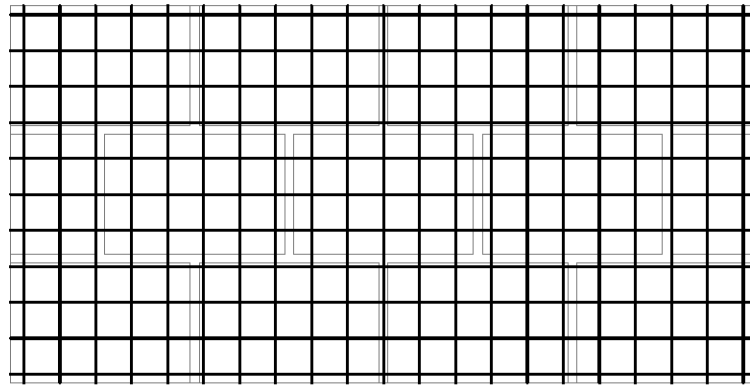
grid 6 cm 22x61 + 11x122 = 27.61 metres
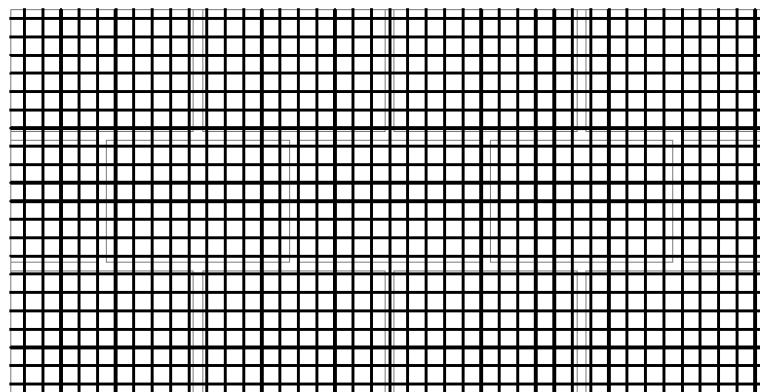
grid 3 cm 43x61 + 21x122 = 53.34 metres

Figure 55. Retrofitting schemes of textile composite meshes composed from the association of composite textile rods

5.2. Mortar control and testing.

The mortar for both the masonry and the rendering was controlled through samples acquired and tested according to UNE EN 1015-11 (1999) – flexural and compressive strength. The sample size was 160x40x40 mm, and they were tested under three-point bending and to compression.

During the building process, a set of three samples was taken for every two walls. Then, during the application of the reinforcement, and given that a different type of pre-mixed mortar was used, new samples were obtained. The samples were kept in the same environmental laboratorial conditions than the walls, even if the standard specifies other type of conditions. The procedure of testing the samples was done immediately afterwards the experimental campaign of the walls, with the equipment and setup as shown in Figure 56.

Figure 56. Mortar flexural strength test.

The obtained data showed a slightly high variation in the results, due probably to the manual elaboration of the mortar, which cannot be controlled as strictly as the one processed mechanically. Detailed data of the results of the tests is available on annexes. The average compressive strength for laying brick units was 9.34 MPa, with the lowest value of 7.9 MPa, and the highest of 11.1 MPa. This value is slightly under the 10 MPa given by the specifications (M10), but again, it can be due to a higher quantity of water required to have a proper workability. The average flexural strength was of 2.94 MPa.

For the render, the average compressive strength was of 9.18 MPa, higher than the minimum value provided by the producer and the average flexural strength of 3.45 MPa. The average compressive Elasticity Modulus estimated in the machine is of 565 MPa.

5.3. Brick control and testing.

The bricks were tested to uniaxial compressive load in the direction of the perforations, given that this is the direction in which it will be compressed when the masonry is tested to bending in the perpendicular direction to the bed joints, as seen in Figure 57. The samples of bricks were selected with as less imperfections as possible, and were prepared for the testing by capping them with two regularizing surfaces of mortar on each end. It should be noticed that the defects such as small cracks resulting from the curing process, variability of dimensions and possible lack of leveling are common is brick units used in infill walls.
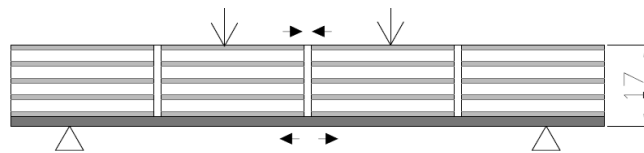
Figure 57. Direction of compression in bricks imposed by flexure perpendicular to the bed joints.

Four samples were tested in a loading machine with a capacity of 2000kN according to UNE EN 771-2 00, using a load rate of 0.05 (N/mm^2)/s (Figure 58). The obtained data is shown in Table 10. It is seen that the maximum stress is lower than the normalized one. Sample 3 is considered non relevant due to unexpected mode of failure caused by irregularities of the regularizing mortar. The obtained average value must be normalized due to the dimensions of the unit. Given the height of 300 mm and the width 140 mm, the correction factor δ is 1.35, and the normalized strength in the parallel direction to the perforation is f_b=6.1 MPa. The typical failure mode of the bricks is presented in Figure 59.

Table 10. Brick compressive strength.

Sample	1	2	3	4	Average
Load (kN)	125.9	117.6	76.6	112.9	118.9
Stress (MPa)	4.7	4.5	2.8	4.3	4.5

Figure 58. Equipment.   *Figure 59. Characteristic failure of the samples.*

5.4. Design of the test setup.

The test setup is composed of a steel frame connected to a reaction walls to which a hydraulic jack, with a load capacity of 500 kN connected to a load cell of 200Kn is associated (Figure 60). Given that it is used in a low load regime in comparison to the maximum capacity, the obtained results present some noise as will be seen later.

With respect to the test setup, some literature was reviewed for other examples of similar tests. It is possible to find three-point bending tests in Papanicolau and Triantafillou (though used for cyclic loading), carried out through control of the displacement at midspan. The used scheme is very similar to the one used in [39], more correspondent to what established in standards UNE-EN-1052-2-99 for flexural strength of masonry. Other tests with similar purposes of assessing different materials for out-of-plane reinforcement of masonry used punching tests [27].

The flexural free span was set as 1000 mm, according to the possibilities of the auxiliary structure. The distance between the two lines of application of the load was designed firstly as 500 mm, according to the standards. Nonetheless, given the bad results from the first tests (2G#6_3 and 4G#6_1 which failed by shear giving higher values than what should correspond to flexure), it was decided to reduce it, see Figure 61. Even if it went under standard measures, it was decided to adjust it to the joints. This way, the length was reduced to 350 mm.

The deformation of the samples was measured through three Linear variable differential transformers (LVDT) with a measuring capacity of 50 mm: one in the mid-span and one under each application of the load, as this were expected to be the most likely points for the formation of the cracks and thus the maximum deflection, see Figure 61.

The simple support structural scheme was achieved through the use of metallic rods, adding an interface in-between the rod and the sample composed by two layers of Teflon painted with mineral oil to avoid any unexpected effect of the friction at the supports.

In this case, the load-application control is through fixed displacement. The testing procedure is composed of three steps, according to the different expected mechanisms:

- First step, with a velocity of 0.004 mm/s during the first 6 mm, corresponding to the lower rate achievable by the machine. This is due to the low displacement required for the cracking of the wall (after the first testing, estimated in the order of 1 mm).
- Second step, with a velocity of 0.01 mm/s during the next 4 mm, increasing the velocity as the reinforcement is loaded after the cracking of the wall.
- Last step, with a velocity of 0.02 mm/s, aiming to make time-affordable tests given the high deformation expected, especially for the braided materials.
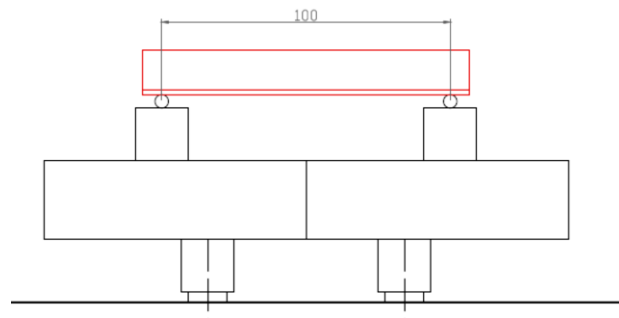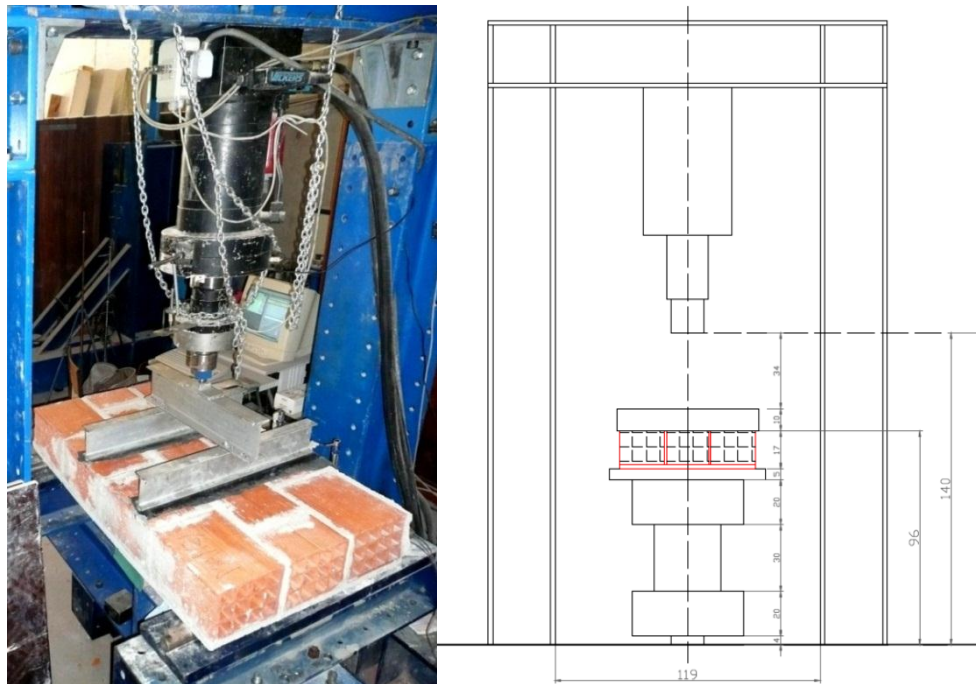
Figure 60. Test setup: arrangement of load cell and auxiliary structure.
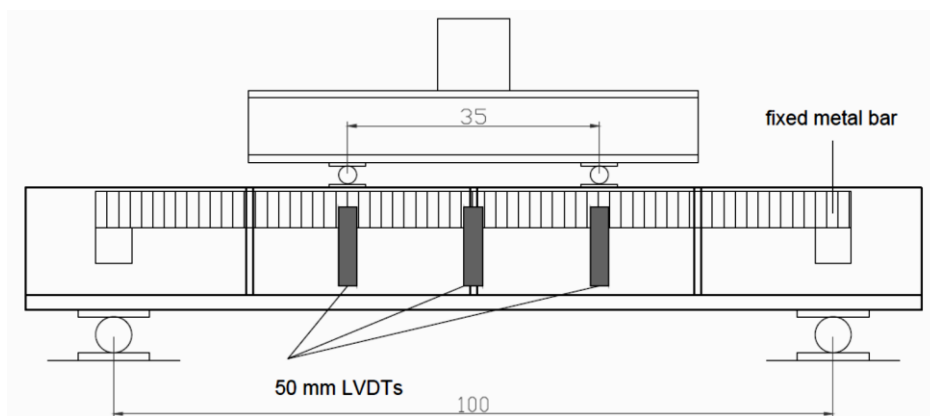
Figure 61. Test setup: supports, load distribution and displacement control.

5.5. Theoretical characterization of the flexural strength of masonry walls

5.5.1. Compressive strength of masonry.

From the properties of the materials analyzed, and according to the formulation from EC6, the compressive strength of the walls can be estimated as follows.

$$f_k = K \cdot f_b^{0,7} \cdot f_m^{0,3}$$

(Eq. 4)

From this value, EC 6 recommends as an estimation of the elasticity modulus of masonry comprised in between 700 and 1000 times the compressive strength:

$$E_m = 1000 \, f_k$$

(Eq. 5)

This compressive strength will be calculated for two directions: the compressive strength in the normal direction to the bed joints, also as a mean of characterization of the masonry quality, and in the direction of the bed-joints, given that this is the direction in which flexural compression will be acting. The strength of the bricks should be considered according to each direction.

The coefficient K used in eq. 4, is taken for the perpendicular direction to the bed joints, according to the type of units. For clay bricks type 4 with general purpose mortar, has a value of 0.35.

The flexural strength is provided directly from EC6, given the type of units and mortar class of resistance, namely: f_{x1} parallel, and f_{x2} perpendicular to bed-joints.

Table 11. Theoretical compressive mechanical of masonry material.

Direction of loading	K	f_b (MPa)	f_m (MPa)	f_k (MPa)	E (MPa)	f_{x1} (MPa)	f_{x2} (MPa)
Perp. to bed joints	0.35	5	9.34	2.11	2111	0.10	0.40
Paral. to bed joints	0.35	6.1	9.34	2.47	2474		

5.5.2. Theoretical estimation of the flexural strength.

This estimation of the flexural strength of the masonry panels tested under four-point loading bending tests will be made based on the classic theory of bending applied to reinforced concrete and reinforced masonry and stated also in EC6. In this approach the equilibrium of forces between the compressive forces conducted by masonry and tensile stresses installed in the reinforcements, as explained in Figure 62. As it will be seen later, this estimation is approximate, mainly due different range of deformations to be assumed, that many times will reach the large displacements and due to

some uncertainty about the tensile strength of the retrofitting materials. Nonetheless, it is valid as a first approach. The derivation of the equations is quite easy but can be seen in [39] and [27]. The values assumed in this calculation will be the estimations on compressive strength of masonry according to EC6, the experimental data obtained in the characterization of both 2G and 4G rods, and the nominal values given by the producers on the commercial meshes.

The use of the equilibrium and compatibility equations implies some assumptions according to the considered material models:

- Plane sections remain plane after bending.
- Strains vary linearly across the section.
- Parabolic distribution of stress in masonry.
- Tensile strength of masonry is neglected.
- Perfect bond among reinforcing layer and masonry.
- The values for the ultimate and peak strains in masonry are taken from Triantafillou [53], as $\varepsilon_{mu}=0.0035$ and $\varepsilon'_m=0.0030$ respectively.
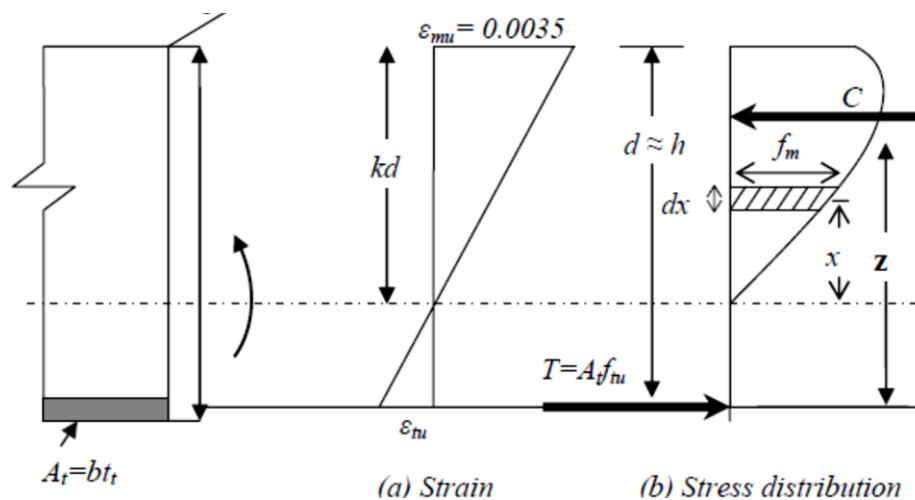
Figure 62. Stress and strain distribution in the wall section [39].

The first step is to verify the reinforcement ratio, and to compare it to the balanced reinforcement ratio, so as to state the failure mode. The balanced reinforcement ratio corresponds to that in which it is expected that there will be simultaneous failure of brick by crushing and of reinforcement by tensile stress. Thus, provided the stress distributions shown in Figure 62, we can have two failure domains, each one implying different formulations, derived from strain compatibility condition and equilibrium in the section: (1) compressive failure of bricks (in case that $\eta_{bal}<\eta$), where ε_{mu}, the ultimate strain defined for the masonry, is the limiting factor or (2) tensile failure of reinforcement, commanded by the value of T_u, or ultimate tensile capacity of the reinforcement (if $\eta_{bal}>\eta$).

The balanced reinforcement ratio, η_{bal}, is given by (Eq. 6:

$$\eta_{bal} = 0.714 f'_m \left(\frac{\varepsilon_{mu}}{\varepsilon_{mu} + \varepsilon_{tu}}\right)$$

(Eq. 6)

The reinforcement ratio, η, is given by the (Eq. 7:

(Eq. 7)

$$\eta = \frac{T}{b \cdot d}$$

The ultimate bending moment is depending on the failure domain. If the failure occurs by crushing of masonry the ultimate bending moment is given by (Eq. 8:

$$M_u = (0.714 - 0.274k) f'_m \cdot b \cdot d^2$$

(Eq. 8)

If the failure occurs by tension of the reinforcement the ultimate bending moment is given by (Eq. 9:

$$M_u = bd^2 f'_m \left(\frac{\varepsilon_{tu}}{\varepsilon'_m}\right) \left[-\left(\frac{k^4}{4(1-k)^2}\right)\left(\frac{\varepsilon_{tu}}{\varepsilon'_m}\right) + 2\left(\frac{k^3}{3(1-k)}\right)\right] + Tu(1-k)d$$

(Eq. 9)

In the previous equations:

b width of the wall, 610 mm; d distance from top surface to the reinforcement, 160 mm

f'_m maximum compressive strength of masonry, estimated in 2.16 MPa

ε_{tu} ultimate strain for each reinforcing solution
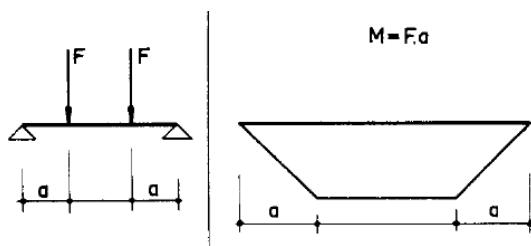
ε'_m peak strain for masonry, taken as 0.003;

ε_{mu} ultimate strain for masonry, taken as 0.0035

$k = \frac{\varepsilon_{mu}}{\varepsilon_{mu} + \varepsilon_{tu}}$ is the ratio between the depth of the neutral axis and d

T_u total ultimate tensile capacity of each reinforcing solution

From moments calculated according to eq. 8 or eq. 9 the estimated load can be derived from the test setup load configuration:

$$M = \frac{F}{2}a \quad ; \quad F = \frac{2}{0.33}M.$$

(Eq. 10)

The estimated values for the ultimate load are indicated in Table 12.

Table 12. Theoretical ultimate loads for each reinforcement type.

	T (kN)	ε_{tu}	k	η	η_{bal}	Failure	M_u (kNm)	F_u (kN)
2g#6	9.22	0.036	0.089	94	156	Tensile	1.48	8.95
4g#6	11.97	0.056	0.059	123	103	Compressive	1.58	9.56
2g#3	18.44	0.036	0.089	189	156	Compressive	2.35	14.23
Mapei	27.45	0.03	0.104	281	184	Compressive	2.75	16.67
sp	57.1	0.0175	0.167	585	293	Compressive	4.28	25.93

5.5.3. Calculation of theoretical ultimate moment for large displacements

Another theoretical approach can be considered under the scope of assessing if the performance of the reinforcement fulfilled the expected values. All the reinforced samples develop their highest load resisting capacity after cracking and undergoing displacements that most of the times are out of the range considered by continuum mechanics models The nominal out-of-plane moment capacity of the wall specimens, Mn, can be calculated using a simple physical model associated with the failure mode shown in Fig. 12, in which the compression force across the depth of the section is assumed to be concentrated at or near the tip of the block, as observed from the failure mode of the specimens. The procedure is adapted from Harajli [50].
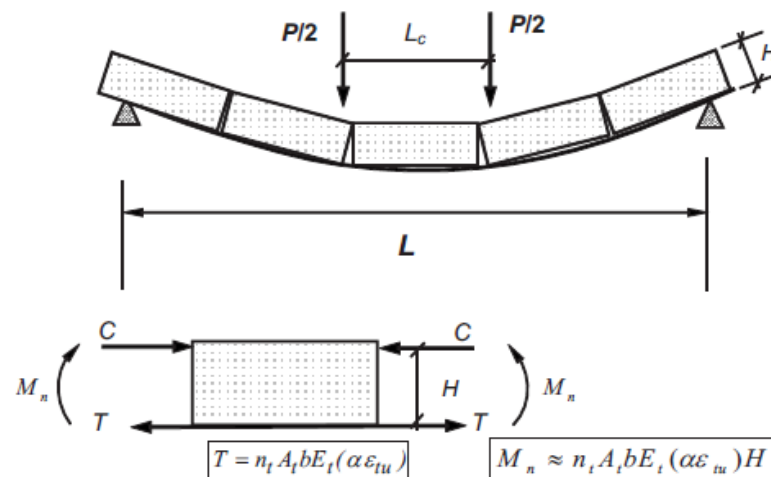
Figure 63. Estimation of ultimate moment from the ultimate elongation in the reinforcements.

The ultimate moment is estimated, considering the equilibrium of the section, as:

$$M_u \cong T_u \cdot H$$

(Eq. 11)

The ultimate tensile capacity is estimated for the braided composite materials as the addition of the tensile capacities of the number of rods composing the mesh, and for the commercial solutions it is given as tensile capacity per metre, as was resumed in Table **9**. The estimated maximum loads to obtain in the procedure are deduced from (Eq. 10, obtaining the values showed in Table 13.

Table 13. Theoretical ultimate loads for each reinforcement type.

	T_u (kN)	M_{max} (kNm)	Max Load (kN)
2g6	9.22	1.4752	8.85
4g6	11.97	1.9152	11.49
2g3	18.44	2.9504	17.70
Mapei	27.45	4.392	26.35
s&p	57.1	9.136	54.81

The comparison of the obtained values with the experimental ones will be a measure of the effectiveness of the reinforcements to attain their maximum theoretical strength, or if some capacity is taken by phenomena as sliding or debonding.

5.6. Assumptions for analysis of experimental results.

In the subsequent section, an overview of the obtained results will be provided on the purpose of extracting the main features of the behaviour that define each reinforcement typology. There will be a special interest on analyzing the parameters that measure the effectiveness of each solution, namely:

- Maximum load in elastic regime, and if it is increased in comparison with the unreinforced samples. This would show that the reinforcement has an effective capacity of diminishing the initial damage to masonry and naturally on the improving flexural strength.
- Post-cracking behaviour, with increase or decrease of the loading capacity.
- Possible modifications on the stiffness of the wall.
- Increase on the ultimate deformation and ductility
- Failure mode, focusing on the existence of redistribution of load, , being this a feature of the safety improvement provided by each solution.

The quantifiable parametres to be obtained, as seen in Figure 64:

- Load and deflection for the limit of the elastic state.
- Maximum attained load.
- Maximum deflection considered until the sample ceases to have load bearing capacity.
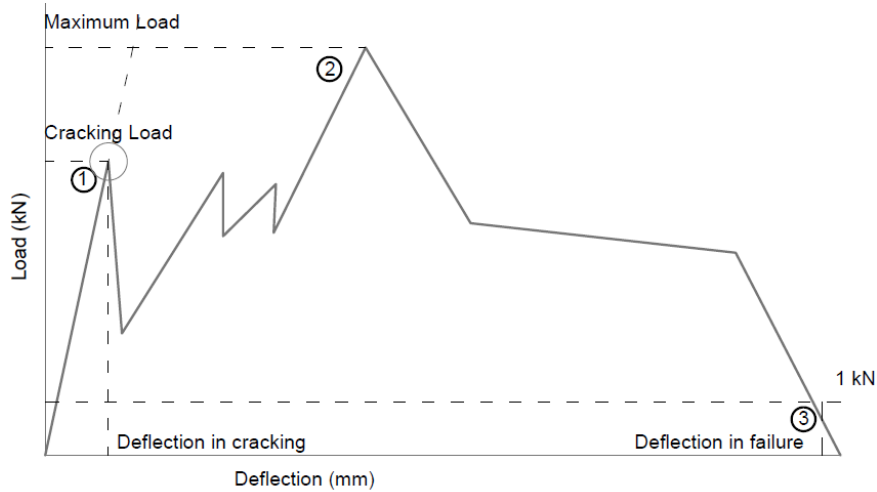
Figure 64. Representative parametres in the load-deflection diagram.

5.6.1. Measurement of displacements.

The displacements are measured using the data acquired through the LVDTs installed in the test setup. Nonetheless, this is only valid for the first range of displacements, given that the high deflections that are obtained for many reinforced samples went out of the measuring range of the LVDTs. This way, the deflections will be measured in two ways:

- For the elastic range, the deflection will be the maximum of the deflections registered in the LVDTs installed in the sample, given that for their distribution (one in the midspan and one on each point of load application) there is always one of them measuring the maximum deflection.

- For big deflections out of the range of the LVDTs, a linear relation will be established among the internal displacement control of the machine and the measured deflections on the point of maximum deflection, as seen in Figure 65. It is noticeable how in the first part of deformation, the measure given by the internal control is not reliable, given the initial deformation of the system of transmission of loads.
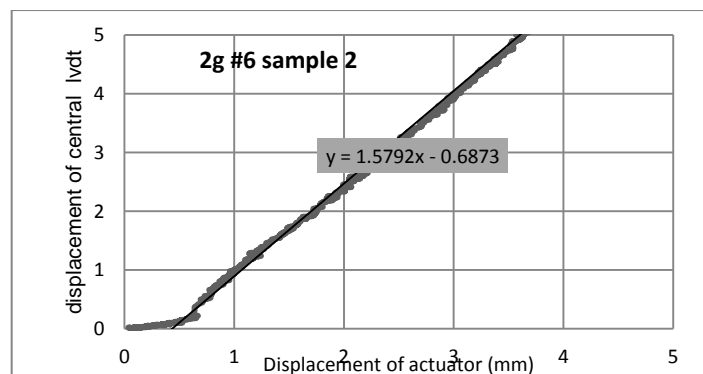
Figure 65. Relation of measured displacements in a given sample.

5.6.2. Calculation of flexural stress within the elastic range.

The flexural stresses in the masonry, from which the tension in the reinforcements can be derived, will be calculated according to the formulation given by the standards for flexural testing of masonry UNE EN 1052-2-99.

$$\text{fxi} = \frac{3F_{i,max} \cdot (l_1 - l_2)}{2bt_u{}^2} \; N/mm2 \qquad \textbf{(Eq. 12)}$$

For all posterior calculations, l_1-l_2= 650 mm, b=630 mm, t_u=170mm.

5.6.3. Estimation of elastic modulus.

For the elastic phase of the deformation of the masonry, it will be used the analogy with beam theory to have an estimation of the elastic modulus, considering that masonry is an homogeneous material. Given that the applied force and the corresponding deflection are obtained experimentally, and knowing the geometry of the samples, it is possible to apply the formulation for deflections in order to estimate the elastic modulus.

Thus, by calculating the deflection of the masonry specimen by eq. 12, corresponding to a deflection of a beam submitted to four point loading configuration and equalize to the measured experimental deflection it is possible to derive and estimated value for the elastic modulus.
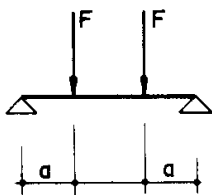
$$\text{deflection} = \frac{F \cdot a}{24\,EI} \cdot (3l^2 - 4a^2) \qquad \textbf{(Eq. 13)}$$

5.7. Typologic analysis for each type of reinforcement.

In the following pages, the data obtained for the tests will be summarized and exposed with a brief description, for each type of reinforcement. This will allow to extract quantifiable values, as well as common features of the behaviour, in order to be able to make comparisons among different types.

5.7.1. Unreinforced masonry. Reference samples.

It is noticeable the uniformity in the results, with low scatter for all the studied parametres. The obtained flexural strength was 11% higher than the EC6 suggested value (Table 14). This means that the experimental load approaches reasonably the estimated value. As expected, the material is very stiff, with a very low displacement until the peak load is attained (Figure 63). This gives even an error of a residual resistance after the failure which is not realistic. Even if the loading rate was set for the minimum possible for the used load cell, the samples broke in an average of 3 minutes.

Table 14. Obtained values for unreinforced masonry.

	ur_1	ur_2	ur_3	AVERAGE
Max. elastic load (kN)	8.498	8.586	8.371	8.485
Max elastic deflection (mm)	0.164	0.175	0.157	0.165
Max elastic flexural stress (MPa)	0.451	0.455	0.444	0.451
Modulus of elasticity (MPa)	3540	3352	3643	3512
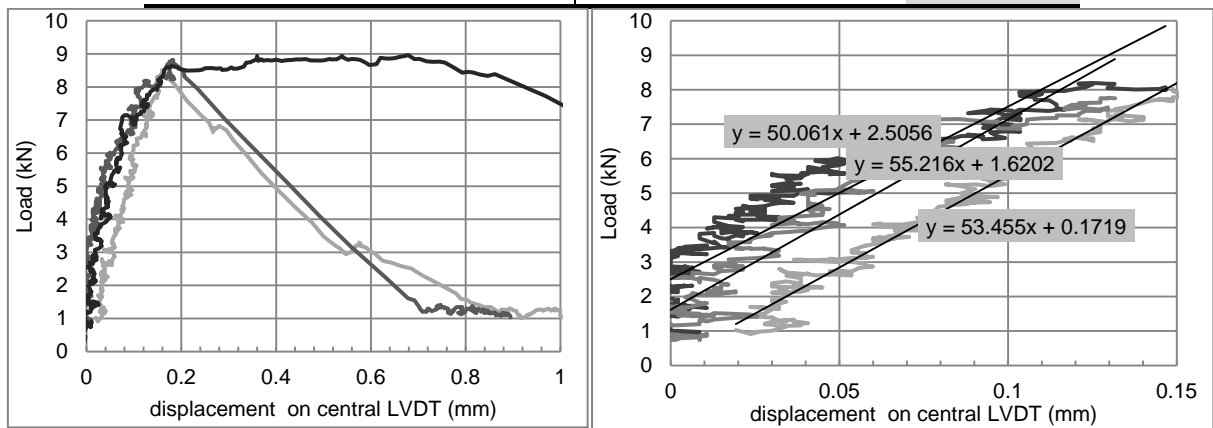
Figure 66. Behaviour of unreinforced samples in elastic range. Estimation of stiffness.
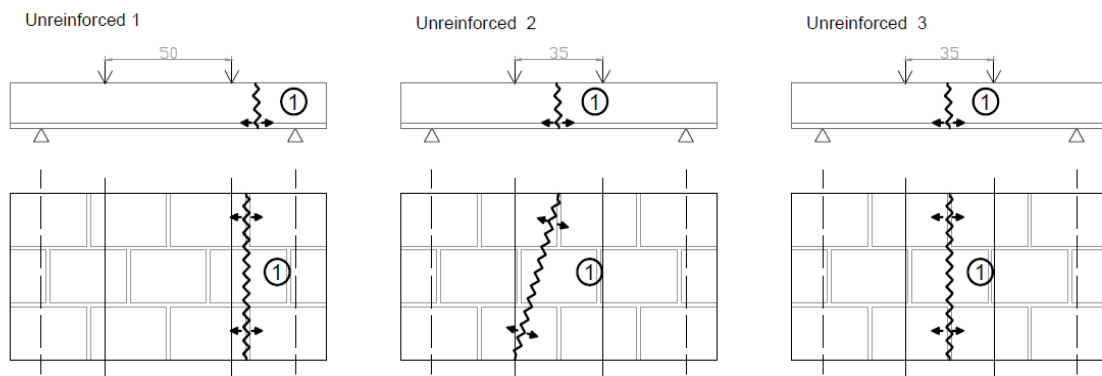
Figure 67. Crack pattern for unreinforced samples

5.7.2. Masonry specimens retrofitted with 2G #6.

This is the sample with the lowest ratio of reinforcement, using rods with two yarns of glass fibre spaced 60 mm.

No improvement of the cracking load is observed, being within the range of the unreinforced samples, as seen in Table 15 and Figure 66

Besides, no redistribution of stresses was observed either. After the development of a localized crack, see Figure 69, the load bearing capacity drops abruptly, and then raises as the deformation increases and the rods develop their strength capacity. This behaviour appears to be related to the behaviour of the polyester external braid, given its low elastic modulus and high deformability. Therefore, the function of glass fibre at this very low reinforcement ratio is not noticeable. This was expected if the values of maximum load for unreinforced walls and the maximum load for this type of reinforcement according to the estimation with large deflections are compared. The function of the reinforcement is mostly keeping the crack opening controlled by promoting the connection between both individual bodies in which the sample is divided after the failure (Figure 69), promoting at the same time a great capacity of deformation of the specimen, see Figure 65. This behaviour corresponds more to kinematic equilibrium of bodies than to pure flexural behaviour. This can be compared with solutions like polymeric grids [40].

After a large deflection of about 28 mm implying an open crack, the rods start to fail individually, leading to a progressive reduction of the load bearing capacity. Nonetheless, this reduction occurs slowly, and it still allows a bigger displacement before the complete failure of the sample.

It should be stressed that sample 3 should not be taken into account, as its failure was in shear mode, within the first samples tested with a different setup of the load distribution, and thus it is not taken into account.

Table 15. Obtained values for 2G#6 reinforcement.

	2g6_1	2g6_2	2g6_3	AVERAGE
Max. Elastic load (kN)	8.157	7.22	13.28	7.68
Max elastic deflection (mm)	0.151	0.148	0.253	0.149
Max elastic flexural stress (MPa)	0.433	0.383	0.705	0.408
Modulus of elasticity (MPa)	3691	3334	3587	3512
Max load (kN)	10.09	8.85	13.28	9.47
Max deflection observed (mm)	54.37	48.55	87.2	51.46
Position max deflection	lateral	central	lateral	
Conversion ratio of deflection	1.11	1.57	1.29	1.34
Max deflection calculated (mm)	60.35	76.22	112.5	68.28
Load redistribution	NO	NO	NO	
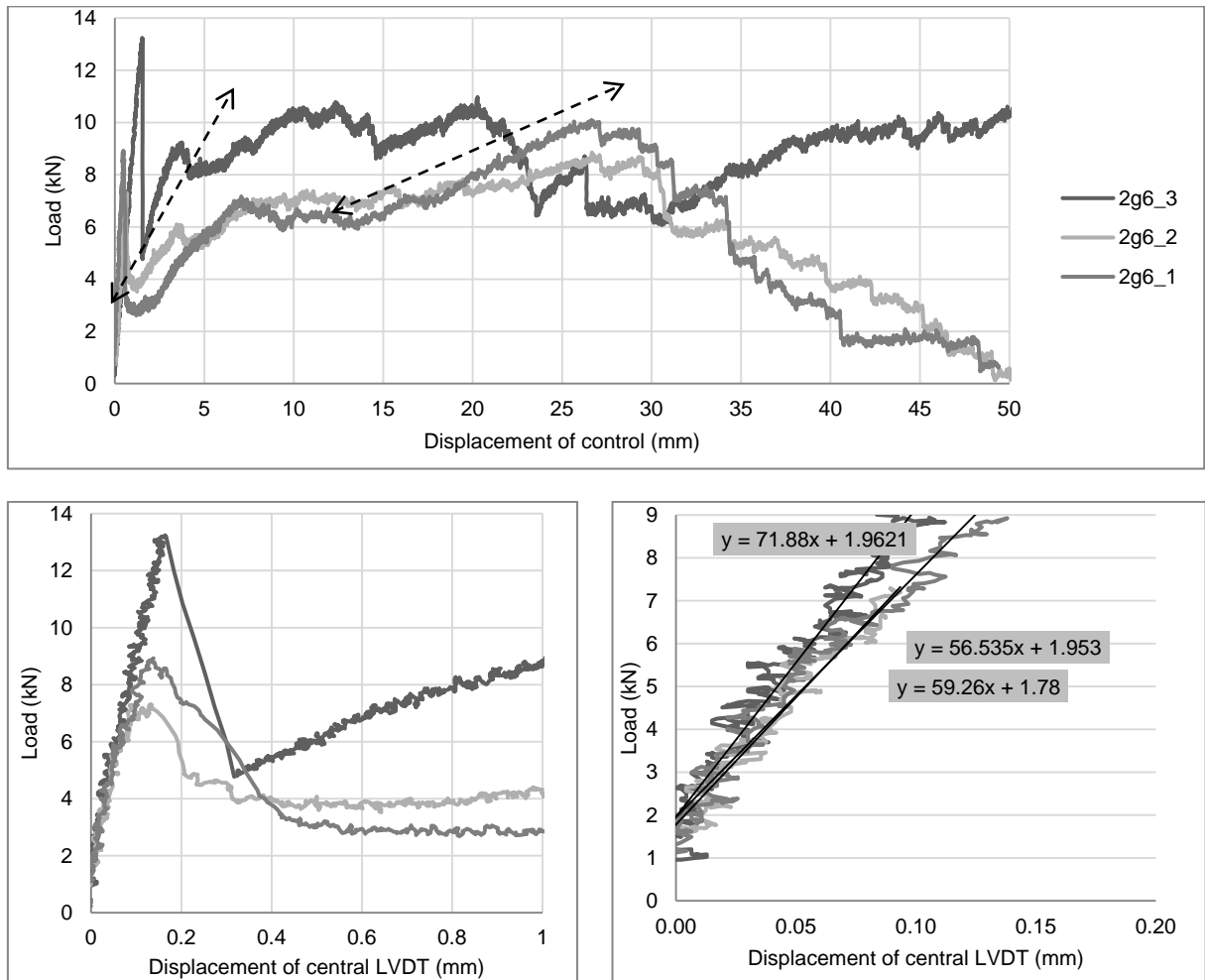
Figure 68. Load-displ. diagrams,2G#6: General behaviour. Elastic range. Estimation of stiffness.
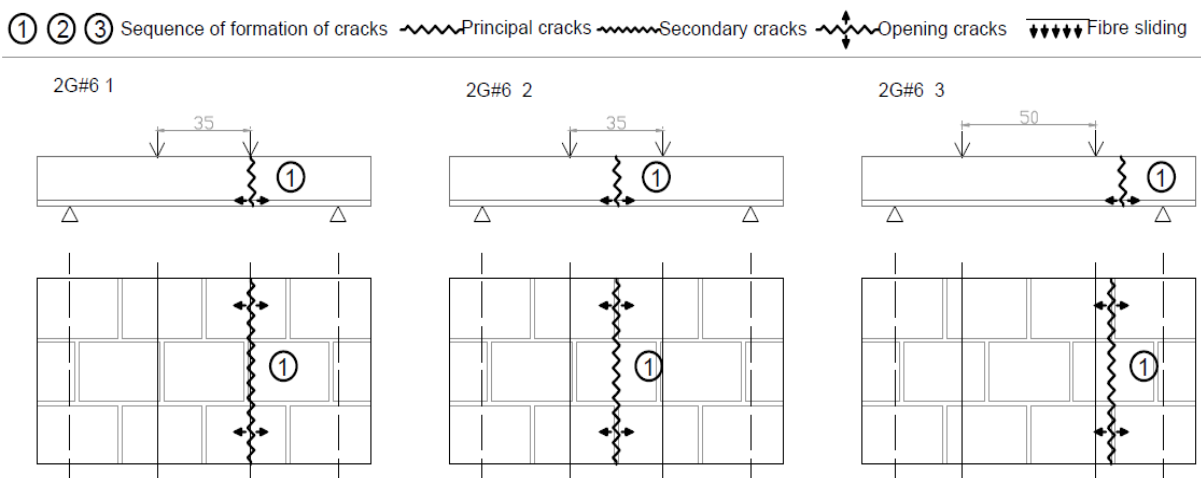
Figure 69. Specimen retrofitted with 2G#6: Crack pattern.

5.7.3. Masonry specimens retrofitted with 4G #6.

By using the mesh 4G#6, glass fibre amount is the double of the one considered for 2G#6. Even if it is the same than in the following series, 2G#3, the expected performance is lower, given that the tensile force of 4G rods is not double that of 2G rods, as was explained in chapter 3.

As in previous series of samples, no improvement of the cracking load is observed compared to the unreinforced control samples, see Figure 67.

Only in one of the samples it is observed a slight redistribution of the stress after reaching the cracking load, maintaining the load bearing capacity for a small increase of deformation. Nonetheless the cracking is localized, and after its development, the load bearing capacity diminishes, and then raises as the deformation increases and the rods develop their strength capacity, see Figure 71.

An increase on the load bearing capacity occurs until a deflection of about 17 mm with the development of an open crack is attained. In average the flexural strength (10.4kN) increases about 19% in relation to the cracking load (8.44kN) At this time, the rods start to fail individually, leading to a progressive reduction of the load bearing capacity as seen in the previous series.

Sample 1 should not be taken into account, as its was within the first samples tested with a different load distribution, and showed an unexpected failure mode.

Sample 2 developed a slight stress redistribution with opening of multiple small cracks previously to the developing a localized macro-crack.

Table 16. Obtained values for 4G#6 reinforcement.

	4g6_1	4g6_2	4g6_3	AVERAGE
Max. Elastic load (kN)	12.69	8.57	8.31	8.44
Max elastic deflection (mm)	0.196	0.27	0.2	0.235
Max elastic flexural stress (MPa)	0.673	0.455	0.441	0.448
Modulus of elasticity (MPa)	4424	2168	2839	2504
Max load	12.69	10.2	10.59	10.395
Max deflection observed (mm)	34.29	32.51	27.47	29.99
Position max deflection	central	central	central	
Conversion ratio of deflection	1.09	1.57	1.26	1.415
Max deflection calculated (mm)	37.37	51.04	34.61	42.82
Load redistribution	NO	YES	NO	

Figure 70. Load-displ. diagrams, 4G#6: General behaviour. Elastic range. Estimation of stiffness.
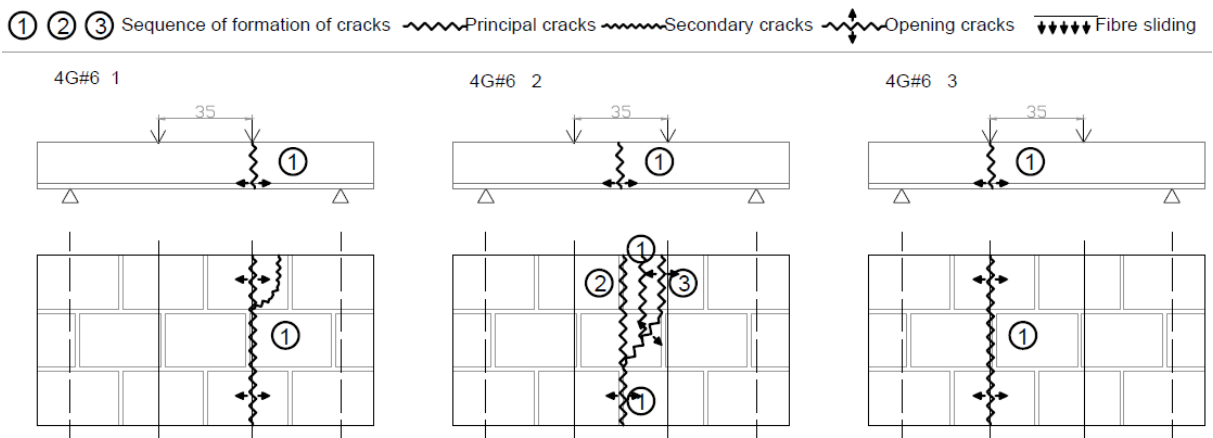
Figure 71. Specimen retrofitted with mesh 4G#6: Crack pattern.

5.7.4. Masonry specimens retrofitted with 2G #3.

The samples retrofitted with the mesh 2G #3 present the highest reinforcement ratio within the innovative materials, using rods with two yarns of glass fibre spaced 30 mm. It is seen that even in this case, no significant improvement of the cracking load is observed. However, it is observed a very good behaviour in terms of stress redistribution. The load bearing capacity only drops significantly in one of the cases, and is maintained or increases slightly in the others in the immediate term, see Figure 72. After this stage, the flexural strength increases significantly, reaching new peaks as new cracks appear, which seems to be the results of the redistribution of stresses resulting in multiple cracking (Figure 73). The increase in load bearing capacity after every peak is very similar in their slope, which is associated with the behaviour of glass fibre. After a new more pronounced peak, one of the cracks starts to open, but the load bearing capacity continues to grow. From here, the governing slope is more associated to the polyester.

The strengthening of the samples increases until reaching an unusually large deflection that in average can be taken as 50 mm (in a span of 1000mm), with the development of a main macro- crack. After this, the rods start to fail individually, leading to a reduction of the load bearing capacity that occurs in a more sudden way than in the previous series. The masonry specimens with this typology of retrofitting presented the more flexural-like failure, with deformations tending to arch shape (bending curvature) and signs of slight brick crush in the compressed part.

It is important to remark that even for this reinforcement ratios, and very large displacements, there was no visible sign of sliding of the fibres within the mortar matrix, which should be taken as a positive assessment of the functions predicted for the braided shell.

Sample 3 was slightly damaged during its manipulation previously to the tests, and possibly some microcracking occurred, which would explain its lower cracking load, as well as its better stress redistribution after the first crack opening.

Table 17. Obtained values for 2G#3 reinforcement.

|	2g3_1	2g3_2	2g3_3	AVERAGE
Max. Elastic load (kN)	9.447	8.58	7.668	8.565
Max elastic deflection (mm)	0.267	0.184	0.344	0.265
Max elastic flexural stress (MPa)	0.501	0.455	0.407	0.454
Modulus of elasticity (MPa)	2417	3186	1523	2802
Max load (kN)	18.05	19.71	15.727	17.829
Max deflection observed (mm)	66.45	79.35	73.68	73.16
Position max deflection	central	central	lateral	
Conversion ratio of deflection	1.09	1.2	1.25	1.18
Max deflection calculated (mm)	72.43	95.22	92.1	86.58
Load redistribution	YES	YES	YES	
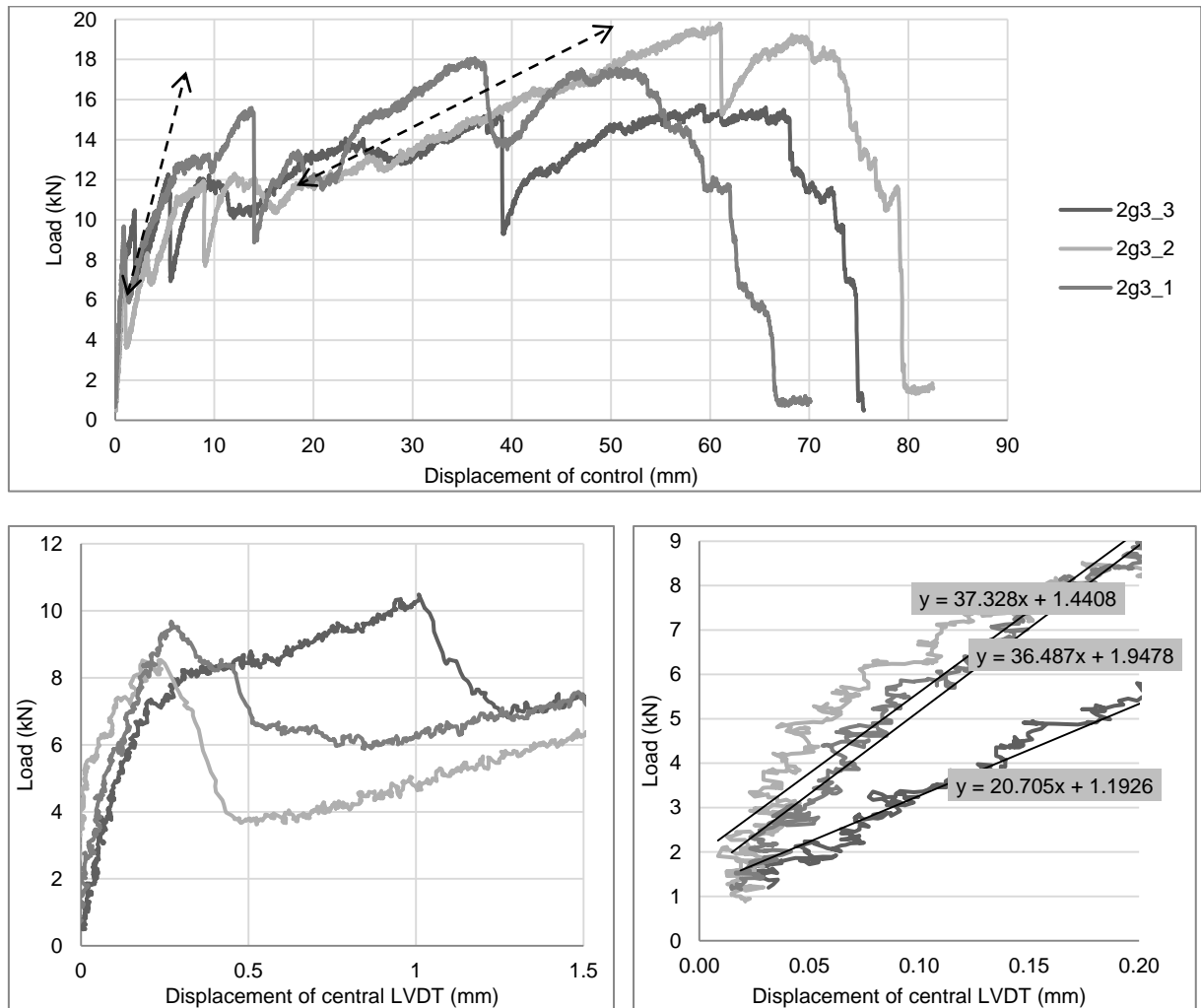
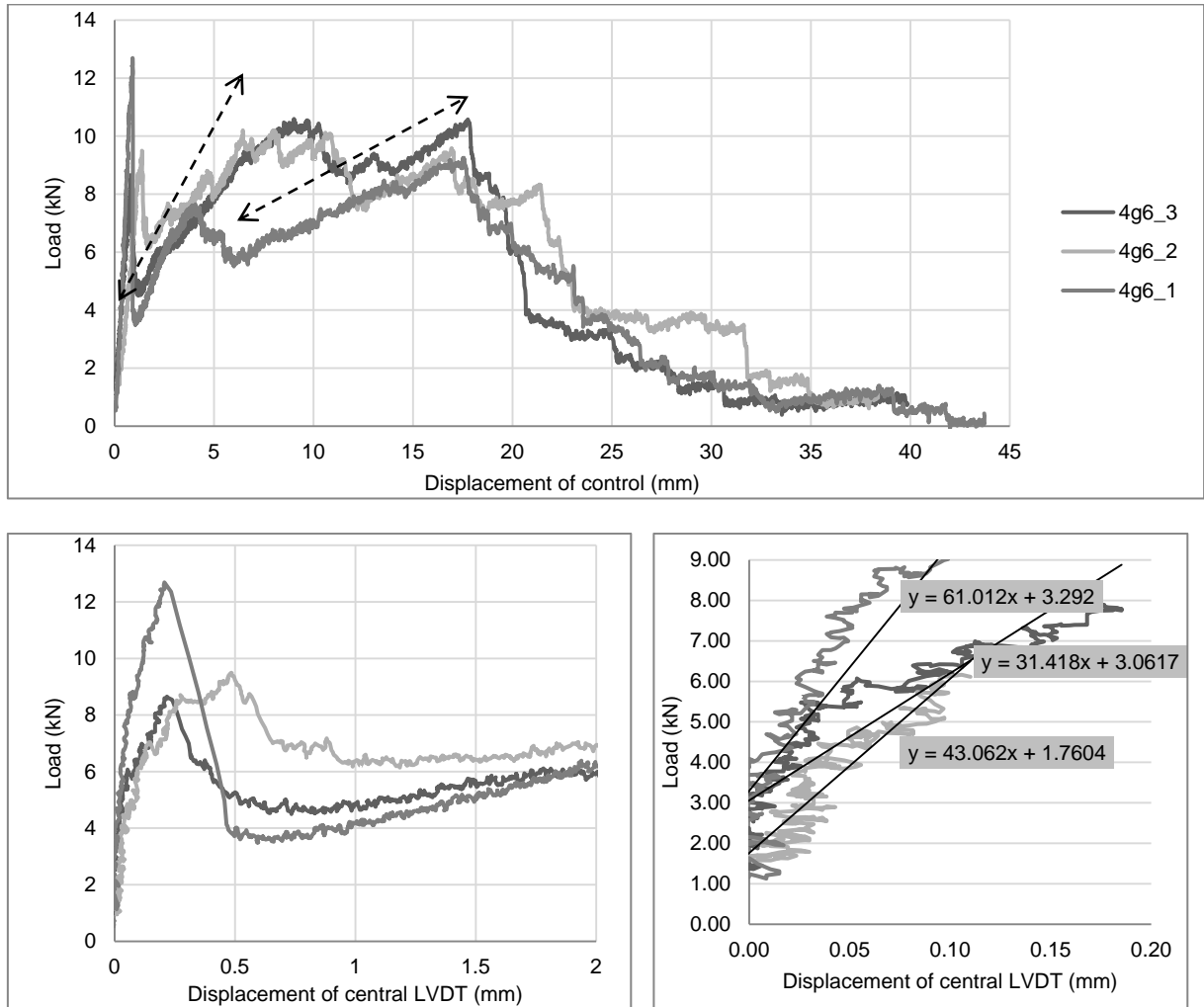Figure 72. Load-displ. diagrams, 2G#3: General behaviour. Elastic range. Estimation of stiffness.
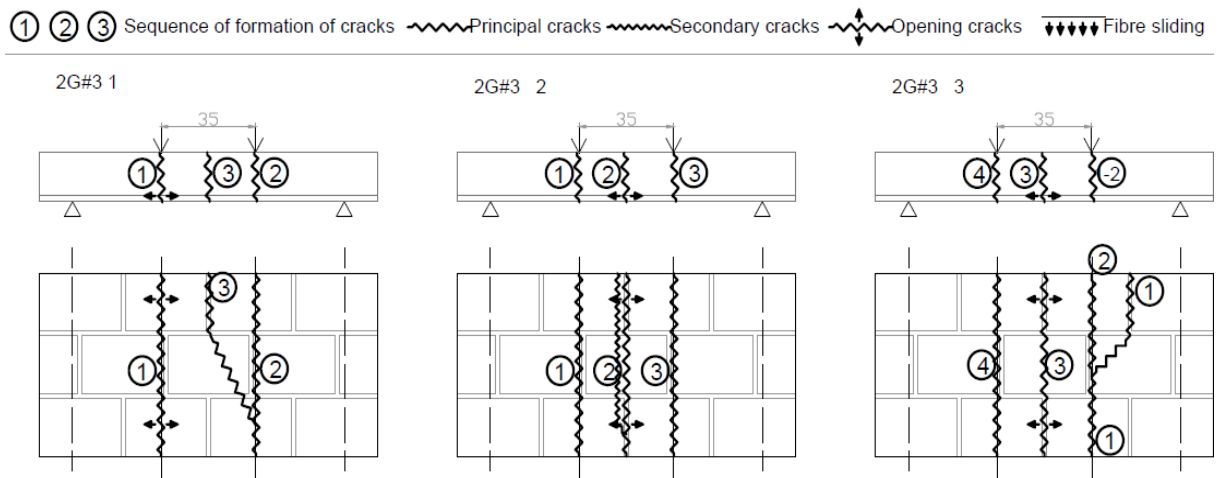
Figure 73. Specimen retrofitted with mesh 2G#3: Crack pattern.

5.7.5. Masonry specimens retrofitted with Mapei Mapegrid.

The commercial mesh from Mapei is composed of the same base reinforcing material than the innovative materials, glass fibres. However, reinforcement ratio is considerably higher. Besides, the small spacing among the yarns guarantees a very uniform behaviour.

A slight improvement of the cracking load is observed, being in average approximately 25% higher than the unreinforced specimens, though with the same displacements, having thence a stiffer behaviour, see Table 18.

After the first cracking, only one of the samples presents a drop of the load bearing capacity, see Figure 71. In general terms, it is maintained, never dropping below the average value of the unreinforced masonry. There is a very good redistribution of the load, with the development of several thin cracks without a definite opening of any of them. The opening of these cracks implies lowerings on the load bearing capacity, though in a growing tendency until reaching a maximum load of about 23 kN is observed. The peak load is attained for a deflection of about 12 mm.

Once this point is reached, there are two different behaviours leading to failure; (1) in samples 1 and 2, the reinforcement fails to tensile strength uniformly, giving a brittle failure; (2) sample 3 continues to deform with a decreasing load bearing capacity and a continuous opening of one of the cracks. This behaviour can be explained as the starting of some sliding of the fibres, though this could not be verified visually.

In samples 1 and 3, the direction of one of the cracks, developing from the load application towards the support, is an indicator of a mixed failure mode of flexion and shear, as can be seen in Figure 75. Specially in sample 3, final failure is due to shear.

Table 18. Obtained values for Mapei reinforcement.

|	mapei_1	mapei_2	mapei_3	AVERAGE
Max. Elastic load (kN)	10.19	12.86	9.65	10.9
Max elastic deflection (mm)	0.132	0.155	0.148	0.145
Max elastic flexural stress (MPa)	0.541	0.682	0.512	0.578
Modulus of elasticity (MPa)	5247	5669	4455	5124
Max load (kN)	24.65	24.09	21.41	23.38
Max deflection observed (mm)	12.58	12.06	39.8	21.48
Position max deflection	central	central	central	
Conversion ratio of deflection	1.006	1.04	1.107	1.051
Max deflection calculated (mm)	12.65	12.54	44.05	12.59
Load redistribution	YES	YES	YES	
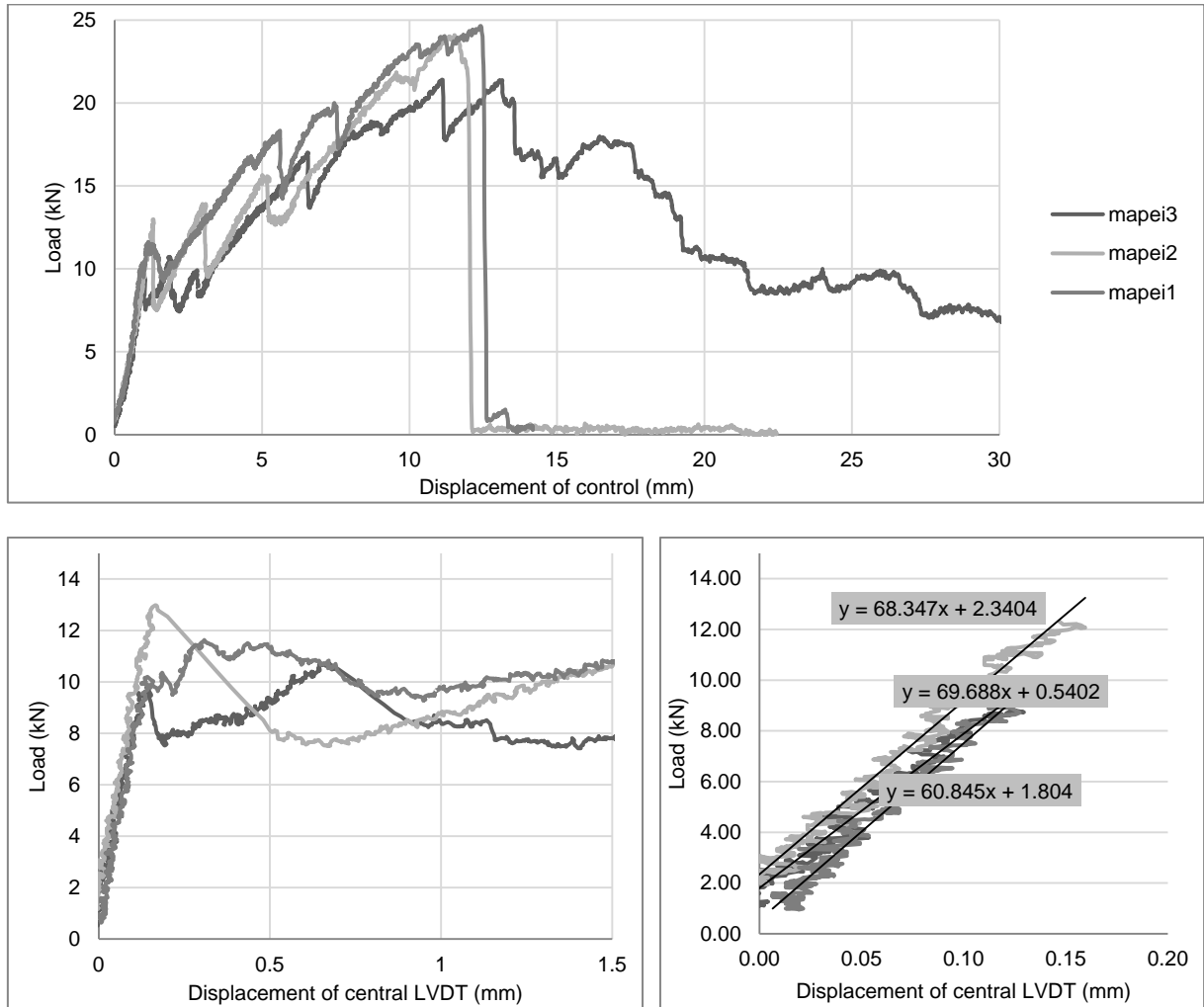
Figure 74. Load-displ. diagrams, Mapei: General behaviour. Elastic range. Estimation of stiffness.
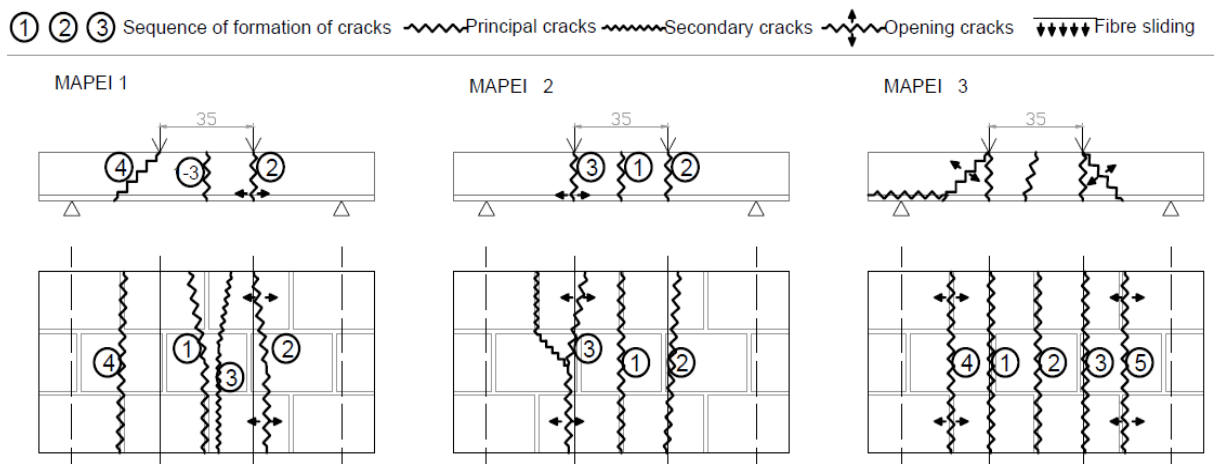
Figure 75. Specimen retrofitted with mesh from Mapei: Crack pattern.

5.7.6. Masonry specimens retrofitted with the mesh from S&P.

This commercial solution presents both the highest reinforcement ratio in terms of mass, the stiffest material, carbon fibres, and a different disposition given that it's an unidirectional reinforcement.

The use of this commercial solution lead to an enhancement of the first cracking load, of around 20 % compared to the unreinforced samples, see Table 19.

The most remarkable feature of its behaviour is the quick redistribution of the loads and the developing of several thin cracks. The formation of cracks does not imply the dropping on the load bearing capacity, but just a lowering of the stiffness (cracked stiffness), see Figure 76. The load bearing capacity continues to increase at a lower rate until a load level that is the triple of the cracking load, at which one of the cracks starts becomes a macro-crack, see Figure 77. Then, the load bearing capacity drops fastly, gets stabilized and regains some magnitude.

Nevertheless, this load recover is quickly stopped, and a slow diminution of the load bearing capacity starts, with a very lineal rate. This is due to the triggering of the sliding of the fibres within the mortar matrix. For this mechanism to happen, it is needed the complete debonding of the fibres, which happens after some fluctuation of load in the post-peak regime. Then, the lowering of the load capacity is linked to the same mechanism of the sliding. Once the stationary sliding begins, the tensile force is a product of the friction and the length of the fibres within the mortar. As it slides, the fibre is taken out of the mortar in the crack, and the length remaining within the mortar diminishes. This is probably an unrealistic representation of reality of masonry panels, given that the sliding starts always from the free border closest to the macro-cracks, meaning that the bond length can not be enough to develop a realistic bonding force.

The tests were stopped before the full failure of the walls, given that this is not a representative behaviour, obtaining all the same very large displacements.

Table 19. Obtained values for S&P reinforcement.

|	sp_1	sp_2	sp_3	AVERAGE
Max. Elastic load (kN)	9.47	11.37	10.97	10.60
Max elastic deflection (mm)	0.207	0.159	0.228	0.198
Max elastic flexural stress (MPa)	0.502	0.603	0.582	0.563
Modulus of elasticity (MPa)	3126	4886	3287	3766
Max load (kN)	30.96	30.44	35.68	32.36
Max deflection observed (mm)	very large	very large	very large	
Load redistribution	YES	YES	YES	
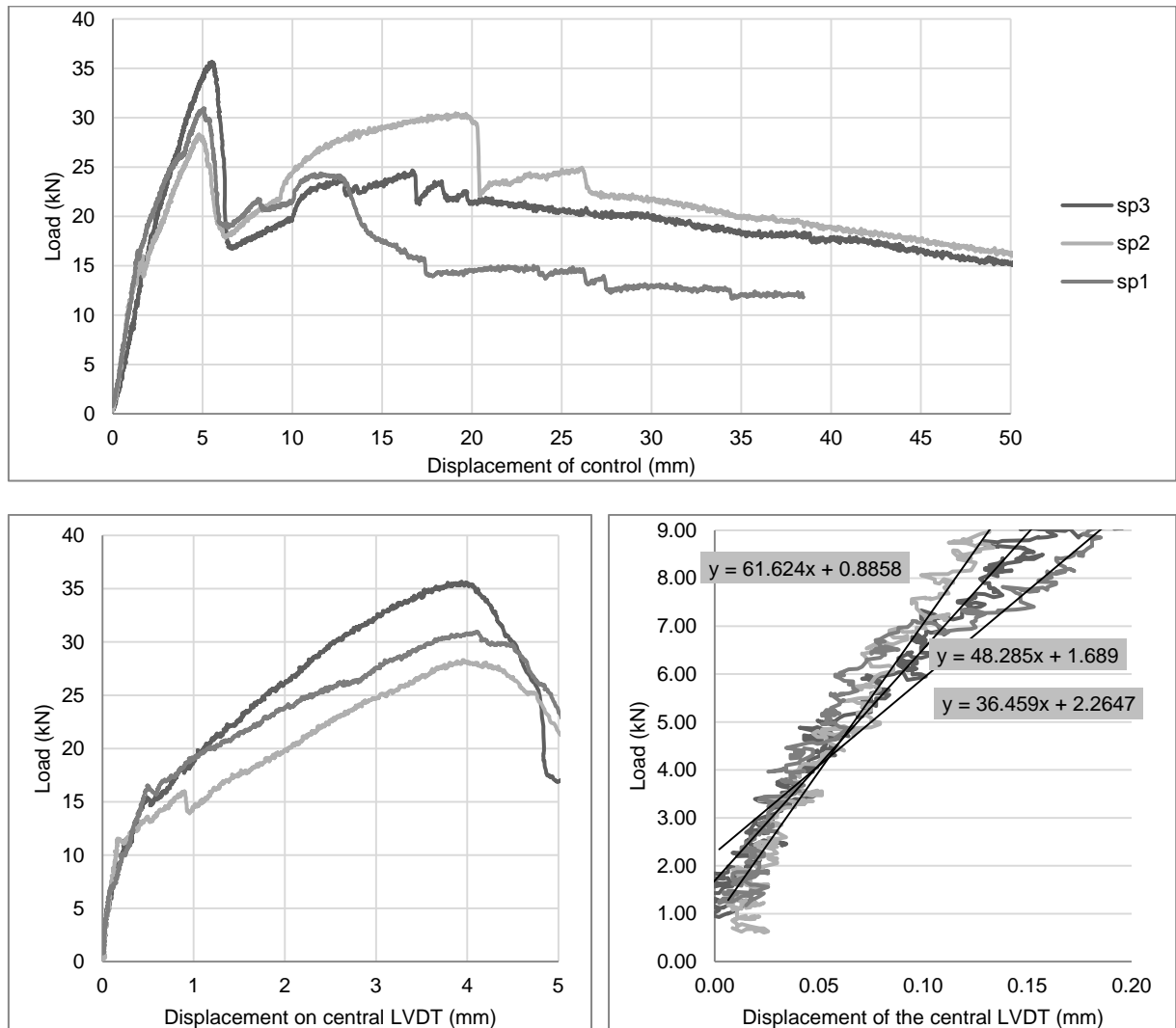
Figure 76. Load-displ. S&P: General behaviour. Elastic range. Estimation of stiffness.
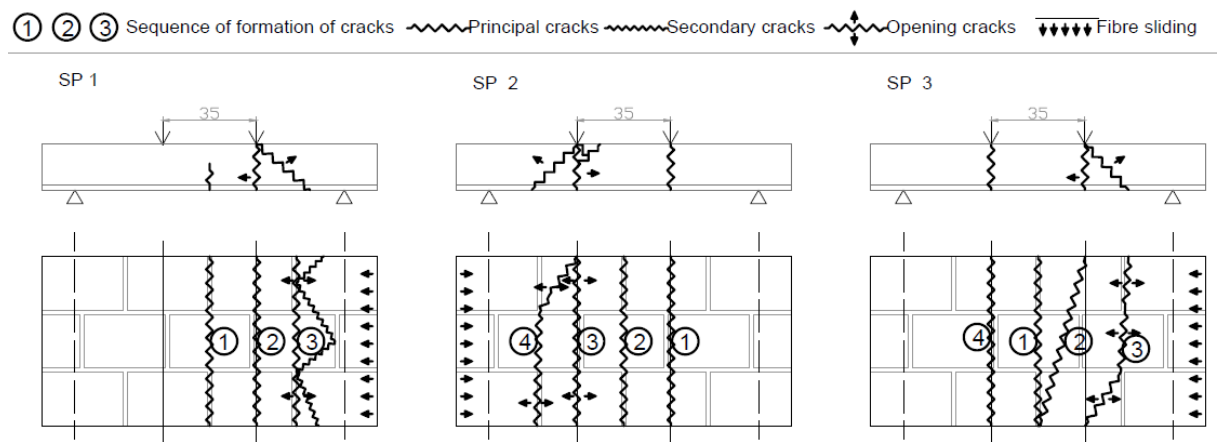
Figure 77. Specimen retrofitted with mesh from S&P: Crack pattern.

5.8. Comparative analysis.

The comparison among the different retrofitting solution must take into account the differences between the used solutions. The samples with the innovative material are comparable among them, given that they have a progressively increasing tensile capacity, and this is noticeable in increasingly better properties. The commercial solutions, having a much higher mass and tensile capacity, give better results in general, though the features of their behaviour are different. Therefore, the comparison among the solutions should be regarded more in a qualitative than in a quantitative scope.

However, for the quantitative comparison, in short, as shown in

Table 20, the following statements can be remarked:

- The composite reinforcements do not provide any noticeable improvement in the elastic range, meanwhile the commercial products increases the maximum elastic flexural stress (load at first crack) in about 26% for Mapei and 24% for SP commercial solutions.

- The maximum load increases progressively with the amount of reinforcement, though not in a linear way. The improvement on the flexural maximum load can be estimated in terms of load bearing capacity (directly related to flexural stress) when compared to the load obtained in unreinforced masonry specimens :

  o 2G#6, improvement on the maximum flexural load of of 11%

  o 4G#6, improvement on the maximum flexural load of of 22.6%

  o 2G#3, improvement on the maximum flexural load is of 110% but it is mobilized for very large deformations. If the range of deformations is considered within the glass fibre domain, the improvement can be estimated as 36%

  o Mapei, improvement on the maximum flexural load of of 175%.

  o S&P, improvement on the maximum flexural load of of 281%.

Table 20. Comparative analysis of resisting and deformation flexural parametres.

	unreinf	2g6	4g6	2g3	mapei	sp
Max. Elastic load (kN)	8.48	7.68	8.44	8.56	10.9	10.6
Max elastic deflection (mm)	0.165	0.149	0.235	0.265	0.145	0.198
Max elastic flexural stress (MPa)	0.450	0.408	0.448	0.454	0.579	0.563
Modulus of elasticity (MPa)	3512	3512	2504	2802	5124	3767
Max load (kN)		9.47	10.395	17.829	23.38	32.36
Max deflection calculated (mm)		68.287	42.826	86.583	12.59	large
Load redistribution		NO	NO	YES	YES	YES

Finally, for the final displacements, it is not possible to directly compare, as they depend on very different behaviours, and are better described in a qualitative way. Nonetheless, it is possible to state that the composite materials give by far the most ductile failure.

5.8.1. Influence of spacing and glass fibre content.

The retrofitting of masonry walls with the innovative materials shows a behaviour that is associated to the behaviour of the components of the composite. The samples were designed so that the mesh with two yearns and 6cm spacing (2g6) was the reference for comparison, 4g6 had double reinforcing material by means of having double glass fibre within the rods, and 2g3 has double reinforcing material by putting double of rods. A more detailed comparative analysis can be made based on the force-displacement diagrams shown in Figure 79 and Figure 80
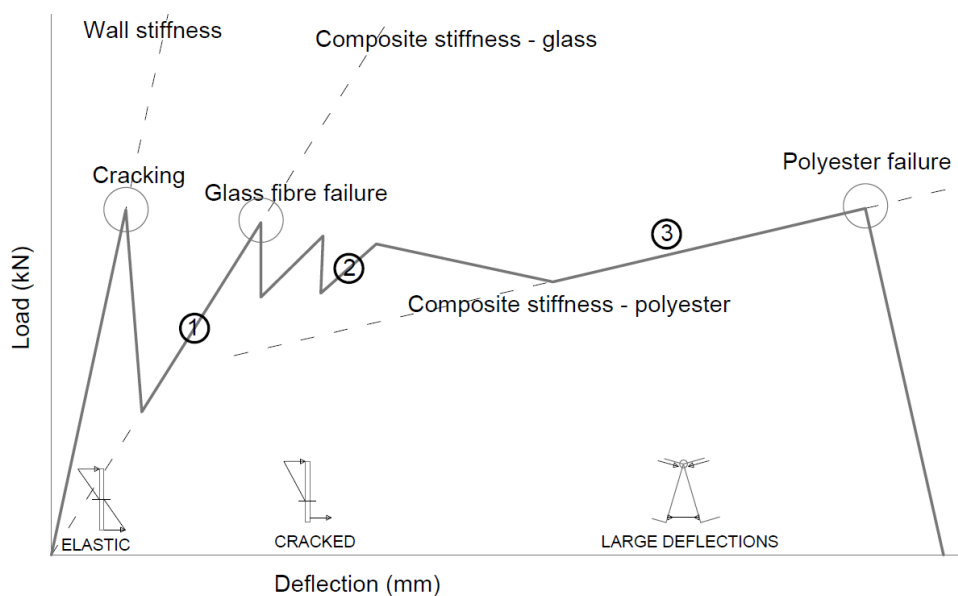
Figure 78. Scheme of the behaviour of composite-reinforced masonry.

After the cracking of the masonry three steps in the deformation and load bearing capacity can be distinguished, as showed in Figure 78:

- The first step implies a quick recover of the load bearing capacity, related to the stiffer behaviour of the reinforcement in the first phase previous to yielding point, in which the glass fibre commands the deformation.

- The second phase can be characterized by a relation among deformation and load bearing capacity with some fluctuation after cracking load. This should be related to the successive yield of different composite rods of the mesh. It is also possible that not all the glass fibres within the reinforcing material fail at the same time, which should be expected from the testing of the single rods, see Figure 80. This could be due to the different rate of loading that result

from two very different circumstances in which the material is tested: free and at standard velocity, or embedded in mortar and as slow as the opening of the cracks.

- A third phase defined by a new recovery of the load bearing capacity develops for a much lower rate, and is associated to the role of the polyester as reinforcing element, once glass fibre has completely failed.
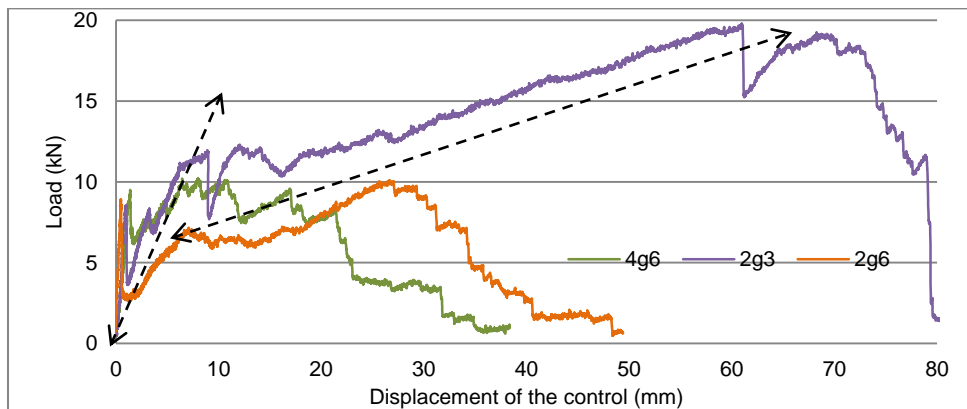
Figure 79. Comparative of general behaviour of significant samples with innovative material.
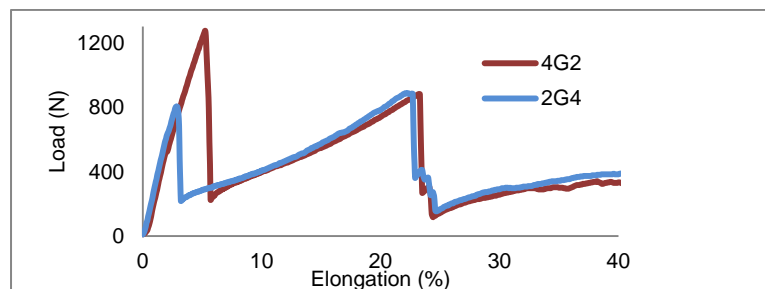
Figure 80. Behaviour of the reinforcements.

From the comparison of the three phases for the three different ratios of reinforcement following conclusions can be drawn:

- 4G#6 mesh has the double of glass fibre but the same amount of polyester of the mesh 2G#6. The specimens with the mesh 4G#6 present a faster recovery of load bearing capacity, as mentioned in the previous Chapter, even with slight stress redistribution. The highest load bearing capacity is achieved with much lower displacements. Specimens with 2G meshes reach almost the same load bearing capacity, but in the range where polyester is working, meaning that it needs much higher displacements. It is also noticeable that the working range of polyester in 4G reinforcement is very short (it is only noticed when putting the diagrams in direct comparison).

- 2G#3 meshes uses the same reinforcement than 2G#6, but has a double quantity. This is noticeable as a very similar behaviour of the reinforcement in qualitative terms, as the drop on

the load bearing capacity after cracking or the big recovery in the phase where the polyester is commanding. In quantitative terms, the maximum values are in the range of double of the ones obtained with the mesh 2G#6: double load-bearing capacity after the first phase, double load bearing capacity after the second phase and double deformation.

- 2G#3 and 4G#6 have the same quantity of glass fibre, but 2G#3 has double quantity of polyester, given that it has double number of rods. This is seems the reason why the load bearing capacity for both cases in the first and second phases of deformation are very similar. However, from that point 2G#3 has much longer deformation capacity and increases its load bearing capacity even over that value, due to the amount of polyester that commands that phase.

5.8.2. Comparation with commercial solutions.

5.8.2.1. Mapegrid 220.

The reinforcement of Mapei, namely MAPEGRID 220, having the same commanding material, fibreglass, shows a behaviour somehow comparable to the composites. The ratio of reinforcement is much higher: 225 g/m^2 of glass fibre compared to 114 g/m^2 of fibreglass in 4G#6 and 2G#3 and 57 g/m^2 in 2G#6. This implies that the final load bearing capacity is much higher, though the observed slope in the increment is very similar to the composites.

However, once the maximum stress in the glass fibres is reached, they break in a very uniform way, leading to a brittle failure, compared to the ductility of the samples reinforced with composites, see Figure 81.

Other important difference is in the masonry cracking point, as seen in Figure 82. The drop in the flexural from the cracking load is evident in case textile braided mesh of and less important when the Mapei grid is used. This is analysed as a possible problem of interfaces within the composite braided material and its definition as a tubular structure infilled with resisting fibres. For the Mapei material, there is only one interface in-between the mortar and the glass fibre. For the braided composites, there are two interfaces: mortar-polyester and polyester-glass fibre. Given that the tubular structure is the same for 2G and for 4G, it is possible to admit that there are more voids within the rod when there are only two yarns inside. This would imply that the material needs some small elongation to let the yarns line up with the axis and contributes more effectively for the resisting flexural mechanism of the retrofitted masonry specimens. Furthermore, this can be also a sign of ineffectiveness of the tensioning of the glass fibres before the application of the resin the external surface of the composite rod is made.

5.8.2.2. SP ARMO 550.

The comparison of the composite materials developed in this thesis with the commercial mesh from S&P I is really difficult due to its completely different properties. However, from the analysis of its

behaviour it is possible to guess that the behaviour of a solution in-between this and the composite materials can give very promising results.

The sliding of the fibres would be avoided due to the bonding of the external tubular structure, which would allow the carbon fibres to develop its maximum potential. In this experimental campaign, the failure of the carbon fibres was never observed. The improving on bonding would result on materials with very good behaviour using only limited amounts of carbon fibres.

The low elasticity of the carbon fibres allows a very high load bearing capacity for small displacements. On the other hand, the more effective redistribution of stresses enables the development of more smeared cracking instead of having important macro-cracks.

The possibility of combining all three materials in composite rods can give promising results combining high load bearing capacity with small damage and a very ductile failure.
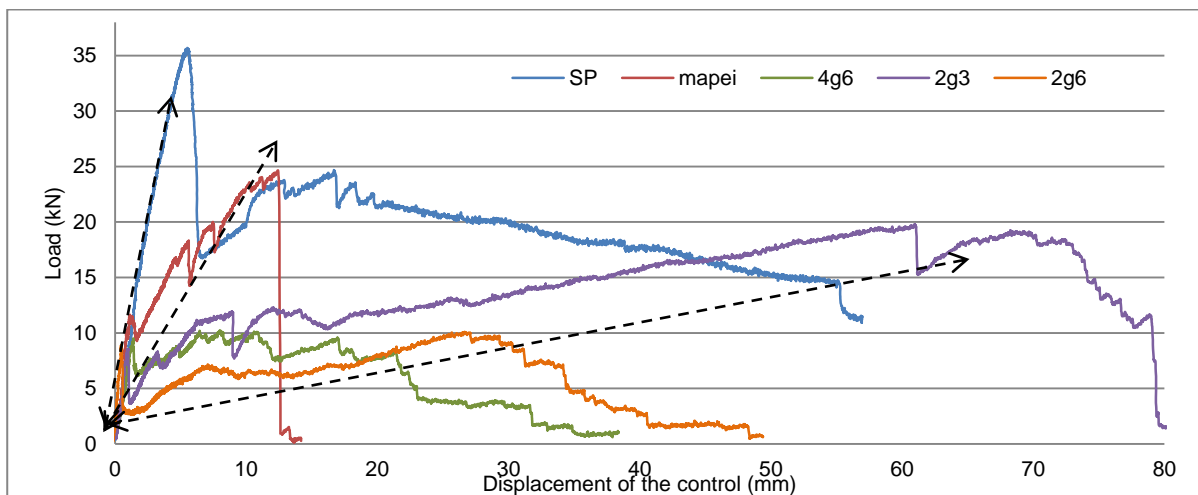
Figure 81. Comparative of general behaviour of significant samples of each type.
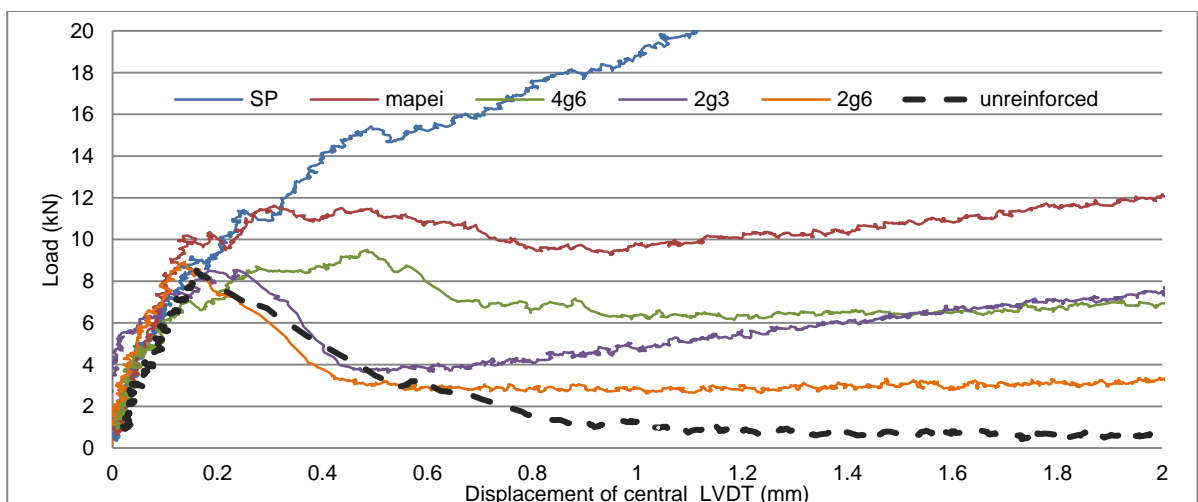
Figure 82. Comparative of cracking behaviour of significant samples of each type.

5.8.3. Comparison of cracking patterns and failure modes.

In the following images shown in Table 21 and Figure 83, the significant features of the deformation of the samples and the failure modes will be depicted. The images have been selected from samples with representative behaviour. In short, the conclusions drawn are as follows:

- The composite braided materials show a progressive failure, allowing thus the samples to develop significant macro-cracks and very large deflections.
- For 2G#6 and 4G#6 reinforced samples, the failure mode and the development of cracking is very simmilar, as seen in the first row of photographies. There is a single localized macro-crack that divides the sample into two blocks. For 4G#6, there was a slight distribution of cracking in one of the samples (Figure 83).
- 2G#3 reinforced samples developed several macro-cracks, always coincident with the position of the head joints, confirming the discretization of the stress distribution. Nonetheless, the typical bending curvature was observed.
- In the Mapei-reinforced samples, there was multiple cracking from the very beginning of the deflection. There was no significant opening of the final macro-crack, though, as the failure was brittle and it happened for a relatively small deflection. The failure showed features of combination of bending and shear, specially for one of the samples.
- In the S&P-reinforced samples there were also multiple thin cracks from the beginning of the deformation. Then, at a given point, one of the cracks, normally under the load application, widened exposing the reinforcement. Large sliding of the reinforcement within the mortar was observed.

Table 21. Significant images for failure modes by typology.

| 2g6: Crack localization and large deformations. | 2g6: Progressive failure of the reinforcement in last phase. | 4g6: Sample corresponding to small redistribution of stress. |

2g3: Stress redistribution with several open cracks.	2g3: Signs of brick crushing in compressed part.	2g3: Bending behaviour with curved deformation.
MAPEI: Multiple thin cracks showing stress redistribution.	MAPEI: Development of a localized crack before failure.	MAPEI: Final shear failure of sample with large deformations.
SP: Multiple thin cracks showing stress redistribution.	SP: Localized large crack opening	SP: Fibre sliding, visible after removing the rendering.
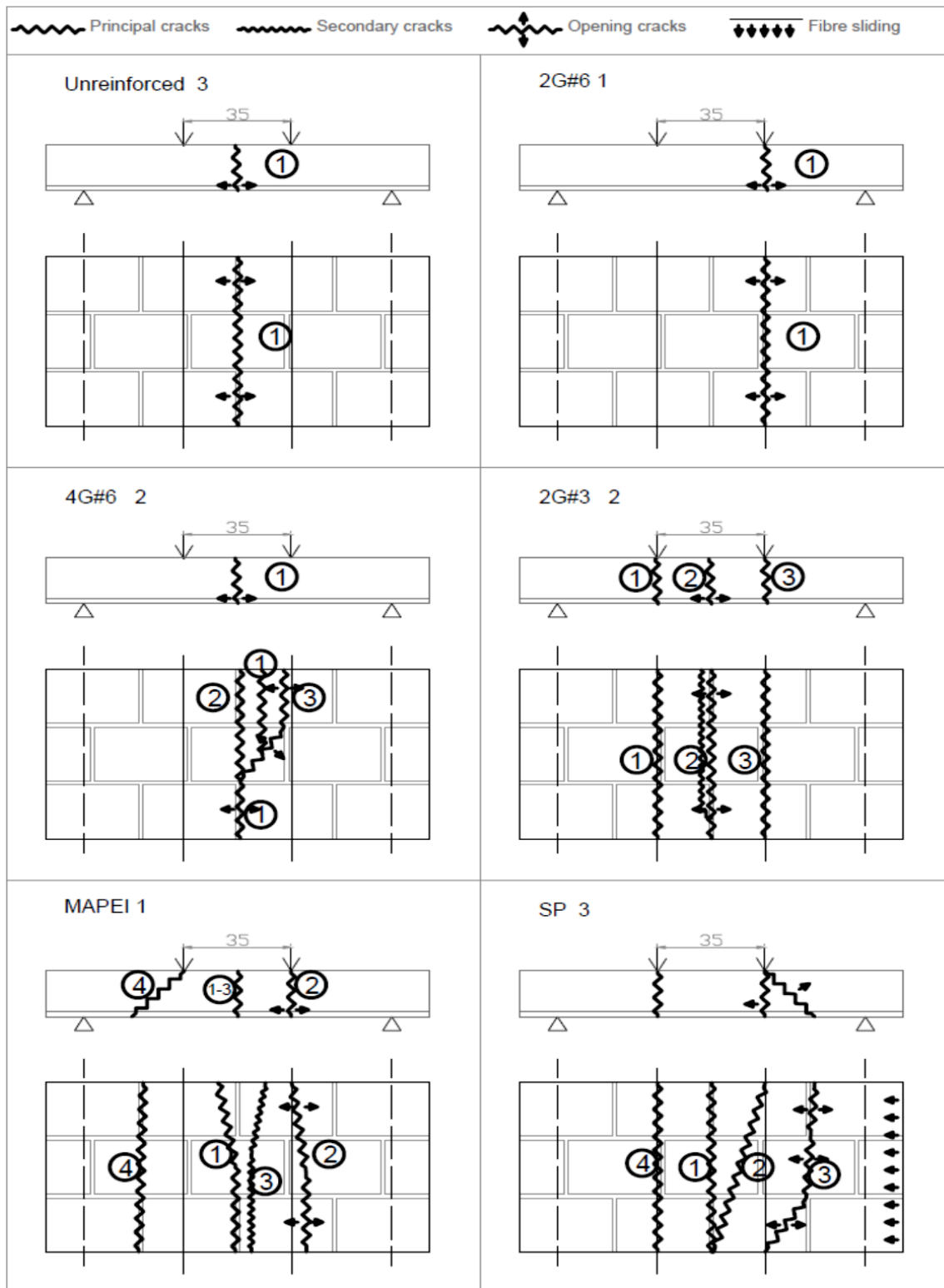
Figure 83. Comparison of typical failure modes of different reinforcements.

5.9.   Analytical vs. experimental results.

Table 22. Final expected load in kN. Estimations according to analytical models and obtained results.

	Analytical		Experimental	
	Cracked model	Large deformations	Elastic	Absolute maximum
2G#6	8.95	8.85	7.68	9.47
4G#6	9.56	11.97	8.44	10.39
2G#3	14.23	17.70	8.56	17.83
Mapei	16.67	26.35	10.9	23.38
S&P	25.93	54.81	10.6	32.56

Table 22 makes a direct comparison of the loads expected according to the different analytical models, and with both the maximum load within the elastic range and the absolute maximum load attained in the experimental campaign, for each type of reinforcement.

It is observed that, corresponding to the real observed behaviour, the most simmilar results are those considering large deformations and division of the masonry in several blocks, joined only by an almost infinitesimal compressed portion of masonry in compression and the elongated reinforcement in tension.

The comparison of the results can give draw important conclussions given that this is a measure of the difference between idealization and reality.

The analytical results for the cracked section model have considerable similarity in their distribution, but the values are lower than the real ones. Nonetheless, the differences show some important conclusions and lighten some errors in the assumptions:

- The strength of the masonry, taken as the EC6 estimation, seems to be low. This is visible by the statement that most cases will fail by crushing of the bricks, which doesn't happen. It also gives a low estimate for the elastic modulus.
- The expected loads, in general, are underestimated. This is even more noticeable for the more reinforced samples.
- It is also noticeable the effect of the small size of the samples. Given its composition by a small number of pieces, the discretization of stresses seems logical. This numerical model

should be also contrasted with larger masonry panels, which will resemble more to the continuous material model.

- It should also be noticed that this formulation is done for small deformations and thin cracking, and the range of this reinforcements go beyond it, which could lead to some error in the calculations.

The results for the model with large deflections, though initially considered just an approximation, shows a very good correspondance with the reality. The most important conclusions to highlight are:

- Except for the S&P reinforced samples, the obtained values correspond to the expected for the ultimate tensile capacity of the reinforcement. This is interpreted as a positive result, showing that there is no debonding between the mortar and the fibres. For the S&P reinforcement, it is interesting to observe that due to debonding, only 65% of its total capacity was used.

- It is important to remark that for both 2G#6 and 2G#3, the results of the maximum load in the experimental campaign correspond to the phase after the glass fibre yielding, which is not considered in the analytical models. This is another sign that 2G rods had a very little amount of glass fibres, and its effect is not noticed in terms of maximum attained load but only enhances the performance of the reinforcement in the first phase of deformation.

- For all the composite reinforced materials, there is some difference among the maximum expected load and the observed one in the yielding point of glass fibres. Given that no debonding of the rods was observed, this could be interpreted as a sign of internal debonding, or of irregularities in the distribution of stresses in the mesh, leading to progressive failure.

5.10. Comparison with other researches and solutions.

Though other studies found in the literature are not directly comparable due to the differences in the design and materials for the masonry samples, in the composition of the embedding mortar and mostly in the reinforcing materials, some remarks on the flexural behaviour can be done.

Papanicolau and Triantafillou have done extensive research on the application of TRM, and thus their publications [49] [54] [47] [48] compare a wide range of reinforced materials, both in-plane and out-of-plane, with flexural action in the direction of the bed-joints and perpendicular to them, and mostly under cyclic loading. They state to obtain always very good results both in terms of increment of the load and of ductile failure. The examples shown in Figure 84 correspond to several different samples reinforced with carbon, using different mortars (R: resin, P: polymer-enhanced, M: general purpose mortar), different techniques (NSM, near-surface mounted) and quantities (one or two layers, with a density around 180 g/m^2). For all of them it is observed a very important increment of the load bearing capacity. The curvature on the load-displacement diagram shows an immediate redistribution of the loads, giving a good flexural behaviour. Similarly to the samples reinforced with carbon in this thesis

(and being also similar in geometry), there is a quick achieving of the maximum load, with a relatively small displacement, followed by a sudden drop on the load bearing capacity, with some residual strength that decreases in almost constant rate, though the failure is defined as "flexure-shear". In this study, the samples using resins as matrix showed a slightly more ductile behaviour, and the ones with NSM, though not achieving as high load bearing capacity, showed the most ductile behaviour, due to the failure by "flexure and sliding".
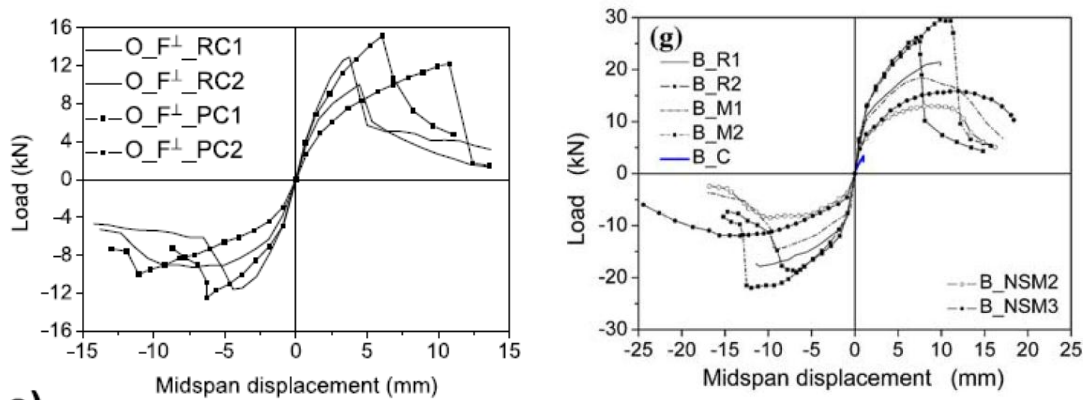
Figure 84. Envelopes for hysteretic curves for masonry reinforced with carbon textile fibres [49] [48].

In research carried out by Harajli [50], it was compared different materials to TRM, namely basalt and glass fibres, and different matrixes, lime mortar and TYFO industrial cement-based mortar, and reinforcing masses of 192 g/m^2 for basalt and 260 g/m^2 for glass. Though the dimensions of the samples and the test setup are similar, the masonry materials have a considerably higher strength. They concluded on the better behaviour of the lime mortar for cyclic loading, given that the cement based mortar failed after few cycles. They also verified that the final load was lower than expected, given that the failure of the fibres was not sudden but was reached progressively. The observed behaviour is defined by, after the first cracking, the load bearing capacity remains practically stable.
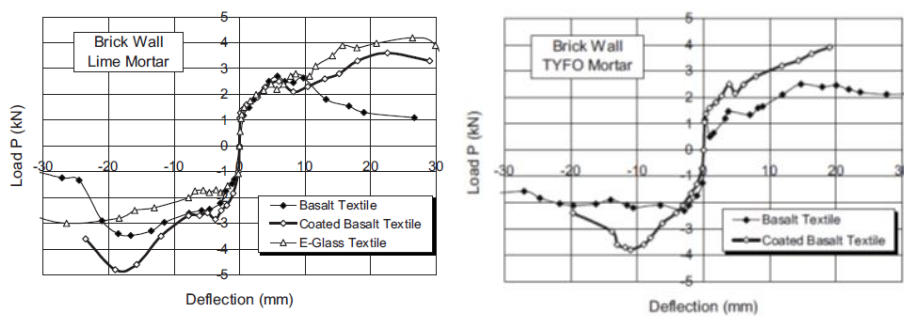
Figure 85. Comparison of the flexural behaviour of specimens reinforced with TRM - basalt and glass with different mortars. [50]

The thesis work by Rupika [39] is very interesting due to its parallelism to the work carried out in this thesis. The test setup and the dimensions of the samples are very similar, though the masonry used

had much higher strength. Ferrocement is interesting under merely comparison, as it is noticeable the really high strengthening effect, but also the very low deformation, given the much lower ultimate strain of steel, that leads to a very brittle failure. But the real interest is to compare both the composite reinforcements with polymeric grids and with glass fibres, since a combination of them could define quite correctly the composite braided materials used in this thesis. The polypropylene bands show a low reinforcing capacity, with an almost constant or slightly raising load bearing capacity after the cracking. Glass fibre gives a high initial strengthening followed by a drop as the reinforcement starts to fail. It is noticeable that as reinforcement ratio increases, the drop in the load bearing capacity for both the glass fibre and the polypropylene gets more irrelevant, and eventually for the samples with highest reinforcement of glass fibre, it disappears.
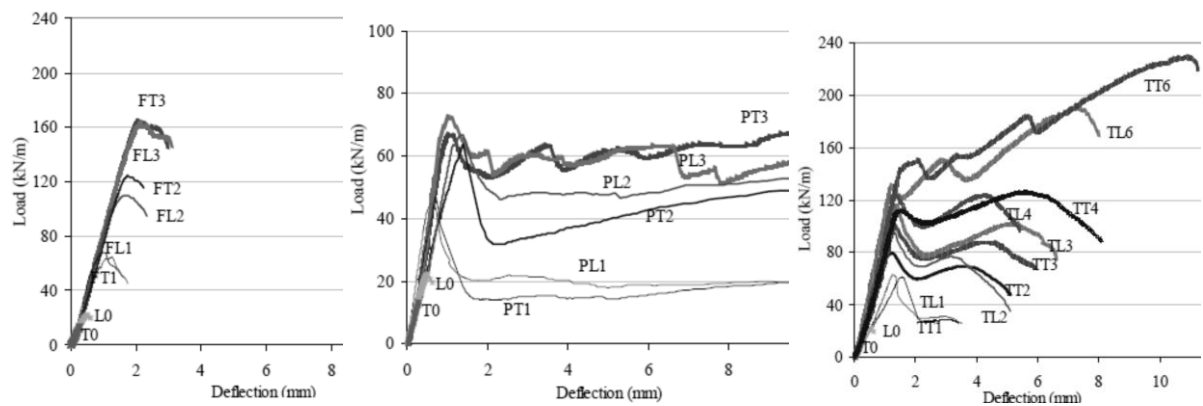
Figure 86. Left: ferrocement. Middle: polypropylene bands. Right: Glass fibre TRM. [39]

CHAPTER 6.   CONCLUSIONS AND FUTURE WORK.

6.1.   Conclusions.

6.1.1. Braided materials

The definition of the behaviour of this composite material under tensile loading is dependent on features of its components. This means that it is possible to distinguish two phases corresponding to two yielding points: (1) a first linear elastic phase with stiffer behaviour associated to the high elastic modulus of the glass fibre core; (2) after the failure of the fibre glass, a second stretch develops allowing very large elongations due to the polyester external tubular structure. This second almost linear stretch is governed by the elasticity of the polyester braided materials.

Given the mixed area in which the polyester accounts for a high percentage, the obtained maximum stress for the whole section is lower than the expected only for glass fibre. Nonetheless, this value is still considerable among reinforcing materials. It is obtained 289 MPa for 2G composite braided and 326 MPa for 4G composite braid, depending on the quantity of glass fibre. This is comparable to reinforcement steel, with about 400-500 MPa. And, though it is a very low value when compared to the 2600 MPa declared for pure glass fibre, the comparison of the performance in the experimental campaign shows that it is similar in the glass-fibre governed phase to the samples reinforced with only glass fibres.

The rods were initially designed considering as resisting material only the glass fibre, but it has been proven that the effect of the polyester cannot be neglected. It accounts for a considerable part of the strength in the first phase of extension, contributing to the force given by the glass fibres. Besides, it is the cause of the very ductile behaviour of the walls after their cracking, giving all its capacity for very large deformations.

Another important conclusion on the behaviour of the material as a composite is the nonlinearity on the correspondence among the quantity of strictly reinforcing material, glass fibre, and the expected resistance. This is due both to the nature (a tubular structure infilled with high resistance material) and to the high component of manual processing of the material. This can be explained somehow as a failure in the expected maximum strength, due to irregularities in the internal bonding between the glass fibre core and the external structure. Possibilities of improvements will be further discussed.

6.1.2. Performance of the materials as reinforcement for clay brick masonry walls.

The enhancement of the ultimate strength should be described in two terms, given that the most significant behaviour for the braided materials implied two peaks in the load bearing capacity:

- The peak corresponding to the maximum linear load, corresponding to the cracking load (load corresponding to the onset of the cracking), associated to a very small deformation. This value is the same for unreinforced walls and for the samples with lower reinforcement ratio, and after its achievement there is a sudden drop in the load bearing capacity. For the samples with higher reinforcement ratio, this load was not improved either, but the load bearing capacity kept stabilized. For the commercial solutions, with a much higher reinforcement ratio, the cracking load was increased of about a 25%, and the load bearing capacity continued to grow after the macro-cracking was reached.

- The absolute maximum load bearing capacity, related to the maximum tension on the reinforcement, increases progressively with the amount of reinforcement, though not in a linear way. This value was improved for all the samples, from an almost insignificant value for the lowest reinforcement ratios, to a 36% in the sample with more braided materials, within the small deformation range (2G#3), and to a 175% in glass fibre (Mapei mesh) reinforcement and 280% for carbon fibres (S&P mesh).

The improvement of the ductility is the most important contribution for the performance of the composite braided material. Even the samples with lower reinforcement ratio show very large ultimate displacements maintaining a high load bearing capacity. This appears to be related to the third phase of the composite braided material, which correspond to the polyester deformation, after the failure of the internal reinforcing core. In the case of the highest reinforcement ratio (2G#3), the ductility is such that the maximum load bearing capacity is only attained for very large displacements, in the order of 6% the span. For the commercial glass fibre, ductility is considerably lower as due to the progressive failure of the fibres, after which a brittle failure was recorded. For the commercial carbon fibres, the behaviour is very ductile as the sliding of the fibres lead to very large displacements, getting out of the range of the capacity of the test setup. However, it should be better studied if this sliding is realistic for conventional size of panels, given that if this phenomenon didn't happen, the failure would be most likely brittle due to brick crushing.

The deformation and the failure mode of the reinforced walls is tightly connected with the reinforcement ratio:

- For low values, there is no stress redistribution and therefore the failure implies the excessive widening of a macro-crack. However, the big capacity of deformation of the polyester braid avoids the complete failure, keeping the separate blocks together and allowing a considerable load bearing capacity for large deformations.

- As the reinforcement ratio increases, a more smeared crack distribution was observed. This implies stress and strain redistribution between masonry and the reinforcement, which implies a higher load bearing capacity before one of the cracks widens more than the others, getting to the range of the polyester command and the sample is finally divided in two blocks.

- For the highest reinforcement ratios, corresponding to the commercial meshes, the multiple cracking is noticeable from the beginning of the deformation. The failure is due to a mix of flexural and shear actions.

Effect of stronger rods and of bigger density. Bigger density implies better redistribution of the loads and therefore avoids the drop in the load bearing capacity after the cracking of masonry.

The use of a composite material implies mixing the features of its components. This way, the innovative rods result on a behaviour that approximately can be described as the addition of two already existing reinforcing techniques:

- Glass fibre textile reinforced mortar, with good reinforcement properties within the range of small deformations but with a brittle failure if there is no sliding of the fibres.

- Polymeric grids, that don't provide much reinforcement in terms of load bearing capacity but have very good performance in allowing the masonry to undergo large deformations.

6.1.3. Comparison of analytical estimation and observed results.

The analytical estimation of the ultimate strength for cracked sections is based in some assumptions that are too idealistic for the behaviour of a sample of masonry. The discrete conformation of the material implies stress concentration and localized failures that are not considered in the model. Possibly, it would be a better representation for bigger panels, given that the smaller size of the units relatively to the sample, it can bear more resemblance with a continuous material. The obtained data showed as well the underestimation of the compressive strength of masonry when using the EC6 formulation.

The approximate model in which the flexural strength was a direct function of the tensile capacity matched much better with the obtained results, indicating thus that the range of deformations to be considered is out of the material continuum.

Anyway, it is important to remark that neither of the models consider the progressive failure of the fibres that is observed in the experimental campaign. This phenomenon might be caused by irregular distribution of the stresses within the mesh, by slight variations of properties within the material or even by small differential sliding of the fibres within the mortar. Nonetheless, it is also observed in the commercial glass fibre mesh, which was produced industrially and is supposed to have very homogeneous properties. The difference among the experimental results and the expected values could be a measure of this effects that make reality differ from theoretical models.

6.2.   Suggestions for further development.

Based on the results obtained in the experimental campaign, both in the mechanical characterization of the composite braid materials and the simple bending tests, some additional work has to be carried out. This work is important to clarify some uncertainties related to the behaviour of the composite and performance of the composite braided meshes.

-        As a starting point, it is necessary a better study on the interface between the external tubular structure and the core in the composite rods to have a complete knowledge of the mechanic characteristics of the material. This might imply a study on the amount of material needed to fulfil the tubular structure in order to avoid voids, or modification of the resin application process. With this respect, microscopic analysis of samples in increasing degree of elongation can be carried out to assess the level of adherence between the components materials of the composite rods.

-        Given the possibility of tailor-made materials, it is clear the importance of experimenting with new combinations of materials. Stiffer reinforcing material such as carbon or basalt fibre will probably result on an earlier action of the reinforcement on the cracking process, giving a better redistribution of the stresses before the development of cracks. Furthermore, the increase of the bonding given by the external shell would avoid the observed sliding of the carbon fibres observed in the commercial solutions. A promising possibility is combining carbon, glass and polyester, giving three steps of breaking to the material and thus an even more gradual failure.

-        Due the importance that the external braid has in the large deformations, other materials should also be tried in this element, as a mean of improving the ductility.

-        Even if one of the reasons for the application of an external polyester braid was the protection of glass fibre to the alkali components of mortars, this has not been experimentally veryfied. It is necessary, then, an experimental campaign on the assessment of the durability of this materials within mortar, and a study on the potential loss of mechanical properties such as strength or bonding.

-        With respect to the braided composite rods and to the manufacture process, it will be very important to evaluate if it is necessary to attain an optimum previous tensioning to be given to the braided textile composites that enable the immediate stress transfer between masonry and reinforced textile mortar. In fact, the important drop in the resistance of the retrofitted masonry panels can in certain extent be attributed to the low tensioning of the reinforcing materials, avoiding the instantaneous stress transfer.

-        Following other researches, experimentation with the application of the braided materials within other kinds of mortar: lime, high ductility, enhanced with polymers, etc., looking for the optimal combination of bonding and ductility.

- With respect to the masonry panels, it is needed to go for new test setups, more realistic for the description of the real earthquake actions on masonry. For instance: punch tests as simulation of bidirectional flexure requirements, consider in-plane and out-of-plane cyclic loading. Nevertheless, this can be only considered once the behaviour of the material is well understood, given the cost and complexity of such tests.

- Real application of the innovative reinforcing technique to the reinforced concrete masonry infill walls, by testing the whole structure. With this respect, it will be very important to study the way of connections between braided rods and enclosure structural elements.

- Exploit the possibility to use sensing features of the reinforcing braided rods to monitor continuously the behaviour of masonry infill walls, mostly for a better understanding of its real behaviour, with research purposes.

REFERENCES.

[1] R. Vicente and others, "Performance of masonry enclosure walls: lessons learned from recent earthquakes," *Earthquake engineering and engineering vibration,* vol. 11, no. 1, pp. 23-34, 2011.

[2] D. D'Ayala and S. Paganoni, "Assessment and analysis of damage in L'Aquila historic city centre after 6th April 2009.," *Bull Earthquake Eng,* no. 9, pp. 81-104, 2011.

[3] S. Abreu, *Retrofitting strategies for masonry infill walls, Master Thesis (in Portuguese),* Guimaraes: Universidade do Minho, 2011.

[4] R. Fangueiro, G. Sousa, F. Soutinho, S. Jalali y M. Araujo, «Application of braided fibre reinforced composite rods in concrete reinforcement,» Guimaraes, 2008.

[5] C. Gonilho Pereira, R. Fangueiro, S. Jalali and others, "Braided reinforced composite rods for the internal reinforcement of concrete," *Mechanics of composite materials,* vol. 44, no. 3, 2008.

[6] C. Gonilho Pereira, R. Fangueiro, S. Jalali y M. Araujo, «Hybrid composite rods for concrete reinforcement,» *Structures and Architecture – Cruz (Ed.),* 2010.

[7] M. Tomazevic, Earthquake - resistant design of masonry buildings., London: Imperial College Press, 1999.

[8] Various, Manual de alvenaria de tijolo., Coimbra: Associaçao Portuguesa da Indústria de Cerâmica, 2000.

[9] M. Tomazevic, M. Lutman y V. Bosiljkov, «Robustness of hollow clay masonry units and seismic behaviour of masonry walls,» *Construction and Building Materials,* vol. 20, pp. 1028-1039, 2006.

[10] Hyspalit, «Catálogo de soluciones cerámicas,» Instituto de ciencias de la construcción Eduardo Torroja, Madrid, 2008.

[11] FEMA_306, Evaluation of earthquake damaged concrete and masonry wall buildings. Basic procedures manual., Washington D.C.: Federal Emergency Management Agency, 1998.

[12] A. Kappos, "Seismic Design and Performance Assessment of Masonry Infilled R/C Frames.," in *12th WCEE*, New Zealand, 2000.

[13] G. Al-Chaar, M. Issa and S. Sweeney, "Behavior of Masonry-Infilled Nonductile Reinforced Concrete Frames," Journal of structural engineering, 2002.

[14] B. Binici, G. Ozcebe y R. Ozcelik, «Analysis and design of FRP composites for seismic retrofit of

infill walls in reinforced concrete frames,» *Composites: Part B,* vol. 38, 2007.

[15] C. Syrmakezys y P. Asteris, «Influence of infilled walls with openings to the seismic response of plane frames,» de *9th canadian masonry symposium*.

[16] E. Vintzeleou y T. Tassios, «Seismic behaviour and design of infilled R.C. frames,» *Journal of European Earthquake Engineering,* vol. 2, pp. 22-28, 1989.

[17] M. M. Kose, "Parameters affecting the fundamental period of RC buildings with infill walls," *Engineering Structures,* no. 31, pp. 93-102, 2009.

[18] A. Madan and others, "Influence of masonry infills on the dynamic response of reinforced concrete framed structures," in *13th International Brick and Block Masonry Conference*, Amsterdam, 2004.

[19] T. Liauw, "An effective strutural system against earthquakes - infilled frames," in *Proceedings of the Seventh World Conference on Earthquake Engineering (7th WCEE)*, Istanbul, 1980.

[20] A. Menon and G. Magenes, "Definition of Seismic Input for Out-of-Plane Response of Masonry Walls: I. Parametric Study," *Journal of Earthquake Engineering,,* no. 15, pp. 165-194, 2011.

[21] A. Menon and G. Magenes, "Definition of Seismic Input for Out-of-Plane Response of Masonry Walls: II. Formulation," *Journal of Earthquake Engineering,* vol. 2, no. 15, pp. 195-213, 2011.

[22] P. Shing and A. Mehrabi, "Behavior and analysis of masonry infilled frames.," *Prog. Struct. Engng Mater.,* no. 4, pp. 320-331, 2002.

[23] FEMA_273, *NEHRP Guidelines for the seismic rehabilitation of buildings,* Washington D.C.: Federal Emergency Management Agency, 1997.

[24] P. Asteris, D. Kakaletsis and others, "Failure modes of infilled frames," *Electric journal of structural engineering,* vol. 11, no. 1, 2011.

[25] R. Angel, D. Abrams and D. Sapphiro, Behaviour of reinforced concrete frames with masonry infills, Department of Civil Engineering, University of Illinois, USA, Report Nº UILU-ENG-94-2005, 1994.

[26] R. Flanagan y R. Bennet, «Bidirectional behaviour of structural clay tile infilled frames,» *Journal of structural engineering,* vol. 125, nº 3, 1999.

[27] S. Hendra, Strengthening of masonry walls against out-of-plane loads using cementitious composite materials, Singapore: University of Singapore, 2007.

[28] G. Verderami, I. Iervolino y P. Ricci, «Rapporto dei danni subiti dagli edifici a seguito dell'evento sismico del 6 aprile 2009 V1.00,» Dipartimento di Ingegneria Strutturale, Università di Napoli

Federico II., Napoli, 2009.

[29] M. Feriche, F. Vidal y C. Aranda, «Efectos del terremoto de Lorca del 11-5-2011,» Universidad de Granada.

[30] «www.reluis.it,» Universitá di Basilicata, Universitá Federico II di Napoli, Universitá di Pavia, Universitá di Trento. [En línea].

[31] V. Kodur, M. Erki y A. Quenneville, «Seismic design and analysis of masonry-infilled frames,» *Canadian Journal of Civil Engineering,* vol. 22, nº 3, 1995.

[32] T. Bashandy, *Behavior of reinforced concrete infilled frames under cyclic loading,* Austin, Texas: University of Texas, 1995.

[33] FEMA_356, *NEHRP handbook for the seismic evaluation of existing buildings - a prestandard.,* Washington D.C.: Federal Emergency Management Agency, 1998.

[34] W. El-Dakhakhni and R. Drysdale, "3D finite element modelling of masonry infilled frames with and without openings," in *13th International Brick and Block Masonry Conference*, Amsterdam, 2004.

[35] X. Li, S. Gong and X. Gu, "Interaction and seismic capacity of brick walls and supporting RC frames," in *13th International Brick and Block Masonry Conference*, Amsterdam, 2004.

[36] S. Chidiac, Z. He y D. Drysdale, «Finite element model of unreinforced hollow concrete blocks subject to out-of plane actions. A parametric study.,» de *13th International Brick and Block masonry conference*, Amsterdam, 2004.

[37] M. ElGawady, P. Lestuzzi and M. Badoux, "A review of conventional seismic retrofitting techniques for URM," in *13th International Brick and Block Masonry Conference*, Amsterdam, 2004.

[38] M. Pereira, *Caracterizaçao experimental da resposta mecânica no seu plano e fora do plano de parede de alvenaria de enchimento,* Porto: Mestrado Integrado em Engenharia Civil - 2009/2010 - Departamento de Engenharia Civil, Faculdade de Engenharia da Universidade do Porto, 2010.

[39] W. Rupika, *Out of plane strengthening of unreinforced masonry walls using textile reinforced mortar systems,* Singapore: Thesis for the degree of Master of Engineering, Department of Civil Engineering, National University of Singapore, 2010.

[40] R. Sofronie, «Seismic strengthening of masonry in buildings and cultural heritage,» de *6º Congresso Nacional de Sismologia e Engenharia Sísmica*, 2004.

[41] A. Penna, G. Calvi and D. Bolognini, *Design of masonry structures with bed joint reinforcement,* 2007.

[42] V. Turco y others, «Flexural and shear strengthening of un-reinforced masonry with FRP bars.,» *Composites Science and Technology,* nº 66, pp. 289-296, 2006.

[43] N. Galati, G. Tumialan and A. Nanni, "Strengthening with FRP bars of URM walls subject to out-of-plane loads," *Construction and building materials,* no. 20, pp. 101-110, 2006.

[44] M. Ismail, J. Ingham y others, «Diagonal shear behaviour of unreinforced masonry wallettes strengthened using twisted steel bars,» *Construction and Building Materials,* nº 25, 2011.

[45] D. Bournas, T. Triantafillou and C. Papanicolau, "Retrofit of Seismically Deficient RC Columns with TRM jackets," in *4th Colloquium on Textile Reinforced Structures (CTRS4)*, 2008.

[46] Various, *Linee guida per la reparazione e il rafforzamento di elementi strutturali, tamponature e partizione (Draft),* Roma: Dipartamento della Protezione Civile, 2009.

[47] C. Papanicolau, T. Triantafilou and others, "Textile-reinforced mortar versus FRP as strengthening material of URM walls: In-plane cyclic loading," *Materials and structures,* no. 40, p. 1081–1097, 2007.

[48] C. Papanicolau, T. Triantafilou and others, "Textile-reinforced mortar versus FRP as strengthening material of URM walls:Out-of-plane cyclic loading," *Materials and structures,* no. 41, p. 143–157, 2008.

[49] C. Papanicolau and T. L. M. Triantafillou, "Externally bonded grids as strengthening and seismic retrofitting materials of masonry panels," *Construction and building materials,* no. 25, pp. 504-514, 2011.

[50] M. Harajli, H. ElKhatib and J. San-Jose, "Static and Cyclic Out-of-Plane Response of Masonry Walls Strengthened Using Textile-Mortar System," ASCE, 2010.

[51] R. Dias Tolêdo, J. Kuruvilla y others, «The use of sisal as fibre for reinforcement in cement based composites,» *Revista Brasileira de Engenharia Agrícola e Ambiental,* vol. 3, nº 2, 1999.

[52] Various, «Raport științific PN II ID_589, faza 3/2009,» http://www.3dknit.tuiasi.ro/.

[53] T. Triantafillou, «Strengthening of masonry structures using epoxy-bonded FRP laminates.,» *Journal of Composites for Construction,* nº 2, pp. 96-103, 1998.

[54] C. Papanicolau and T. Triantafilou, "TRM versus FRP as strengthening material of concrete structures," FRPRCS-7 Fiber Reinforced Polymer Reinforcement for Reinforced Concrete

Structures S-230-6.

[55] E. 6. EN-1996-1-1, *Design of masonry structures - Part 1-1: General rules for reinforced and unreinforced masonry structures,* Brussels: CNE, 1996.

[56] E. 8. EN-1998-1, *Design of structures for earthquake resistance - Part 1 General rules, seismic actions and rules for buildings.,* Brussels: CEN, 1998.

[57] F. Crisafulli, A. Carr and R. Park, "Capacity design of infilled frame structures.," in *12WCEE*, 2000.

[58] S. Altin, Ö. Anil and M. Kara, "Strengthening of RC nonductile frames with RC infills: an experimental study," *Cement & Concrete Composites,* no. 30, pp. 612-621, 2008.

[59] A. Peled and A. Bentur, "Geometrical characteristics and efficiency of textile fabrics for reinforcing cement composites," *Cement and Concrete Research,* no. 30, pp. 781-790, 2000.

[60] W. Curtin, G. Shaw and others, Structural masonry designers' manual, Blackwell science, 1995.

[61] C. Gonilho Pereira, «Varoes em material composito para monitorizaçao e reforço do betao,» de *Fibrenamics na construçao civil*, Guimaraes, 2012.

ANNEXES.

A1 Technical data of the commercial solutions used in the experimental campaign.

Table 23. Technical data for the yarns of glass fibre.

property information		Individual Package
Binder	Type	611
	% Nominal LOI %	0.70%
	% Tolerance LOI %	+/- 0.30%
Yardage	Bare Glass, Nominal	1215 yds / 408 tex
	With Binder, Nominal	1205 yds / 412 tex
	% Tolerance	+/- 6.0%
Broken Filaments per plane, maximum		10.0
% Moisture Content, Maximum		0.25%
Tensile Strength, Minimum		36.7 lbs / 163 Newtons
Twist	Turns per Inch	+/- 0.20 tpi
Tolerance	Turns per Meters	+/- 8 tpm

Table 24. Technical data for Mapegrid G220.

DATI TECNICI (valori tipici)	
DATI IDENTIFICATIVI DEL PRODOTTO	
Tipo di fibra:	fibre di vetro A.R.
Grammatura (g/m²):	225
Dimensione delle maglie (mm):	25 x 25
Classificazione di pericolo secondo Direttiva 99/45/CE:	nessuna
Voce doganale:	7019 90 99
DATI APPLICATIVI	
Resistenza a trazione (kN/m):	45
Allungamento a rottura (%):	< 3

Table 25. Technical data for SP ARMO L500

Technical data	ARMO-mesh L500
Elastic modulus (theoretical) [kN/mm^2]	240
Reduction factor on elastic modulus due to application	1.5
Elastic modulus (reduced) for design [kN/mm^2]	**160**
Ultimate tensile strength C-fibre (theor.) [N/mm^2]	4'300
Weight of C-fibre in main direction [g/m^2]	200
Density C-fibre [g/cm^3]	1.7
Elongation at rupture (therotical) [%]	1.75
Theoretical thickness of C-fibre for design (fibre weigh t ÷ density) [mm]	0.117
Theoretical cross section C-fibre for design [mm^2/m]	117
Ultimate tensile force at 1.75 % **(theoretical)** **[kN/ m]**	**500**
Tensile force for desing (S&P recommendation) **Flexural (~ 800 N/mm^2)** (Limit strain at ultimate state 0.5 %) **[kN/m]** **Axial (~ 640 N/mm^2)** (Limit strain at ultimate state 0.4 %) **[kN/m]**	 93.6 74.8

A2. Mortar flexural and compressive strength data.

		Element	flexural stress (MPa)	mean compressive stress (MPa)
17-may	1a	unreinforced1; 4g#6-1	0.12	11.12
	1b	unreinforced1; 4g#6-1	2.99	9.31
	1c	unreinforced1; 4g#6-1	non valid	non valid
		average	2.99	10.22
	2a	unreinforced2; 4g#6-2	non valid	
	2b	unreinforced2; 4g#6-2	2.85	8.53
	2c	unreinforced2; 4g#6-2	2.31	8.23
		average	2.58	8.38
	3a	unreinforced3	2.91	10.15
	3b	unreinforced3	3.24	9.49
	3c	unreinforced3	2.87	9.31
		average	3.01	9.65
	4a	4g#6-3	2.87	8.95
	4b	4g#6-3	non valid	non valid
	4c	4g#6-3	0.18	8.69
		average	2.87	8.82
	5a	S&P1; 2g#3-1	non valid	non valid
	5b	S&P1; 2g#3-1	3.03	8.78
	5c	S&P1; 2g#3-1	2.70	8.52
		average	2.87	8.65
	6a	S&P2	1.21	8.18
	6b	S&P2	3.29	9.13
	6c	S&P2	2.77	8.85
		average	2.42	8.72
18-may	1a	2g#3-2	3.21	10.76
	1b	2g#3-2	3.20	10.75
	1c	2g#3-2	3.25	10.95
		average	3.22	10.82
	2a	S&P3; 2g#3-3	2.86	9.70
	2b	S&P3; 2g#3-3	3.22	10.56
	2c	S&P3; 2g#3-3	3.21	10.76
		average	3.10	10.34
	4a	MAP1; 2g#6-1	2.98	7.92
	4b	MAP1; 2g#6-1	3.07	8.90
	4c	MAP1; 2g#6-1	3.47	10.07
		average	3.17	8.96
	5a	MAP2; 2g#6-2	0.11	8.32
	5b	MAP2; 2g#6-2	3.29	9.71
	5c	MAP2; 2g#6-2	3.00	9.77
		average	3.15	9.27
	6a	MAP3; 2g#6-3	3.13	8.94
	6b	MAP3; 2g#6-3	2.90	8.76
	6c	MAP3; 2g#6-3	2.79	8.91
		average	2.94	8.87
	average		2.94	9.34
31-may	1a	RENDER	4.53	9.87
	1b	RENDER	1.99	9.55
	1c	RENDER	3.97	9.80
01-jun	1a	RENDER	3.11	7.84
	1b	RENDER	3.17	7.84
	1c	RENDER	3.11	7.66
	2a	RENDER	4.38	10.46
	2b	RENDER	3.34	9.54
	2c	RENDER	0.10	10.08
	average		3.45	9.18